Further development of marine mammal dynamic energy budgets models for application to environmental assessments and integration into the iPCoD framework

October 2023

Scottish Government
Riaghaltas na h-Alba

SMRU Consulting

understand ♦ assess ♦ mitigate

Further development of marine mammal dynamic energy budgets models for application to environmental assessments and integration into the iPCoD framework

Authors: John Harwood, Magda Chudzinska, Cormac Booth

Report Code: SMRUC-MSC-2021-015

Date: Sunday 2nd May 2022

This report is to be cited as: Harwood, J; Chudzinska, M; Booth, CG 2021. Final Report: Further Development Of Marine Mammal Dynamic Energy Budgets Models For Application To Environmental Assessments And Integration Into The IPCoD Framework. SMRUC-MSC-2021-015 Provided to Marine Scotland, May 2022 (unpublished).

1 Non-Technical Summary

The offshore wind industry is in the process of a significant expansion with a move towards clean energy and a green economic recovery. The sustainable expansion of offshore wind requires a robust understanding of the impacts of construction and operation and appropriate levels of conservatism and realism in assessments. The potential risk of injury and/or disturbance to marine mammals during construction of offshore renewable energy developments (e.g., pile driving, removal of unexploded ordnance, increased vessel presence offshore) has been identified as a key consenting risk for projects in UK waters. Possible consequences of exposure to underwater noise include disturbance that could cause marine mammals to either move away or change behaviour (which could result in reduced net energy intake) or suffer temporary and permanent hearing damage.

The scale of offshore wind farm developments means there is the potential for significant cumulative impacts on marine mammals, which would need to be considered and mitigated at a project and regional level. The interim framework for assessing the Population Consequences of Disturbance (iPCoD) relies on the relationship between the disturbance experienced by an animal and how that disturbance impacts vital rates such as the probability of surviving to the next year or the chance of giving birth to a viable pup or calf. The relationships used in iPCoD were obtained from formal expert elicitation approaches (EE). The iPCoD tool has been updated with new elicitations and other improvements in recent years (including updated elicitations). Despite these model updates, the reliance on expert judgement is a source of uncertainty in assessments and risk for decision makers (as it relies on the carefully solicited judgments of experts rather than empirical datasets).

Disturbance can cause behavioural, physiological and health changes which can have subsequent effects on an individual's vital rates, such as survival and reproduction. The cost of disturbance is in most cases mediated by the state of the individual (e.g., life history stage and exposure history) and the environment that the individual is in (e.g., resource availability). By modelling health, we have an explicit scalar link between individual health, response to disturbance and the consequential population demographic effects of this disturbance. A wide range of bioenergetic models exist for marine mammal species and other taxa, and the principles behind these models are well established.

The overall objective of this project was to describe Dynamic Energy Budget (DEB) frameworks for harbour seal (*Phoca vitulina*), grey seal (*Halichoerus grypus*), bottlenose dolphin (*Tursiops truncatus*) and minke whale (*Balaenoptera acutorostrata*) (building on an existing DEB model for harbour porpoise (*Phocoena phocoena*)) to help improve marine mammal assessments for offshore renewable developments. The intention is that these models can provide new tools that can potentially be applied to project level assessments to help address potential risk to

marine mammals from offshore wind and other developments. These DEB models can also be used to generate transfer functions for use in the interim PCoD model and reduce the need for EE.

Section 3 provides background the energetics and disturbance and an introduction to DEB theory. In **Section 4** we outline the overview, design and details of DEB models – following the ODD (Overview, Design concepts, and Details) protocol of Grimm et al. (2020). **Section 5, 6, 7 and 8** describes the data used to parameterise the models for harbour seals, grey seals, bottlenose dolphins and minke whales respectively. This provides complete transparency of the main data gaps that remain as we move towards a more empirically-based framework. In each of these sections there are explorations of the simulated effects of disturbances. **Section 9** explores how we can account for uncertainty in energetics models. **Section 10** covers another important feature of assessments of disturbance – considering the movement ecology of species (which affects the probability of exposure – a key determinant of impacts). The report concludes in **Section 11**, with consideration of future developments required with respect to energetics, movement and understanding the effects of disturbance.

These new models can be added to the suite of DEB models, all based on the template developed by Hin et al. (2019), that already includes models for harbour porpoise, long-finned pilot whale (*Globicephala melas*), Cuvier's beaked whale (*Ziphius cavirostris*), Blainville's beaked whale (*Mesoplodon densirostris*), beluga whale (*Delphinapterus leucas*) and Pacific walrus (*Odobenus rosmarus divergens*). The model descriptions in this report have been structured using the ODD protocol recommended for documenting agent-based models. The models have also been calibrated using the pattern-oriented modelling (POM) approach. While this study provides new tools to move towards a more empirically-based framework to reduce this uncertainty, all models require subjective decisions in the selection of parameters and so we cannot remove all expert judgment from such processes. However, we can provide greater transparency of where the knowledge gaps are and the key sensitivities of models. Such models are yet to be used in formal assessments, but by developing the models, it adds to the suite of tools available when an energetic pathway is being considered (as is largely the case with disturbance effects). In the future, this will help understand the potential knock-on effects population demographic of disturbance, therefore, providing a more in-depth assessment of how disturbance might affect population growth rate (over a longer time periods) and highlight life history stages that are particularly vulnerable to disturbance.

We have also described how the uncertainty associated with the many model parameter values can be accounted for, and developed a novel, and potentially cost-effective, method for quantifying uncertainty associated with parameters that are not directly observable. This method can be readily applied to any of the existing DEB models developed using the Hin et al. (2019) template. DEB models can also

be used as standalone tools to assess the predicted effects of disturbance, and resulting foraging disruption, at an individual level (unless a population level version is available). We investigated the effects of disturbance on vital rates for harbour seals, grey seals, bottlenose dolphins and minke whales (**Sections 5.3, 6.3, 7.3** and **8.3**). Grey seals appear to be more vulnerable to the effects of disturbance than the other three species, but these results should be treated with caution because only a relatively small set of plausible model parameter values was used in the simulations for the other three species.

We have demonstrated in **Section 9.3** how the DEB models developed for this study and the harbour porpoise DEB model are capable of generating the relationships required to replace the transfer functions in iPCoD. The current transfer functions established the relationship between days of disturbance experienced and their effect on vital rates and were derived using formal EE approaches. It is critical to stress that, whilst it is possible, the DEB derived results will still be based on two key sets of assumptions. The first is that the DEB models (as outlined above) rely on a number of parameters sourced from across the marine mammal and energetics literature. This is true of many models for any taxa, but it cannot be overlooked. The second is that, in order to generate empirically derived transfer functions (to replace the EE-derived ones in iPCoD), it is necessary to specify an appropriate effect of disturbance (i.e., the number of hours without foraging on each day of disturbance). This is still a poorly understood field, but any new DEB-derived transfer functions (and how similar or different they are to the EE-derived functions) will be heavily dependent on the hours of lost foraging specified (N.B. 6 hours was used in **Section 9.3**). This will need to be carefully considered when replacing EE transfer functions into iPCoD.

Beyond the integration of DEB-derived transfer functions into iPCoD, future research should involve exploring the use of movement models to more accurately estimate the probability of exposure (which remains a key sensitivity in population assessments). Additionally, the DEB models themselves can be updated and improved in the future and further bioenergetic and physiological research is funded to improve how these pathways are modelled.

These could include improved understanding of Field Metabolic Rates (FMR) (and how it varies with life stage, time of year and activity) and the ontogenetic development of foraging efficiency in calves, pups and juveniles. Furthermore, increased knowledge on how the prey environment changes (environmental stochasticity); individual variation in the parameters that determine growth, feeding efficiency; and the body condition (energy reserve) thresholds for reproduction and mortality are very important.

Understanding the effects of disturbance in terms of lost foraging remains critical to energetic models and their integration into population models like iPCoD.

Contents

Figures

Tables

2 Introduction

The offshore wind industry in the process of a significant expansion with a move towards clean energy and a green economic recovery. The sustainable expansion of offshore wind requires a robust understanding the impacts of construction and operation and appropriate levels of conservatism and realism in assessments. The potential risk of injury and/or disturbance to marine mammals during construction of offshore renewable energy developments (e.g., pile driving, removal of unexploded ordnance, increased vessel presence offshore) has been identified as a key consenting risk for projects in UK waters. Possible consequences of exposure to underwater noise include; disturbance that could cause marine mammals to either move away or change behaviour (which could result in reduced net energy intake) or suffer temporary and permanent hearing damage.

The scale of offshore wind farm developments means there is the potential for significant cumulative impacts on marine mammals, which would need to be considered and mitigated at a project and regional level. The interim framework for assessing the Population Consequences of Disturbance (PCoD) was released in 2014 (Harwood et al. 2014, King et al. 2015). The iPCoD model relies on relationships between disturbance experienced by an animal and how that disturbance impacts vital rates like the probability of surviving to the next year or the chance of giving birth to a viable pup or calf. The relationships used in iPCoD were obtained from expert elicitations. In these elicitations, experts are asked to estimate the number of days of disturbance an animal can tolerate before a vital rate is affected, and the number of days of disturbance required to cause the maximum effect of disturbance in order to parameterize the transfer function required. The iPCoD tool has been updated with new elicitations and other improvement in recent years (including updated elicitations) (e.g., Booth and Heinis 2018, Booth et al. 2019). This resulted in version 5 of the iPCoD code which is publicly available – this tool is currently being integrated into the Cumulative Effects Framework. Despite these model updates, the reliance on expert judgement is a source of uncertainty in assessments and risk for decision makers (as it relies on the carefully solicited judgments of experts rather than empirical datasets).

The overall objective of this project is to describe Dynamic Energy Budget (DEB) frameworks for harbour seal (*Phoca vitulina*), grey seal (*Halichoerus grypus*), bottlenose dolphin (*Tursiops truncatus*) and minke whale (*Balaenoptera acutorostrata*) to help improve marine mammal assessments for offshore renewable developments. The aim is to produce final models for these species, to go along with the harbour porpoise DEB model (Harwood et al. 2020) that can be applied to project level assessments to help address potential risk to marine mammals from offshore wind and other developments.

This study provides new tools to move towards a more empirically-based framework to reduce this uncertainty. Of course, all models require subjective decisions in the selection of parameters and so we cannot remove all expert judgment from such processes. But we can provide greater transparency of where the knowledge gaps are and the key sensitivities of models. Such models are yet to be used in formal assessments, but by developing the models, it adds to the suite of tools available when an energetic pathway is being considered (as is largely the case with disturbance effects). In the future, this will help understand the potential knock-on effects population demographic of disturbance, therefore providing a more in-depth assessment of how disturbance might affect population growth rate (over a longer time periods) and highlight life history stages that are particularly vulnerable to disturbance.

2.1 Document Structure

Section 3 provides background the energetics and disturbance and an introduction to DEB theory. In **Section 4** we outline the overview, design and details of DEB models – following the ODD (Overview, Design concepts, and Details) protocol of Grimm et al. (2020). **Section 5, 6, 7 and 8** describes the data used to parameterise the models for harbour seals, grey seals, bottlenose dolphins and minke whales respectively. This provides complete transparency of the main data gaps that remain as we move towards a more empirically-based framework. In each of those sections there are explorations of the simulated effects of disturbances. **Section 9** explores how we can account for uncertainty in energetics models. **Section 10** covers another important feature of assessments of disturbance – considering the movement ecology of species (which affects the probability of exposure – a key determinant of impacts). The report concludes in **Section 11**, with consideration of future developments required with respect to energetics, movement and understanding the effects of disturbance.

3 Background

Disturbance can cause behavioural, physiological and health changes which can have subsequent effects on an individual's vital rates, such as survival and reproduction. The cost of disturbance is in most cases mediated by the state of the individual (e.g., life history stage, exposure history), and the environment that the individual is in (e.g., resource availability). By modelling health, we have an explicit scalar link between individual health, response to disturbance, and the consequential population demographic effects of this disturbance (Pirotta et al. 2018a). To date, many PCoD studies have used only changes in an individual's energy stores (e.g., body condition) as a proxy metric of health (Schick et al. 2013, Nabe-Nielsen et al. 2014, New et al. 2014, Villegas-Amtmann et al. 2015, McHuron et al. 2017, Villegas-Amtmann et al. 2017, Nabe-Nielsen et al. 2018, Pirotta et al. 2018b). To build on this, bioenergetics models also consider the variance in energetic demands on an individual and their associated behavioural and physiological state during different

life history stages and take into account the state of the environment the individual is in (e.g., resource density, presence of predators). The role of energy reserves in different reproductive strategies can be thought of as being on a theoretical spectrum relating to how reproduction is fuelled. This spectrum runs between relying solely on capital reserves accrued through the preceding year (capital breeding) through to exclusive reliance on increasing energy intake to cover the increased costs reproduction (income breeding). As with other taxa, marine mammals show a variety of life history patterns, between the 'capital breeding' end of the reproductive spectrum (e.g., minke whale, grey seal) through to the 'income breeding' end (e.g., harbour porpoise, bottlenose dolphin, harbour seal). The choice of reproductive strategy can have a great impact on the energetic consequences of disturbance, varying each individual's vulnerability to disturbance based on both its reproductive strategy and stage. Accounting for life history stage and the associated energetic demands in PCoD models means the model can account for how these demands might affect the individual's response to disturbance. An example of variation in disturbance response based on context would be that a lactating female in a resource poor environment would likely respond very differently to a non-lactating female in a resource-rich environment (Hin et al. 2019).

Bioenergetic models have been used to infer changes in an individual's energy stores with behavioural state or as a consequence of disturbance (see Table 1 for a comprehensive list of examples), and have been widely used to investigate potential impacts of disturbance (both natural and anthropogenic) on marine mammals at both individual and population level (see Pirotta et al. 2018a for a review). However, many bioenergetic models assess the effects of disturbance on marine mammals by focusing on a single reproductive cycle of a female's life history (Braithwaite et al. 2015, Christiansen and Lusseau 2015, Villegas-Amtmann et al. 2015, McHuron et al. 2016, Pirotta et al. 2018c). For an in-depth assessment of how disturbance might affect population growth rate over a longer period, it is necessary to model female energetics over the entire lifespan in order to highlight life history stages that are particularly vulnerable to disturbance (Villegas-Amtmann et al. 2017, McHuron et al. 2018, Pirotta et al. 2018a). Hin et al. (2019) used the DEB model presented by De Roos et al. (2009) as a baseline model to simulate the life history of a female pilot whale from weaning age onwards (including during pregnancy and lactation), and for a calf from birth until weaning. Incorporation of this DEB model into a PCoD framework allowed the authors to predict how vulnerability to different disturbances varied with resource availability and life history stage.

3.1 An introduction to DEB models

DEB theory (Nisbet et al. 2000, Kooijman 2010) provides a mechanistic framework that predicts the consequences of an organism's acquisition of environmental resources for energy demanding traits, such as growth and reproduction, via internal physiological functions. DEB models employ a set of differential or difference equations and parameters that are based on unifying metabolic theory and can theoretically be used to model any species. These equations describe the life history processes of a cohort of organisms, based on energy fluxes. Resources assimilated from the environment are allocated to maintenance, growth and reproduction via a reserve compartment. In the standard DEB model, both structure and reserves contribute to total biomass, but only structure requires maintenance, and all metabolic processes are fuelled from reserves. These two state variables (structure and reserves) can be difficult to measure directly in many species, but they can be linked to more easily observable traits such as body size or age at first reproduction.

3.1.1 DEB models for marine mammals

In many marine mammal species, subcutaneous blubber appears to act as their main energy reserve. The size of this reserve can be estimated directly from dead animals by dissecting out the tissue and weighing it (e.g., Worthy and Lavigne 1987). It can be estimated indirectly using hydrogen isotope dilution techniques (e.g., Costa et al. 1986), although this technique provides an estimate of total body lipid, rather than just blubber. However, blubber performs a number of other functions in marine mammals: it insulates; adjusts buoyancy; defines body shape and streamlines; and acts as a spring (Koopman 2007). In addition, the blubber of beaked whales and sperm whales is largely composed of waxy esters, which are much more difficult to catabolise than the fatty acids that are the main component of most other species' blubber. As a result, individual marine mammals may not be able to use all of the lipid stored in blubber as an energy reserve without compromising their survival.

The most detailed information on the way in which marine mammals manage their energy reserves comes from studies of fasting seals. Although >90% of the energy required by fasting northern elephant seal (*Mirounga angustirostris*), harp seal (*Pagophilus groenlandicus*) and grey seal pups comes from the catabolism of lipids (Worthy and Lavigne 1987, Noren et al. 2003, Bennett et al. 2007), they also obtain energy from the catabolism of lean body tissue. In fact, the decrease in their lean body mass may actually exceed the decrease in the size of their lipid reserves, because lean tissue is mostly comprised of water (Noren et al. 2003). Blubber may be preferentially mobilized if ambient water temperature increases, thus reducing the need for extra insulation (e.g., as documented in fasting harbour seal pups by Muelbert and Bowen 1993). Similarly, lactating females may preferentially catabolize blubber lipids to provide the energy and raw materials for milk production (Costa et al. 1986).

To date, a range of DEB models for marine mammals have been published (either in peer-review or grey literature) and more are currently in development. Klanjscek et al. (2007) developed a DEB model for right whales (*Eubalaena* spp.). Although their primary concern, as noted above, was to understand the factors that might affect the bioaccumulation of lipophilic toxicants, the same model structure could be used to investigate the effects of disturbance that reduced daily energy intake on reproduction and calf survival. Goedegebuure et al. (2018) developed a DEB model for southern elephant seals (*Mirounga leonina*) and used it to examine the potential effects of changes in resource availability on breeding success and juvenile survival.

Hin et al. (2019) developed a DEB model for North Atlantic long-finned pilot whales (*Globicephala melas*), which they used to investigate the effects of disturbance that resulted in reduced energy intake on lifetime reproductive success (i.e., fitness). A subsequent manuscript (Hin et al. 2021) expands this model to consider the effect of density dependence. Hin et al. (2019) found that the calves of females breeding for the first time were particularly sensitive to disturbance, but that all calves – and even lactating females – were at risk as the duration of disturbance increased. Moretti (2019) adapted Hin et al.'s model for Blainville's beaked whale (*Mesoplodon densirostris*) and used this model to investigate the potential population consequences of changes in foraging behaviour resulting from exposure to navy sonars. In addition, outputs from DEB models developed for harbour porpoise and Pacific walrus (*Odobenus rosmarus*) have been used to inform expert elicitations for these species (Booth et al. 2019, Harwood et al. 2019). This model framework has been adapted for a model for harbour porpoise (Harwood et al. 2020) and this report summarises the development of similarly structured DEB models for grey seal, harbour seal, bottlenose dolphin and minke whale.

4 Overview, design and details of DEB models for iPCoD

Below we present a generic description of the DEB models used in this report following the ODD protocol (Grimm et al. 2020), which was developed for describing agent-based models. The sub-models developed for each species are described in later sections.

4.1 Purpose and patterns

The purpose of the models is to explore the link between disturbance and population vital rates for five UK species of marine mammal (harbour porpoise, bottlenose dolphin, harbour seal, grey seal and minke whale), particularly in the context of offshore renewable developments. The models use the same approach as a previously published dynamic energy budget model for harbour porpoise (Harwood et al. 2020). The approach is based on first principles and explicitly accounts for the ways in which the energy budget of each individual varies, depending on its age, size, life history stage, and the environment it encounters (i.e., resource availability). Table 1 provides an overview of the variables considered in the models.

Table 1. state variables and deduced state variable (calculated using other state variables) of the modelled individuals.

Variable	Code	Unit	Description
For all individuals			
a	age	days	Age
L	L	cm	Structural length
S	Sa	kg	Structural (core) mass
F	F	kg	Reserve mass
W	W	kg	Total body mass (S + F)
	GR	kg/day	Daily growth rate (derived from S)
ρ	rho	-	Relative body condition (F/W)
	life_expectancy	days	Life expectancy derived from cumulative survival curve
I	Ir	MJ/day	Assimilated energy
C_M	Cm	MJ/day	Field metabolic costs
For pregnant or lactating females and their offspring			
life history stage	-	-	One of four: resting, pregnant, lactating and pregnant & lactating
$F_{neonate}$	F_preg, skipping_point	kg	Threshold for starting or continuing pregnancy
S_{foetus}	S_foetus	kg	Foetus size
GR_{foetus}	GR_foetus	kg/day	Growth rate of foetus
IM_C	Im_C	MJ/day	Calf/pup assimilated energy from milk
I_C	Ir_C	MJ/day	Calf/pup assimilated energy from prey
C_L	CLact	MJ/day	Daily cost of lactation
CM_C	Cm_C	MJ/day	Field metabolic costs for calf/pup

To evaluate if the model simulations appear to be realistic, model outputs were compared to published and grey empirical datasets using the pattern-oriented modelling approach: seasonal changes in body condition, weight and assimilated energy of females and their offspring; calf/pup survival; and birth rate (proportion of reproductively mature females giving birth each year).

4.2 Entities, state variables, and scales

The model is a non-spatially explicit and is composed of one kind of entity: individuals of the modelled species. It follows individual females from an initial age (age_day1) until their death, the time of which is determined at the beginning of each simulation. Their offspring are followed from embryonic implantation up to age_day1 (described further see Table 2). The model proceeds in discrete time steps of 1 day, and each year consists of 365 days.

Individuals are characterised by the following state variable: age, length, structural (core) mass, reserve mass, and energy assimilation. These vary over time depending on an individual's life history stage and the resource densities it encounters.

Females can be in one of four life history stages: 'resting' (i.e., neither pregnant nor lactating, this includes the juvenile period from weaning to first conception); 'pregnant (but not lactating)'; 'lactating (but not pregnant)'; and 'lactating & pregnant'.

4.3 Process overview and scheduling

Figure 1 provides a flow chart outlining the model processes. We describe it further below. An individual's assimilated energy varies with resource density, its body condition, structural mass and life history stage. Pregnancy begins on the day on which the embryo implants, which is determined by the day of the year on which the simulated individual was born. Foetal mass is included in maternal structural mass for the calculation of metabolic and growth costs. At any point in the pregnancy (the "decision day",–see - Section 4.4.12), a female can abort the foetus if her reserves are too low. A calf/pup depends entirely on milk provided by its mother until a specified day of lactation (T_N,–see - Section 4.4.12). Calf/pup demand for milk depends on its body condition and age. The amount of milk provided by the female depends not only on calf/pup demand but also on her body condition. Females abandon lactation if their relative body condition is close to the starvation threshold. At a specified point during the lactation period, the calf/pup starts foraging on its own and its foraging efficiency increases with age. Grey seal and harbour seal pups fast for a period after weaning, and their foraging efficiency is set to zero during this time.

If assimilated energy on a particular day exceeds the combined costs of metabolism, growth and reproduction, the surplus energy is converted to reserves tissue. Otherwise, individual females give priority to lactation. If lactation costs can be met from assimilated energy, a predefined proportion of the remaining assimilated energy is assigned to growth (including growth of the foetus if any). If this is less than the energy required for growth, the growth rate of the female and her foetus is reduced accordingly. The remaining balance of the energy intake is allocated to metabolism. Any unfulfilled energetic costs of lactation and metabolism are met by catabolism of reserve tissue. If the relative body condition of an individual falls below the starvation threshold (ρ_S - Section 4.4.12), they have an increased chance of death.

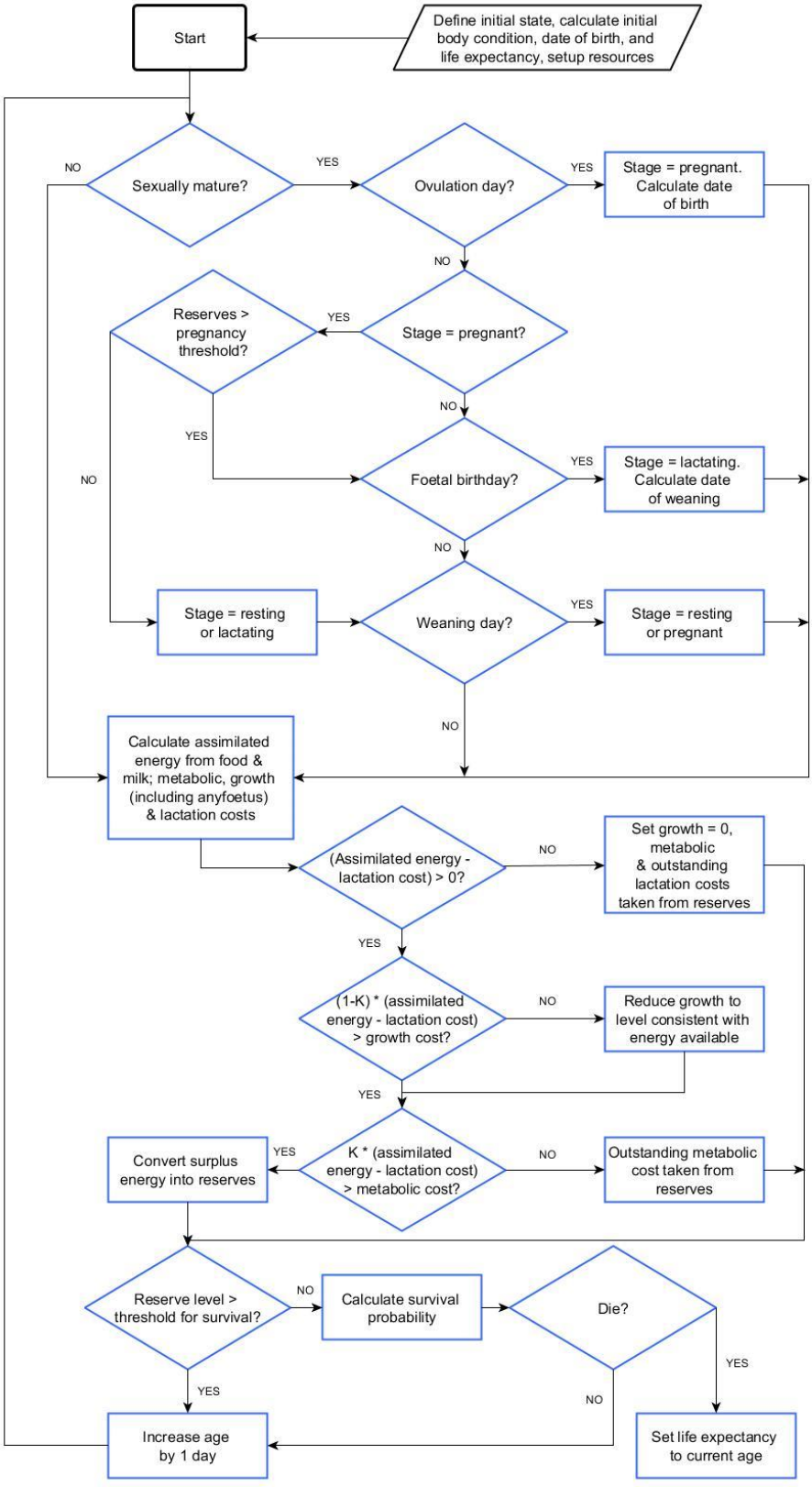

Figure 1. Flow diagram describing the details of the model. The same set of processes is applied to females and their offspring, but calves/pups are only followed to an age equivalent to the minimum inter-birth interval. Parallelograms indicate model inputs and rectangles indicate calculations or changes of life history stage. Females also change life history stage if their foetus or calf/pup dies but these

changes are not illustrated here. A detailed account of all elements of this flow diagram can be found in the submodel descriptions.

4.4 Design concepts

4.4.1 Basic principles

This model follows the approach developed by (Hin et al. 2010) for long-finned pilot whales, which uses the basic principles of DEB theory (Kooijman 2010). The model tracks the way in which individual female marine mammals assimilate energy over the course of their lives from age_day1 to death, and how this energy is allocated to field metabolism, growth, foetal development and lactation. If assimilated energy on a particular day exceeds the energy required for these activities, the surplus energy is stored in a reserve compartment (De Roos et al. 2009, Kooijman 2010)(De Roos et al., 2009; Kooijman, 2010), primarily – but not exclusi–ely - as fat tissue around internal organs and as blubber. If energy expenditure exceeds energy assimilation, the balance is provided by catabolizing tissue from this reserve compartment. The model also tracks these energy fluxes up to age_day1 for every calf/pup that a female produces.

4.4.2 Emergence

Although individual life-history traits such as growth, non-resource driven survivorship, and maturation time are imposed, others emerge from rules of metabolic organization and are driven by the influence of seasonal differences in resource density and energy balance.

The use of a maximum probability for successful fertilization/implantation above a specified age imposes a cap on the annual birth rate. However, the actual number of pups/calves born and the actual age at first reproduction emerge from the current physiological state (body condition) of females. Age-related and seasonal fluctuations in body condition emerge from variations in the resource density experienced by individuals and seasonal changes in energy demand. Body condition then influences the individual's probability of reproducing or dying. In this way, it is possible to use the lifetime reproductive output of each simulated female to examine the population consequences of different conditions (including a changing environment and/or the effects of disturbance).

4.4.3 Objectives

Animals attempt to maximize their fitness by allocating available energy to different life history processes in order of necessity. If processes necessary to survival are not covered by energy intake, stored energy will be used to cover them. As storage levels decrease, the animal has an increasing probability of dying.

4.4.4 Prediction

Females can predict whether they can successfully continue with pregnancy using proxies of their current body condition.

4.4.5 Sensing

Individuals can sense their storage levels and make decisions specific to their current body condition and life history stage, e.g., abort foetus or use energy converted from stores.

4.4.6 Interaction

The only interactions between individuals in the model are between mother and offspring. The foetus and calf/pup are linked to their mother via energy and mass transfer.

4.4.7 Stochasticity

The following processes can be stochastic: life expectancy of females, their foetuses and pups/calves; successful fertilization/implantation; dates relating to reproduction (e.g., calving/pupping date); deaths due to starvation (see Section 4.4.19 for further details); and the resource density that an individual encounters on a particular day.

4.4.8 Collectives

Collective behaviour is not modelled.

4.4.9 Observation

The values of all state variables for each individual are recorded daily. For model output corroboration, the following variables and follow-up calculations were used: length, structural mass, reserves and body condition, assimilated energy, cause of death, proportion of adult females breeding each year, calf/pup survival till age1 (reproductive success), inter-birth intervals, and population growth rate.

4.4.10 Initialization

The model is initialised by creating a number of individuals defined by the user (*sim_number*), all of which have the same initial age (*age_day1*) and body condition ρ_{start} (Table 2). Initial body condition is determined iteratively from the mean condition of simulated calves/pups at *age_day1*. Initial reserve level (F_{start}) is then calculated as:

$$F_{start} = \frac{\rho_{start} * S_{start}}{(1 - \rho_{start})}$$

where S_{start} is the female's structural mass at *age_day1* derived from the growth curve.

Table 2. Initial body condition (ρstart) and age for the modelled species.

Species	ρ_{start}	Initial age
Harbour seal	0.20	1 year
Grey seal	0.22	1 year
Bottlenose dolphin	0.2	3 years
Minke whale	0.28	1 year

Life expectancy of each individual at *age_day1* is determined by sampling from a cumulative survival curve.

4.4.11 Input data

The time series of resource densities that will be encountered by an individual during its lifetime is created at the beginning of each simulation.

4.4.12 Submodels

The original model is cast as a set of differential equations (Table 1 in Hin et al. (2019)), which we have converted to difference equations. Throughout, we use the parameter symbols and names from Table 1 and Supplementary Information 1 (S1) in Hin et al. (2019).

Table 3. Description of parameters used in the model. for all the equations refer to Hin et al. (2019).

Variable, parameter	Code	Units	Description
Resource density			
R	Rmean		Annual mean resource density
a_{beta}	a_beta	-	Shape parameters of beta distribution defining stochasticity in resource density
b_{beta}	b_beta	-	
	amplitude	-	Parameter defining the amplitude of seasonal variation in resource density
	offset	-	Parameter determining when during the year *Rmean* has its maximum value

Variable, parameter	Code	Units	Description
Timing of life history events			
min_age	min_age	years	Minimum age for reproduction
mean_birthday	mean_birthday		Mean date on which calves/pups are born
T_P	Tp	days	Gestation period
T_L	Tl	days	Age at weaning (duration of lactation)
T_R	Tr	days	Age at which calf's resource foraging efficiency is 50%
max_age	max_age	years	Maximum age
	max_age_calf	days	Maximum modelled age of calf/pup
moult_duration	moult_duration	days	Duration of moult (seals only)
Reserves			
ρ	rho	–	Target body condition for adults
ρ_c	rho_C	–	Target body condition for calves/pups
θ_F	Theta_F		Relative cost of maintaining reserves
Growth			
L_0	L0	cm	Length at birth
L_∞	Linf	cm	Female maximum length
k	K	1/days	Von Bertalanffy growth function: growth rate parameter
X_0	x0	days	Von Bertalanffy growth function: length at age zero
ω_1	omega1	kg/cm	Structural mass-length scaling constant
ω_2	omega2	–	Structural mass-length scaling exponent
Energetic rates			
σ_M	Sigma_M	–	Field metabolic maintenance scalar
σ_G	Sigma_G	MJ/kg	Energetic cost per unit structural mass

Variable, parameter	Code	Units	Description
ε	epsi	MJ/kg	Energy density of reserve tissue
ε-	epsi_minus	MJ/kg	Catabolic efficiency of reserve conversion
ε+	epsi_plus	MJ/kg	Anabolic efficiency of reserve conversion
ε_{+pups}	epsi_plus_pups	MJ/kg	Anabolic efficiency of reserve conversion for pups
η	eta	–	Steepness of assimilation response
ϒ	upsilon	–	Shape parameter for effect of age on resource foraging efficiency
K	Kappa	–	Proportion of the daily assimilated energy allocated to growth
	moult_reduction	–	Reduction in resource assimilation during moult (seals only)
	moult_duration	–	Duration of the moult period (seals onlu)
Pregnancy			
fert_success	fert_success		Probability that implantation will occur
decision_day	decision_day	days of gestation	Day of pregnancy when female decides whether or not to continue
$F_{neonate}$	F_preg	kg	Reserve threshold for continuing pregnancy (cetaceans)
Lactation			
φ_L	phi_L	–	Lactation scalar
σ_L	Sigma_L	–	Efficiency of conversion of mother's reserves to calf/pup tissue
T_N	Tn	days	Calf/pup age at which female begins to reduce milk supply
ξc	xi_c		Non-linearity in milk assimilation-calf age relation

Variable, parameter	Code	Units	Description
	lact_feed	days	Day of lactation when female starts foraging (harbour seals only)
	R_prop_lactation	–	Proportion of time female spends foraging during lactation (harbour seals only)
ξ_M	xi_m	–	Non-linearity in female body condition-milk provisioning relation
	pw_fast	days	Duration of calf/pup's post-weaning fast (seals only)
Mortality			
foetal_mortality	foetal_mortality		Background foetal mortality rate
α_1	alpha1	–	Coefficients of age-dependant mortality curve
α_2	alpha2	–	
β_1	beta1	–	
β_2	beta2	–	
ρ_S	rho_s	–	Starvation body condition threshold
μ_s	mu_s	–	Starvation mortality scalar
Disturbance			
$Dist_{dur}$	days.of.disturbance	days	Number of days on which disturbance occurs
$Dist_{start}$	first_day	day of year	First day of disturbance period
$Dist_{end}$	Last_day	day of year	Last day of disturbance period
$Dist_{effect}$	disturbance.effect	-	Reduction in resource density caused by disturbance
Age_{Dist}	age.affected	years	Age class that will be affected by the disturbance

4.4.13 Resource

Resource density (*R*) To avoid having to account for differences among prey in energy density, catchability, and digestibility, and differences among individuals in their ability to assimilate energy, the model of Hin et al. (2019) characterises the resources on which a species feeds in terms of the amount of assimilated energy they can provide to a female. Although it would be virtually impossible to measure resource density defined in this way, *R* provides a useful quantitative index of environmental quality, with high resource density indicating high quality environments, and low resource density associated with poor environments. Seasonal variation in *R* is modelled using a sine function, following Hin et al. (2019).

R is the most important determinant of lifetime reproductive success (the number of female offspring raised to age_day1 in a female's lifetime). It is therefore possible to choose an appropriate value for *R* based on what is known about the status of the population being modelled. For example, if the population is stable, *R* can be tuned so that lifetime reproductive success is 1.0.

Resource density can be deterministic or stochastic. In the latter case, *R* for each day is multiplied by a random number drawn from beta distribution with mean 1. An example showing the differences between fixed and stochastic *R* is given in Figure 2.

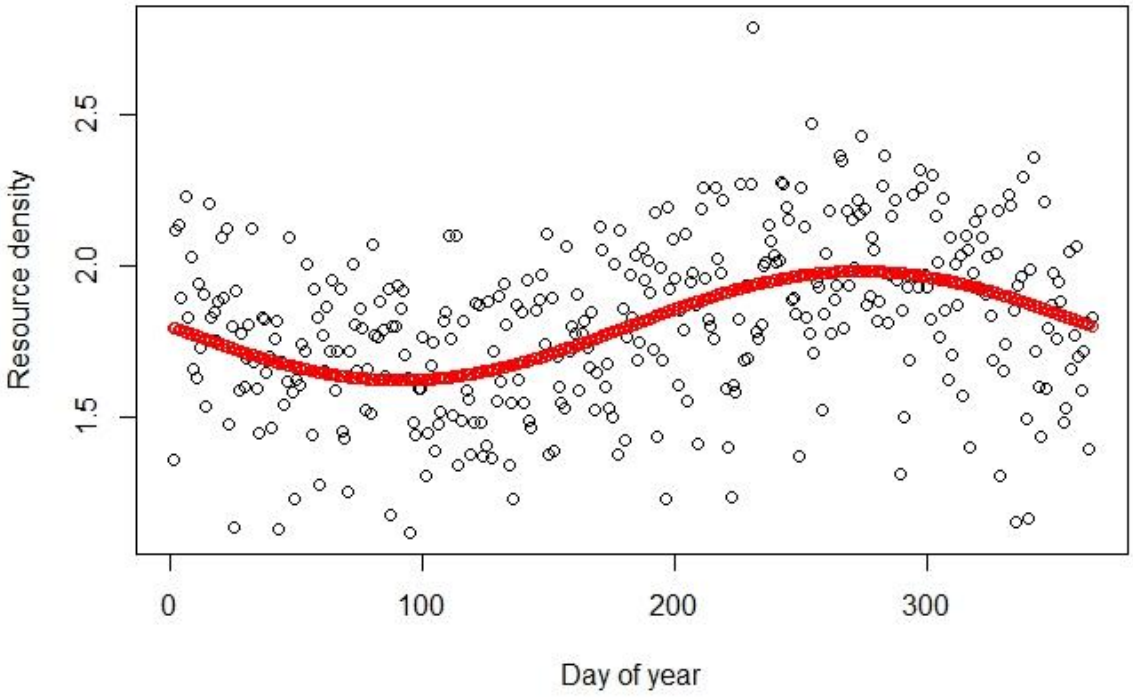

Figure 2. Example of changes in resource density over 1 year modelled deterministically (red) and stochastically (black).

4.4.14 Timing of life history events

Gestation period (T_P) This is usually estimated from a combination of estimates of foetal growth rate and mean length at birth, using the assumption that foetal growth in length is approximately linear (Perrin and Reilly 1984).

Lactation period/age at weaning (T_L) Perrin and Reilly (1984) provide a review of the methods used to determine lactation period and age at weaning. These include estimates of the ratio of lactating to pregnant animals in a sample of mature females, estimates of the age of the largest calf observed associating with a female, stomach content analysis, and behavioural observations.

4.4.15 Reserves and growth

Reserve thresholds (ρ, ρ_S) In the Hin et al. (2019) model the rate of energy assimilation on a particular day is affected by an individual's current body condition (ρt) relative to the **target body condition** (ρ). It is tempting to simply set ρ to the maximum recorded blubber: total body mass ratio for a particular species. However, captive harbour porpoises show strong seasonal variations in blubber thickness and total mass (Lockyer et al. 2003, Kastelein et al. 2019), which are closely correlated with water temperature and probably reflect a requirement for less insulation in summer. This suggests that in some species ρ may vary seasonally and that blubber mass cannot always be equated with reserve mass.

Relative cost of maintaining reserves (Θ_F) According to DEB theory, reserve mass does not require any maintenance (i.e., $\Theta_F = 0$). However, the large lipid reserves maintained by most marine mammal species probably do incur additional costs in terms of drag and buoyancy. Hin et al. (2019) set Θ_F to 0.2 in order to account for these costs.

Structural length and structural mass ($K, L_0, L_\infty, \omega_1, \omega_2, k, x_o,$) Most marine mammal DEB models have used a von Bertalanffy growth curve to describe changes in L_0 with age, and then converted length to mass using a simple power function (e.g., $S_a = \omega_1 . L_a^{\omega 2}$). However, there is no requirement to use this approach, and any empirically derived relationship between weight and age can be used in the model.

4.4.16 Energetic rates

Field metabolic maintenance scalar (σ_M) The Hin et al. (2019) model assumed that an individual's Field Metabolic Rate (FMR) is a simple multiple σ_M of the Resting Metabolic Rate (RMR) predicted by the Kleiber (1975) relationship (i.e., $K.M_t^{0.75}$, where K = 0.294 MJ/kg/day). Estimates of σ_M can be obtained from respirometry studies of captive animals (e.g., Sparling et al. 2006, Worthy and Lavigne 1987), or they may simply be assumed. For example, Hin et al. (2019) used a value of 0.75 for

$\sigma_{M}.K$ based on the assumption that the FMR for pilot whales is 2.5x their RMR (Lockyer, 1993).

Energetic cost per unit structural mass (σ_G) This is the amount of energy required to produce 1 kg of tissue (i.e., the energetic content of the new tissue and the energetic overheads required to produce it). Hin et al. (2019) obtained an indirect estimate of σ_G = 30 MJ/kg from Brody's (1968) formula for the heat of gestation and Lockyer's (1993, 2007) estimate of the energy density of pilot whale calf tissue. However, direct measurements of this cost can also be obtained from captive animals (e.g., Noren et al. 2014 for Pacific walrus).

Catabolic efficiency of reserve conversion (ε-) This is the amount of energy produced by metabolising 1 kg of reserve tissue. It can be calculated from measurements of the changes in mass of fasting animals and estimates of their metabolic requirements during that fast (Bennett et al. 2007, Muelbert and Bowen 1993).

Anabolic efficiency of reserve conversion (ε+) This is the amount of energy required to produce 1 kg of reserve tissue. Since anabolism is likely to be less efficient than catabolism, Hin et al. (2019) used a value for ε+ that was ~40% higher than ε-. However, it may be possible to estimate this parameter from measurements of the amount of additional food consumed by captive animals that have experienced fasting. For example, Kastelein (2019) report that fasted, captive harbour porpoises recovered their original body weight within 2 days when they were offered twice the normal amount of food on those days. Estimates of the actual amount of additional energy consumed by these animals could be used to calculate ε+.

Steepness of assimilation response (η) The amount of assimilated energy obtained from feeding each day depends on the resource density, the structural size of the animal to the power 2/3 following Kooijman (2010), and the individual's body condition (ρt). Individuals are assumed to assimilate energy at half of the maximum possible rate when their body condition is at the target body condition (ρ) and to increase their energy assimilation progressively if their body condition is reduced below the target value. This relationship also allows animals to compensate for the effect of lost foraging opportunities on their body condition by increasing energy assimilation on subsequent days, provided sufficient resources are available. Energy assimilation (I_t) on day t is described by:

$$I_t = \frac{R.S_t^{2/3}}{1 + e^{-\eta(\frac{\rho}{\rho t} - 1)}}$$

Figure 3 shows the effect of body condition relative to the target value ($\frac{\rho t}{\rho}$) and η on energy assimilation with η ranging from 5 to 25. The value of 15 used by Hin et al. (2019) is shown in bold. With higher values of η, energy assimilation is close to its maximum level over a wide range of value for ρt. Lower values of η result in a wider

range of variation in energy assimilation with ρt. Information on how quickly fasting individuals that are in good condition recover the weight lost during the fast (e.g., Kastelein et al. 2019) could provide guidance as to a suitable value for η.

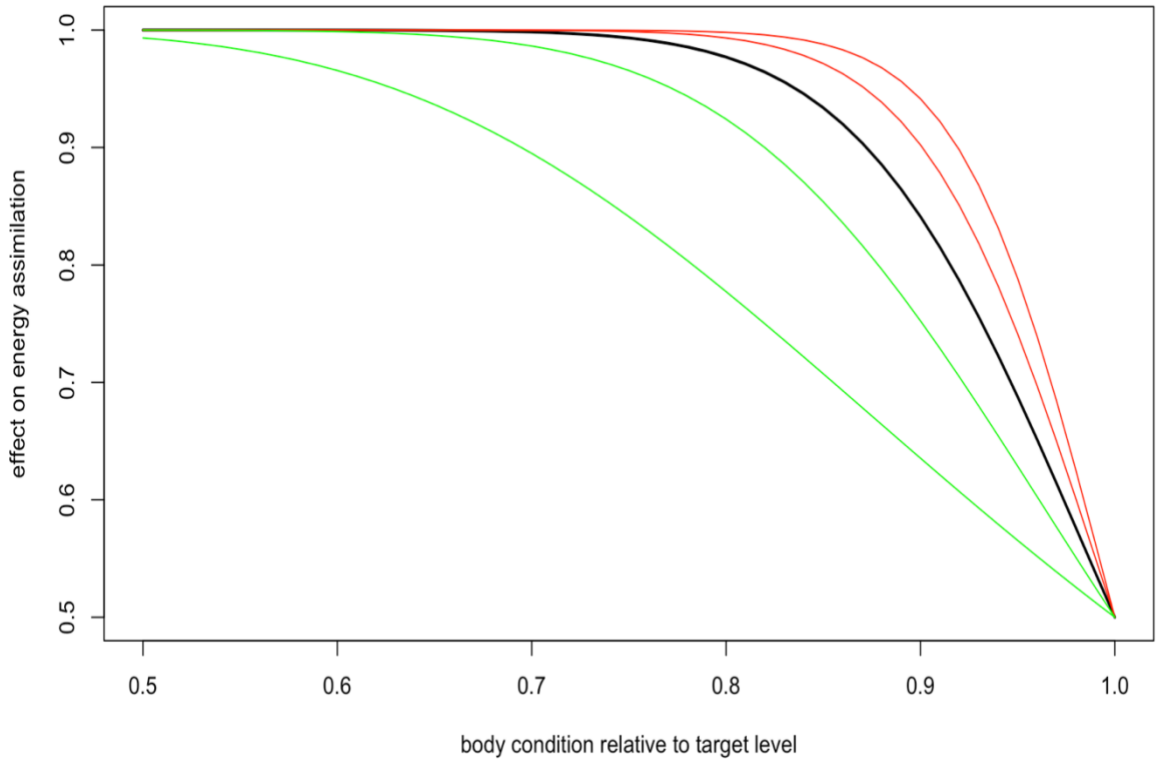

Figure 3. The effect of body condition relative to the target level ($\frac{\rho t}{\rho}$) and the steepness of the assimilation response (η) on energy assimilation as a proportion of its maximum rate. The relationship for η = 15 is shown in solid black. Curves in green are for values of η = 5 and 10; curves in red are for values of η = 20 and 25.

Effect of age on resource foraging efficiency (*Y*, $T_{R,}$ *pw_fast*): These parameters take account of the fact that newly-weaned pups/calves will not be 100% efficient at foraging and that, for species with long lactation periods, calves may begin feeding during lactation. In addition, harbour and grey seal pups undertake a post-weaning fast, whose duration is set by the parameter *pw_fast*. The shape of the feeding efficiency relationship is controlled by $T_{R,}$ the age at which a calf/pup achieves a foraging efficiency that is 50% of an adult, and a shape parameter (γ) that determines how rapidly foraging efficiency approaches 100%. Figure 4 shows the effects of different values of γ on the shape of the function determining foraging efficiency. The value of γ = 3 used by Hin et al. (2019) is shown in bold. As an example, if T_R is 1 year, the function predicts that 100% foraging efficiency would be achieved by age 5. Lower values of γ result in higher ages for 100% efficiency and higher values of γ result in lower ages for 100% efficiency. Although it may be

possible to determine when pups/calves begin feeding independently from an examination of stomach contents (e.g., Figure 3 in Muelbert and Bowen 1993), direct estimation of these parameters is unlikely to be feasible. However, it will affect post-weaning survival and age at first reproduction. Independent information on current values for these demographic characteristics can therefore provide insights into the feasible range for this parameter.

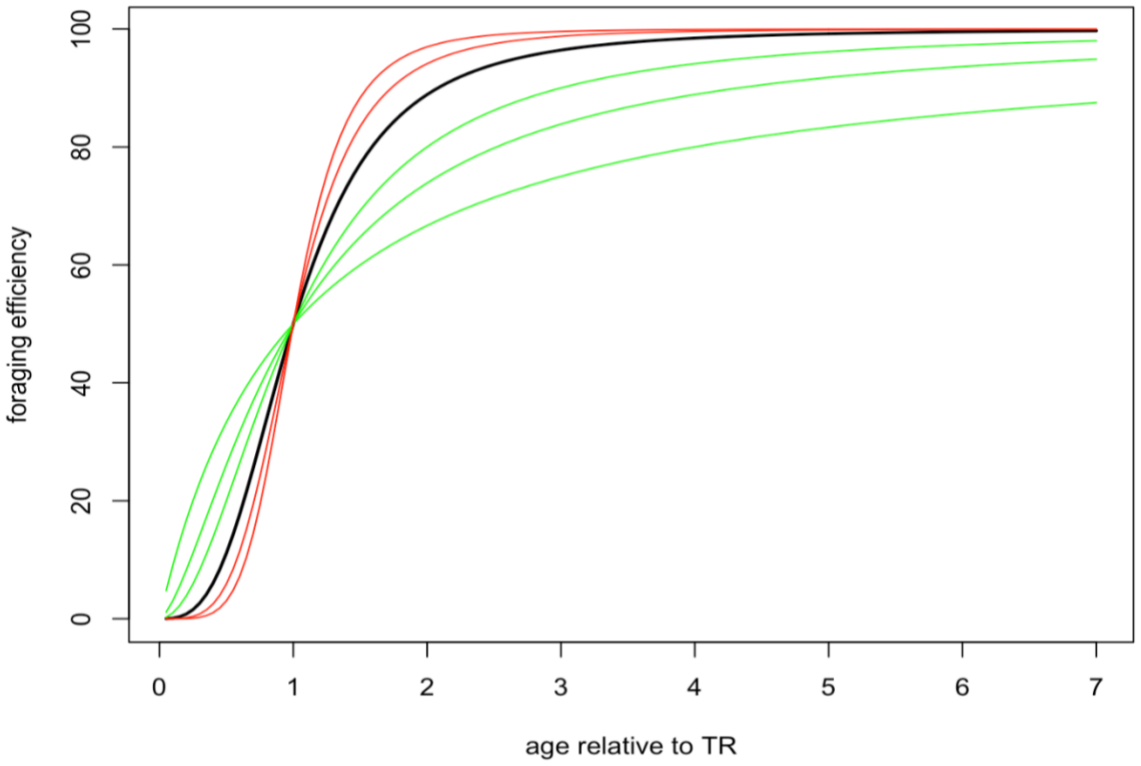

Figure 4. The effect of the shape parameter γ on the relationship between foraging efficiency and age (shown as a multiple of the age at which a calf/pup achieves 50% foraging efficiency). TR is 1 year. The curve for γ = 3 is shown in solid black. Green curves show the relationship for values of γ <3; red curves represent values >3.

4.4.17 Pregnancy

Pregnancy threshold ($F_{neonate}$, *decision_day, skipping_point*) The Hin et al. (2019) model assumes that females can only become pregnant when the size of their reserves exceeds $F_{neonate}$. They used a value equivalent to the energetic costs of foetal growth and development plus the amount of reserves needed to avoid the onset of starvation for pilot whales, but other formulations have been used (e.g., for beaked whales New et al. 2013). This effectively sets a minimum value for the age at first conception, because the absolute size of a female's reserves is determined by S_a and young females are too small to build up sufficient reserves, even if their foraging efficiency has attained its maximum level. Estimates of age at first

conception are available from many marine mammal populations and these can be compared with predictions from the DEB model to provide a “reality check” on the appropriateness of the value chosen for $F_{neonate}$.

Smout et al. (2019) documented a relationship between a female grey seal’s total mass at the end of lactation and the likelihood of giving birth in the following breeding season. The threshold mass that resulted in a 0.5 probability of giving birth was lower if prey abundance was greater than average in the subsequent year. Given that females do not increase their body mass from the end of lactation until implantation (Boyd 1984), this implies that in grey seals the decision to give birth to a pup is made some time during pregnancy, rather than at implantation. However, the exact time at which females should make this decision is not entirely obvious, and the model allows the user to define when this decision is made (*decision_day*). Further details are provided in the section on the grey seal model.

4.4.18 Lactation

Efficiency of conversion of mother's reserves to calf/pup tissue (σ_L) This parameter combines the efficiency with which a female converts ingested or reserve energy to milk and the assimilation efficiency of the calf/pup. Lockyer (1993) assumed that efficiency of milk assimilation is 95% and that the efficiency of milk production in the mammary gland is 90%. Combining these estimates yields a value of 0.86, which was used by Hin et al. (2019) and may also be useful for other cetacean species. Direct estimation of this parameter should be possible from studies of energy transfer in lactating pinnipeds (e.g., Costa et al. 1986, Lang et al. 2011). For example, Figure 3 in Costa et al. (1986) implies that conversion efficiency in northern elephant seals is close to 100%. However, it is not possible to calculate a precise value for σ_L from the results presented in this and other pinniped studies.

Effect of calf/pup age on milk assimilation (T_C , ξ_C) Hin et al. (2019) proposed that females will provide all their calf’s energy demands until the calf is T_C days old, and after this they will gradually reduce the amount of energy they supply according to the formula:

$$\left(1-\frac{(a-T_C)}{(T_L-T_C)}\right) \Big/ \left(1-\frac{\xi_C(a-T_C)}{(T_L-T_C)}\right)$$

Where a is calf age and T_L is age at weaning. Figure 5 shows the effect of the value of ξ_C on the shape of this relationship. For capital breeding species, such as many

pinnipeds, which provide almost all of their pup's energy demands up until the age at weaning, T_C should be close to T_L and ξ_C will be close to 1. Species, such as bottlenose dolphins, with an extended period of maternal care will have relatively small values of T_C and ξ_C.

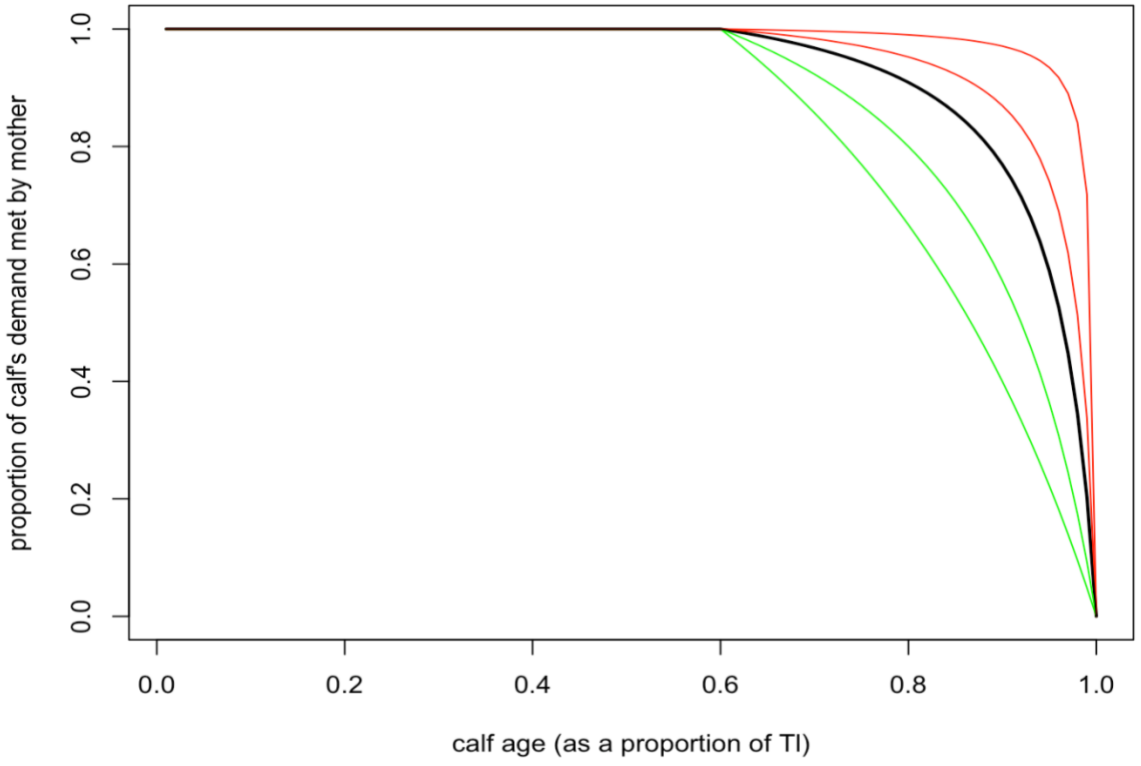

Figure 5.The effect of the non-linearity parameter ξc on the proportion of a calf/pup's milk demand provided by its mother at different stages of lactation. TN (the calf/pup age at which the mother begins to reduce the amount of milk she supplies) was set at 60% of the duration of lactation (TL). The solid black line shows the relationship for ξc = 0.9 (the value used by Hin et al. 2019). Green lines show the relationships for smaller values of ξc (0.5 and 0.75). Red lines show the relationship for larger values (0.95 and 0.99).

Effect of female body condition on milk provisioning (ξ_M) Hin et al. (2019) assumed that females will reduce the amount of milk they provide to their calf as their own body condition declines. They used the function:

$$\frac{(1+\xi_M).(\rho_t-\rho_s)}{\{(\rho-\rho_s)+\ \xi_M.(\rho_t-\rho_s)\}}$$

to predict this reduction, where ρ_t is the female's body condition on day t, and ξ_M is described as the "non-linearity in female body condition-milk provisioning relation". Figure 6 shows how the shape of this relationship varies, depending on the value of ξ_M. Lower values of ξ_M represent a more conservative strategy, with females

reducing the amount of milk they supply by 50% if their body condition falls below 60% of ρ if ξ_M = 0.5. Larger values reflect a strategy that is more "generous" to the calf/pup. For example, if ξ_M = 10, body condition must be reduced close to ρ_S before milk supply is reduced by 50%.

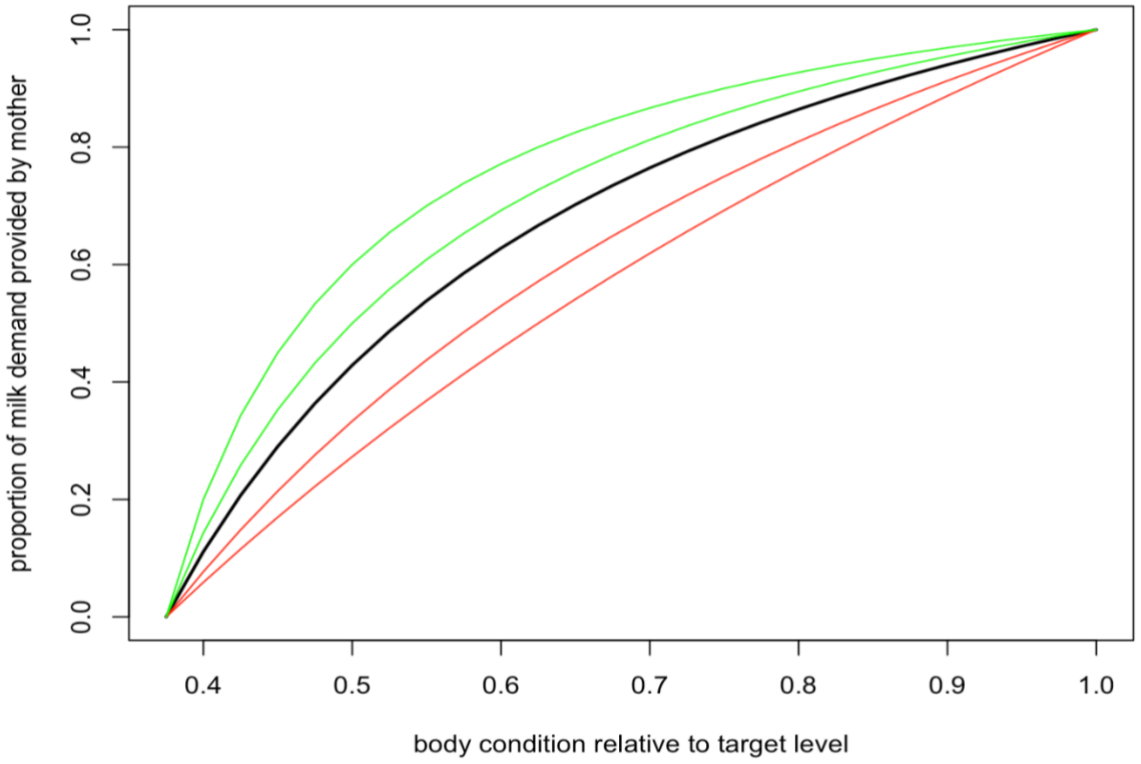

Figure 6. The effect of body condition relative to the target level ($\frac{\rho}{\rho t}$) of the female and the non-linearity parameter ξM on the proportion of a calf/pup's milk demand provided by its mother. The solid black line shows the relationship for ξM = 2 (the value used by Hin et al. 2019). Green lines show the relationships for larger values of ξM (3 and 5). Red lines show the relationship for smaller values (0.5 and 1.0).

Lactation scalar (Φ_L) is analogous to R; because $\Phi_L . S_{c,t}^{2/3}$ determines the maximum amount of energy a calf/pup can obtain from milk on day t, where $S_{c,t}$ is the structural mass of the calf/pup on day t. Hin et al. (2019) estimated Φ_L for pilot whales on the assumption that the female provides all of her calf's energy needs up to age T_C. They calculated the mean amount of energy expended each day by the calf during this period for maintenance and growth, and then divided this by the average structural mass of the calf x 0.5 (on the assumption that the body condition of both mother and calf was equal to ρ). Similar calculations can be performed for other species, provided a value for σ_G (the energetic cost per unit structural mass) is available.

4.4.19 Mortality

Age-dependent mortality rate Hin et al. (2019) calculated an age-varying mortality rate for pilot whales based on published estimates of age-specific survival rates. A similar procedure can be used to estimate this rate for the five species modelled here from the age-specific survival rates provided in published estimates (Winship 2009, Arso Civil et al. 2019, Sinclair et al. 2020)

The **starvation body condition threshold** *(ρ_s)* represents the point at which further reduction in body condition is likely to have a negative effect on survival. It can be estimated from the ratio of blubber: total body mass of dead or dying animals that exhibit symptoms of terminal starvation (Kastelein and Van Battum 1990, Koopman et al. 2002).

Starvation-induced mortality rate (μ_s) This parameter determines how long an individual is likely to survive if its body condition falls below the starvation body condition threshold (ρ_s). Probability of survival is modelled as:

$$\phi_t = e^{-\mu_s(\frac{\rho_s}{\rho_t}-1)}$$

Higher values of μ_s result in a lower probability of survival (Figure 7). Hin et al. (2019) used a value of 0.2, which implies that 50% of starving individuals will survive for one week if their body condition remains below the threshold.

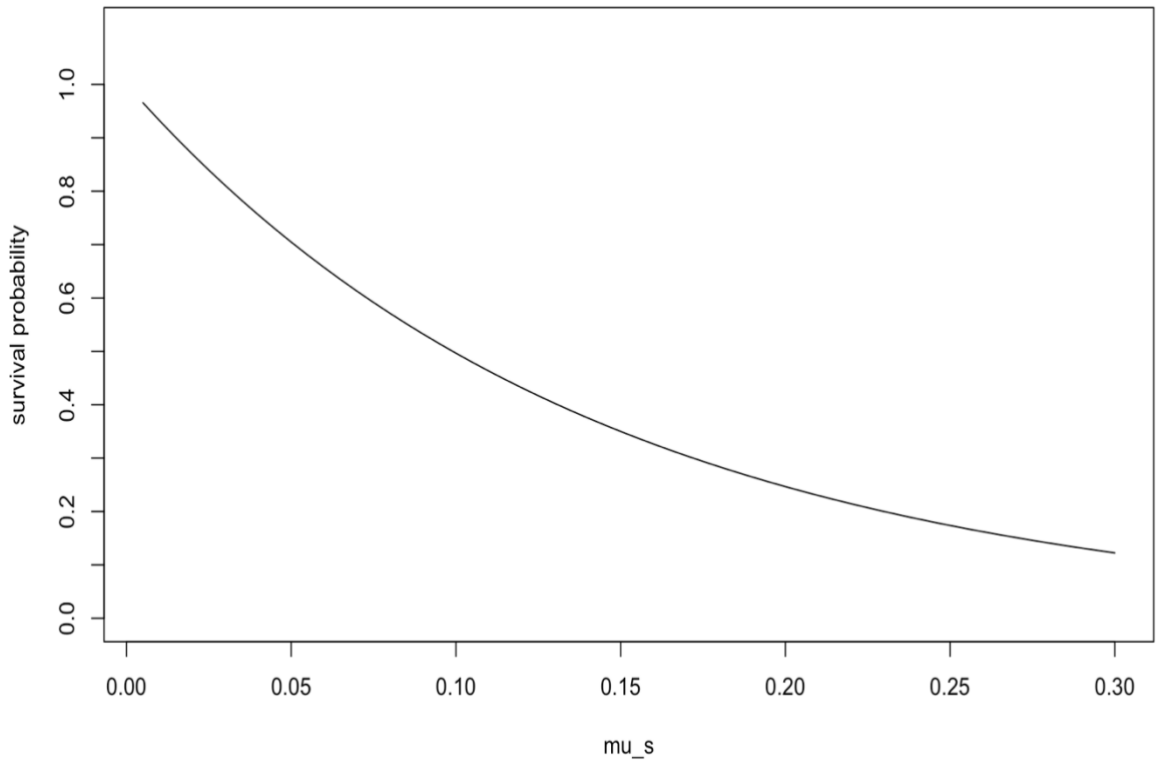

Figure 7. The effect of the starvation-induced mortality parameter (mu_s = μs) on the probability that an individual whose body condition has fallen to ρs/2 will survive for 1 week.

4.4.20 Modelling disturbance

Users can define the start and end points (Diststart and Distend) of the period during which disturbance can occur, and the number of days on which disturbance occurs (Distdur). Specific days when disturbance occurs are chosen at random within the defined period. During each day of disturbance, the resource density experienced by a simulated individual, and consequently the amount of energy it assimilates, is reduced by Disteffect. The effects of this reduction on energy assimilation will depend on the age and life history stage of the affected individuals, and the user can define the age classes that are affected using the parameter Agedist. In the current version the disturbances occur in a single year and their effect on vital rates are determined within the same time frame (for example, the survival of calves/pups that are alive at the time of the disturbance or are born shortly after it).

5 Harbour seal DEB model

5.1 Model parameters

The parameter values for harbour seals in most of the simulations described in this Chapter are shown in Table 4, and details of how these parameters were derived are outlined below. We use the parameter symbols and names as in Tables 1 and S1 in Hin et al. (2019).

Table 4. Parameter values for harbour seals used in this Chapter.

Variable, parameter	Code	Units	Value	Description	Source and description
Resource					
R_{mean}	Rmean	-	2.1	Annual mean resource density	See text
a_{beta}	a_beta	-	23.65	Parameters of beta distribution defining stochasticity in resource density	See text
b_{beta}	b_beta	-	19.35		See text
	amplitude	-	0.1	Parameter defining the amplitude of seasonal variation in resource density	See text
	offset	-	184	Parameter determining when during the year *Rmean* has its maximum value	See text
Timing of life history events					
min_age	min_age	years	4	Minimum age for reproduction	Härkönen and Heide-Jørgensen (1990), Sinclair et al. (2020)
mean_birthday	mean_birthday		17th June	Mean pupping date for UK harbour seals	Reijnders et al. (2010), Härkönen and Heide-Jørgensen (1990)
T_P	Tp	days	240	Gestation period	Reijnders et al. (1993)
T_L	Tl	days	23	Age at weaning (duration of lactation)	Meulbert and Bowen (1993),

Variable, parameter	Code	Units	Value	Description	Source and description
					Cordes et al. (2013)
T_R	Tr	days	60	Age at which calf's resource foraging efficiency is 50%	See text
max_age	max_age	years	30	Maximum age	Hall et al. (2019)
	max_age_calf	years	1	Maximum modelled age of pup	
moult_duration	moult_duration	days	20	Duration of moult	See text
Reserves					
ρ	rho	–	0.43	Target body condition for adults	See text
ρ_c	rho_C	–	0.55	Target body condition for pups	See text
θ_F	Theta_F		0.2	Relative cost of maintaining reserves	Hin et al. (2019)
Growth					
L_0	L0	cm	82.9	Length at birth	Hall et al. (2019), Härkönen and Heide-Jørgensen (1990)
L_∞	Linf	cm	140.5	Female maximum length	Hall et al. (2019)
k	K	$days^{-1}$	0.0012	Von Bertalanffy growth function: growth rate parameter	Hall et al. (2019)

Variable, parameter	Code	Units	Value	Description	Source and description
X_0	x0	days	-2.02*365'	Von Bertalanffy growth function: length at age zero	Hall et al. (2019)
ω1	omega1	kg/cm	3..6*10^{-5}	Structural mass-length scaling constant	Härkönen and Heide-Jørgensen (1990)
ω2	omega2	–	2.86	Structural mass-length scaling exponent	Härkönen and Heide-Jørgensen (1990) but see text
Energetic rates					
σ_M	Sigma_M	–	2.3	Field metabolic maintenance scalar	See text
σ_G	Sigma_G	MJ/kg	25	Energetic cost per unit structural mass	Derived using the approach of Hin et al. (2019)
ε	epsi	MJ/kg	25.8	Energy density of reserve tissue	Reilly et al. (1996)
ε-	epsi_minus	MJ/kg	23.2	Catabolic efficiency of reserves conversion	See text
ε+	epsi_plus	MJ/kg	35.5	Anabolic efficiency of reserve conversion	See text
ε_{+pups}	epsi_plus_pups	MJ/kg	28.5	Anabolic efficiency of reserve conversion for pups/calves	See text
μ_s	mu_s	–	0.2	Starvation mortality scalar	Hin et al. (2019)

Variable, parameter	Code	Units	Value	Description	Source and description
η	eta	–	20	Steepness of assimilation response	See text
ϒ	upsilon	–	1.8	Shape parameter for effect of age on resource foraging efficiency	See text
K	Kappa	–	0.2	Proportion of the daily assimilated energy allocated to growth	See text
	moult_reduction		0.5	Reduction in resource assimilation during moult	See text
Pregnancy					
fert_success	fert_success		1	Probability that implantation will occur	See text
	skipping_point	kg	45	Threshold for continuing pregnancy	See text
decision_day	decision_day	days	160	Day of pregnancy when female decides whether or not to continue	See text
Lactation					
φ_L	phi_L	–	4.02	Lactation scalar	See text
σ_L	Sigma_L	–	0.86	Efficiency of conversion of mother's reserves to calf tissue	Lockyear (1993)
T_N	Tc	days	0.90*TL	Pup age at which female begins to reduce milk supply	See text

Variable, parameter	Code	Units	Value	Description	Source and description
lact_feed	lact_feed	days	10	Day of lactation when female starts foraging	Boness et al. (1994), Thompson et al. (1994)
R_prop_lactation	R_prop_lactation	–	0.6	Proportion of resources density at which female forage during lactation after lact_feed	See text and Bowen et al. (2001)
ξ_M	xi_m	–	-2	Non-linearity in female body condition-milk provisioning relation	See text
pw_fast	pw_fast	days	15	Duration of post-weaning fast	Meulbert and Bowen (1993)
pup_mass_gain	pup_mass_gain	kg/day	0.55	Daily mass increase of pups	Bowen et al. (1992), Harding et al. (2005), Jørgensen et al. 2001
daily_pup_ee	daily_pup_ee	MJ/day	8.3	Daily energy expenditure of pups during lactation	See text
Mortality					
foetal_mortality	foetal_mortality		0.1	Foetal mortality not related to body condition	
α_1	alpha1	–	0.0022	Coefficients of age-dependant mortality curve	Sinclair et al. (2020) and see text
α_2	alpha2	–	0.0019		

Variable, parameter	Code	Units	Value	Description	Source and description
β_1	beta1	–	$2.1*10^{-4}$		
β_2	beta2	–	$0.3*10^{-6}$		
ρ_S	rho_s	–	0.1	Starvation body condition threshold	See text
μ_s	mu_s	–	0.2	Starvation mortality scalar	
Disturbance					
$Dist_{dur}$	days.of.disturbance	days		Number of days on which disturbance occurs	See text for values
$Dist_{start}$	first_day	day of year		First day of disturbance period	See text for values
$Dist_{end}$	Last_day	day of year		Last day of disturbance period	See text for values
$Dist_{effect}$	disturbance.effect	-	0.16	Reduction in resource density caused by disturbance	Russell et al. (2016)
Age_{Dist}	age.affected	years	>1	Age threshold defining which age class of simulated animals is affected by the disturbance	

5.1.1 Resource

Resource density *(R_{mean}):* Although some females harbour seals start increasing their body mass soon after weaning, other individuals do not change their body mass until implantation (Renouf and Noseworthy 1991). We, therefore, assumed that resource density varied cyclically over the year, as for grey seals, with maximum resource density occurring at around the mid-point of pregnancy. This would equate to a peak in resource density in mid-March and a minimum value in mid-August for

animals with a birth date of around 17 June. The predicted pattern of resource density is shown in Figure 8.

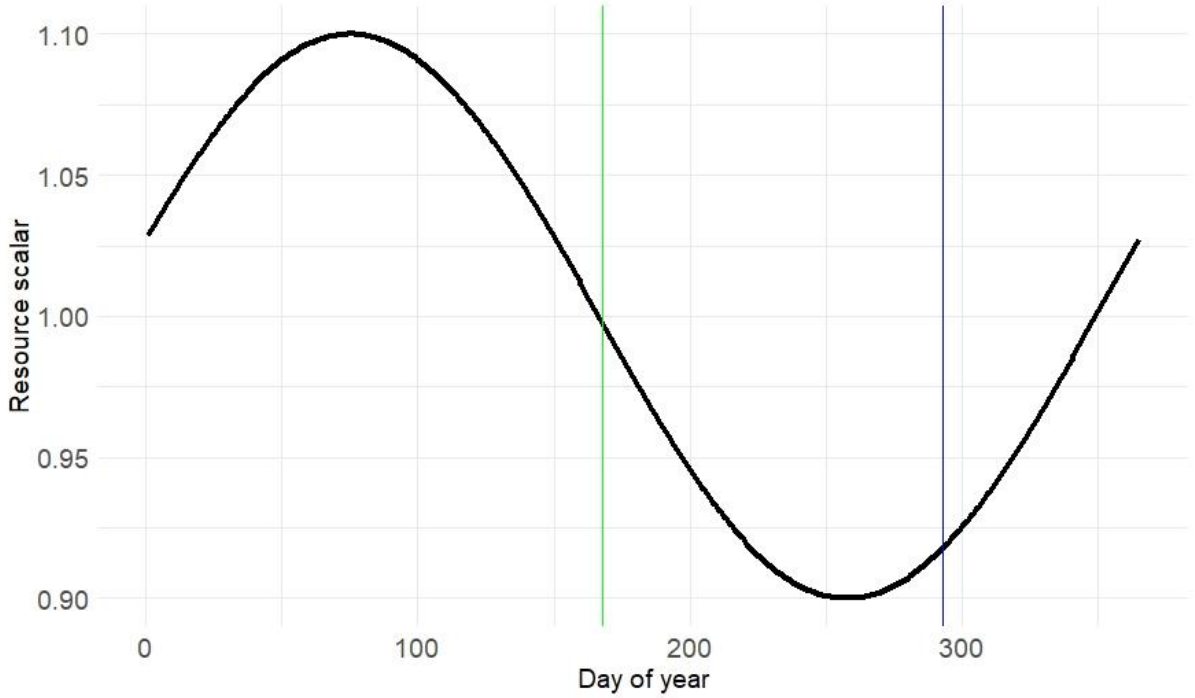

Figure 8. Modelled variation in resource density over the course of the year for a female whose mean pupping date is 17 June (indicated by the vertical green line). The vertical blue line indicates the day on which implantation occurs.

5.1.2 Timing of life history events

Timing of life history events *(min_age, $T_{p,}$, mean_birthday)***:** We used a mean pupping date for each modelled population and assigned a specific birth date for each simulated female. These dates were symmetrically distributed around the mean pupping date, which is 17 June for the North Sea harbour seal population (Härkönen and Heide-Jørgensen 1990, Reijnders et al. 2010). Simulations were started at the start of the 2nd year of life so that we could include the effects of resource density on the survival of a female's pups in the calculation of individual fitness.

All females that were at least 4 years old (min_age, Härkönen and Heide-Jørgensen 1990, Sinclair et al. 2020) were assumed to become pregnant each year, with implantation occurring (365-Tp) days after that individual's birthday. The fert_sucess is therefore assumed to = 1.

Gestation period (T_P): We used a value of 240 days (~ eight months) as suggested by Reijnders et al. (1993).

Lactation period/age at weaning (T_L): There is a large variation in duration of lactation reported for harbour seals, even for the same population, with a range of 17

– 33 days (Bowen et al., 1992, 2001; Cordes and Thompson, 2013; Härkönen and Heide-Jørgensen, 1990; Muelbert and Bowen, 1993; Sauvé et al., 2014). We used the middle of this range (23 days), which is the most commonly reported mean duration.

5.1.3 Reserves and growth

Reserve thresholds (ρ, ρ_s, ρ_{pup}): Total body weight of female harbour seal is at a minimum at the end of lactation but increases soon after, because females may start foraging during lactation. Thereafter total body weight increases to a maximum at the start of the next birth (Renouf et al. 1993). Bowen (2001) documented that the mean reserve mass of females at parturition is 43% of the total body mass, and that females lost 32.3% of their postpartum body mass during the initial 80% of lactation. We, therefore, set a value of ρ = 0.43, which is consistent with these observations. We used a value of 0.55 for ρ at weaning (ρ_{pup}). This is slightly higher than the value of 0.43 reported by (Muelbert et al. 2003).

These values result in female body condition declining to around 0.15 at the end of lactation, which would suggest a value of 0.1 for ρ_s (Figure 9).

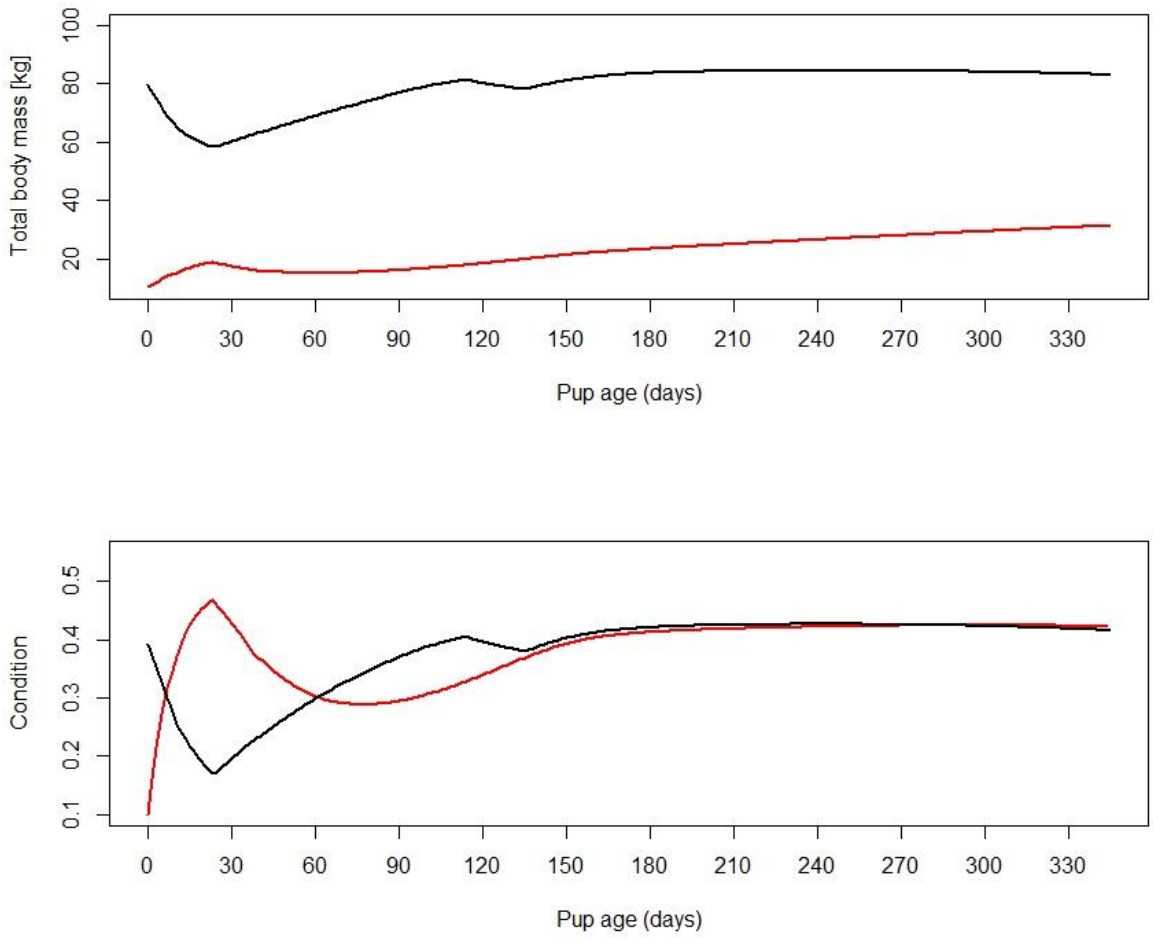

Figure 9. Predicted variation in total body weight (top panel) and Condition (bottom panel) of a female (solid black line) and her pup (solid red line) over 1 year. The dip

in condition and total body of the female around day 130 indicates the effect of the moult – when females spend more time hauled out - on energy assimilation.

Relative cost of maintaining reserves (Θ_F): We were unable to find any published data that would allow a value specific to harbour seals to be calculated for this parameter. We therefore used the value of 0.2 assumed by Hin et al. (2019).

Structural length and mass (K, L_0, L_∞, ω_1, ω_2, k, x_0): The model developed by Hin et al. (2019) assumes that growth in length and core mass continues unabated, regardless of energy intake. This is clearly not the case in harbour seals. For example, the weight-at-age of yearling harbour seals is highly variable (Hall et al. 2012), presumably as a result of variations in foraging success among individuals. We therefore assumed that growth in harbour seals may be reduced if energy intake is less than the combined costs of metabolism, growth, and reproductive activities (pregnancy and lactation). We modelled these circumstances using a modification of the kappa (K) rule which is a fundamental component of classic DEB models (Kooijman 2010). We assumed that an individual will allocate a proportion of the assimilated energy (I_t) it acquires on a particular day to growth (including growth of the foetus, because this is treated as part of the female's core mass), up to a maximum of (1-K)I_t . If this amount of energy is less than the energy required for growth, the growth rate of the female and her foetus is reduced accordingly. The balance of the energy intake is allocated to metabolism. If this balance is insufficient to cover all of the costs of metabolism, reserves must be metabolised. Values of K < 0.5 indicate that growth is prioritised over metabolism. In the baseline calculation we used a value of 0.1, but we explored the implications of other values (see Sensitivity analysis – Section 5.4). Growth is assumed to cease during the lactation period and the cost of lactation is given priority over metabolism.

One consequence of this approach to modelling growth is that pregnant females who experience reduced energy intake may give birth to smaller pups than those that are able to meet their total energy requirements every day.

Growth was modelled with the modified Von Bertalanffy growth curve fitted to 659 harbours seals by Hall et al. (2019)

$$L_a = L_\infty\left(1 - e^{-(k(a+x_0)}\right)$$

where a is age in days, k = 0.441/365, and x_0 = (- 2.02 x 365). The estimated size at birth (L_0) from this equation is 82.8 cm, as also observed by Härkönen and Heide-Jørgensen (1990).

We modelled foetal growth in terms of T_P and L_0 as:

$$L_{af} = af.L_0/T_p$$

Where af is foetal age in days.

The relationship between structural length and structural mass for harbour seals was modelled using $\omega_1 = 0.000033$ and $\omega_2 = 2.875$, close to values estimated by Härkönen and Heide-Jørgensen (1990). We had to decrease ω_1 in order to get mass at birth similar to observed values, because the masses used by Härkönen and Heide-Jørgensen (1990) included some reserve tissue. With L_0 = 82.8 cm, the estimated mass at birth is 10.8 kg. There is very little information on pup mass at birth for the North Sea population. Härkönen and Heide-Jørgensen (1990) reported a range of 7.9 - 9.5 kg, which is slightly lower than our estimate, but our estimate is within the range observed for other populations (means 10.5 – 11.6 kg, Jørgensen et al. 2001, Bowen et al. 1992, 2001). Decreasing ω_2 further resulted in a maximum structural mass of females that was too low. With the current values, maximum structural mass is 49.3 kg, which results in total mass of 87 kg for post-partum females, which is in the middle of the observed range of 60-110 kg (Bowen et al. 1992, 1994, 2001).

5.1.4 Energetic rates

Field metabolic maintenance scalar (σ_M): Although there are many estimates of the metabolic rate of harbour seals in captivity, we were unable to locate any field estimates. We used σ_M = 2.3. Other values were explored in the sensitivity analysis.

Energetic cost per unit structural mass (σ_G): We calculated growth efficiency using the same approach as Hin et al. (2019) and an energy density for foetal tissue of 6.5 MJ/kg (the mean of the values for new-born harp and harbour seal pups reported by Worthy and Lavigne(1987)). This produced a value of 25 MJ/kg for σ_G.

Catabolic and anabolic efficiency of reserve conversion (ε_-, ε_+): We used the same values as for grey seals because there was no information for these two parameters for harbour seals. See the corresponding section for grey seals for further details

Steepness of assimilation response (η): We were unable to find any data in the literature that could be used to set a feasible range for this parameter. We explored the implications of values between 5 and 40 and found that mean reproductive success was maximized when η = 20.

Effect of age on resource foraging efficiency (Y, T_R, *pw_fast, moult_reduction, moult_duration*): Harbour pups undertake a post-weaning fast of approximately 15 days (pw_fast) (Muelbert and Bowen 1993) and continue to lose weight after this time. They regain their initial weight at weaning around the age of 5-6 months (Harding et al. 2005). We set T_R = 65 days and Y = 1.8 and assumed that foraging efficiency was 0 up to the age of 38 days (T_L + *pw_fast*). We chose a combination of T_R and Y which resulted in a foraging efficiency of 0.95 at 1 year of age. This is considerably earlier than the foraging efficiency at this age predicted in the grey seal model because harbour seals pups accompany their mothers into the water during

the lactation period, and pups have been observed catching fish at that time (Jørgensen et al. 2001).

To take account of the fact that moulting seals spend more time hauled out (Paterson et al., 2012), and are therefore likely to acquire less energy, we reduced foraging efficiency by 50% for 10 days before and after implantation (*moult_duration*). Figure 10 shows the modelled variation in foraging efficiency over the first 5 years of life.

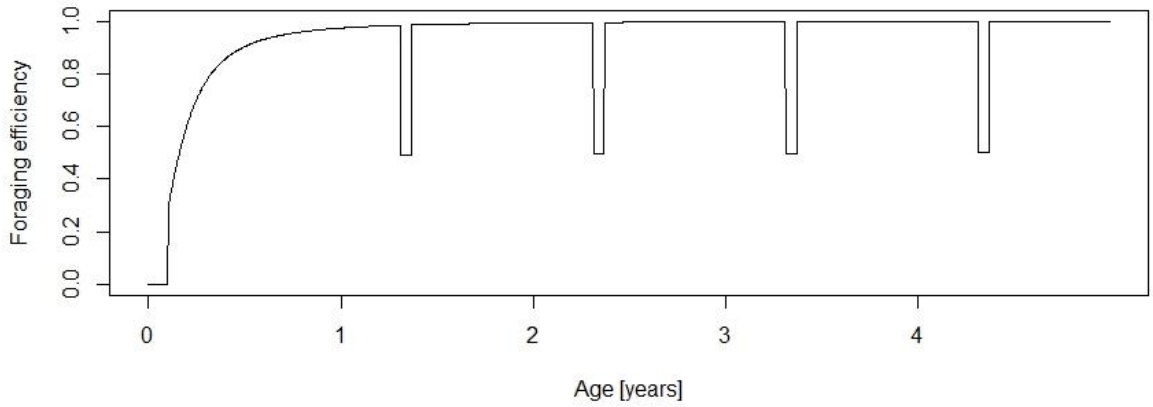

Figure 10. Predicted variation in foraging efficiency with age, showing the reduction in efficiency during the annual moult, which begins in the second year of life.

5.1.5 Pregnancy

Pregnancy threshold (decision_day, skipping_point):

To our knowledge, there is no information for harbour seals equivalent to that for grey seals on the relationship between a female's mass at the end of lactation and the likelihood of giving birth in the following breeding season. Unlike grey seals, harbour seals also forage regularly during lactation and increase their mass from the end of lactation until implantation (e.g., Renouf et al. 1991). We therefore estimated the combination of *decision_day* and weight at weaning that results in a 50% probability of giving birth in the next year (*skipping_point*), which resulted in most mature females (age > = 4) becoming pregnant every year. The interpretation of this point is not equivalent to this interpretation for grey seals due to different breeding strategies of these two species.

We also looked at whether our parameter choice resulted in the probability of giving birth being close to one for females which weigh 60 kg at the last day of pregnancy– the lowest weight reported for harbour seal females just before giving birth (Bowen et al. 2001, Figure 11). For the final simulations, we used *decision_day* – 160 (as for grey seals) and *skipping_point* = 45 kg. See sensitivity analysis for further analysis.

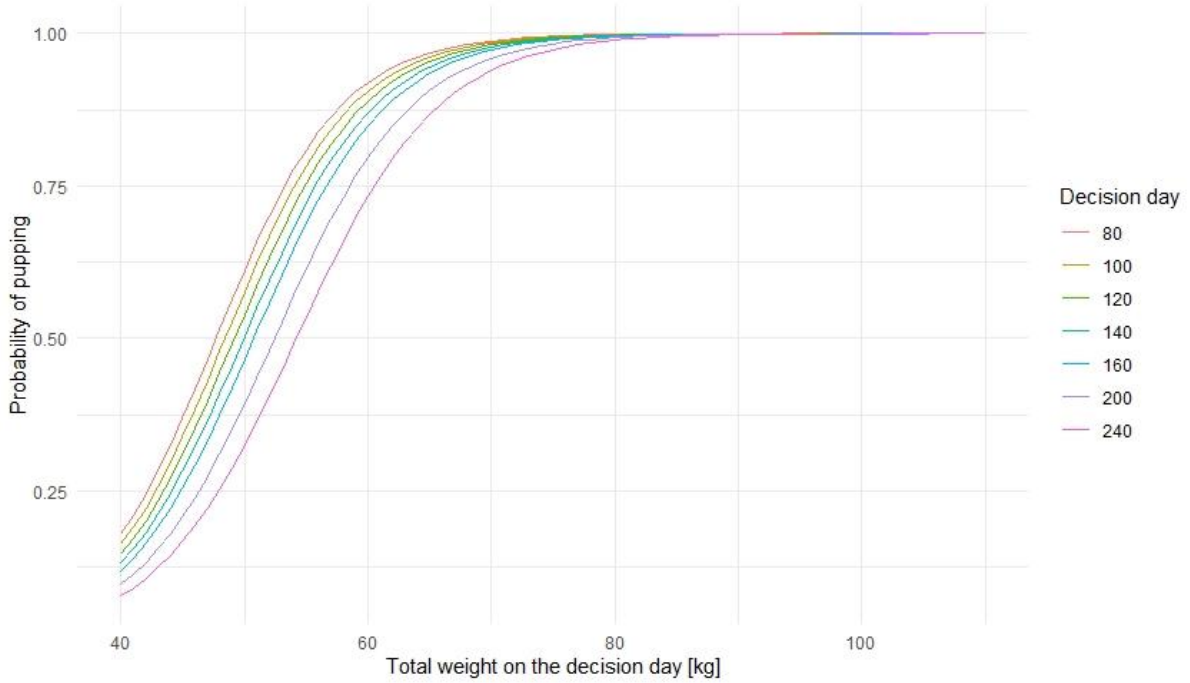

Figure 11. Predicted effect of total body weight at different times during pregnancy (decision day) on the probability of pupping assuming that weight at weaning of 45 kg results a probability of 0.5 that a pregnancy will occur in the following year.

5.1.6 Lactation

Efficiency of conversion of mother's reserves to pup tissue (σ_L): Lang et al. (2011) estimated that approximately 70% of the energy obtained by grey seal pups from milk was converted into tissue. However, this "storage efficiency" includes the costs of maintenance. We, therefore, used the value of 0.86 from Hin et al (2019), as for the grey seal model.

Effect of pup age on milk assimilation ($T_{C,}$ *lact_feed, R_prop_lactation*): The reproductive strategy of harbour seals is intermediate between capital and income breeding, because females start foraging before the end of lactation. We, therefore, modelled a 10% decrease in milk provisioning by female at $T_c = 0.70 * T_L$ (equivalent to day 16 of lactation) and assumed that females start foraging at *lact_feed* = 10 days with a foraging efficiency of 0.6 (*R_prop_lactation).* These days correspond to values reported by Boness et al (1994); Thompson et al (1994), and Bowen et al (2001). There is little information, however, on the amount of food females obtain during lactation, and various values of *R_prop_lactation* were therefore explored (see Sensitivity analysis).

Effect of female body condition on milk assimilation (ξ_M): the value of ξ_M had little effect on model results (not presented in this report) and we chose value 2.

Lactation scalar (Φ_L ,*pup_mass_gain, daily_pup_ee*, ε, ρ_{pup}). All of a pup's energy requirements during the lactation period must be supplied by milk. Although harbour seal pups are reported to start foraging before weaning, it applies to small number of individuals and is more common in pups that have a long lactation period (Jørgensen et al. 2001, Sauvé et al. 2014). There is no information on energy expenditure of harbour seal pups. We used calculation by Reilly et al. (1996) estimating that grey seal pups expend 13.5 MJ/day during lactation, corresponding to 3.7 * RMR and, therefore, resulting in *daily_pup_ee* = 8.3 MJ/day for a 15 kg harbour seal pup. (Bowen et al. 1992, Dubé et al. 2003, Muelbert et al. 2003, Sauvé et al. 2014) reported daily mass increase of harbour seal pup to be between 0.40 and 0.80 kg/day. Assuming the estimated mass at birth to be 10.8 kg and T_L = 23, values of *pup_mass_gain* = 0.55 kg/day would result in simulated mass at weaning of 23.45 kg, as observed (Muelbert et al. 2003, Jørgensen et al. 2001) Assuming that mass at birth is entirely composed of structural mass, this implies that a pup's body condition at the end of lactation is 0.5. Using this value in Hin et al.'s (2019) formula gives Φ_L = 4.51 if ε = 25.8 MJ/kg.

5.1.7 Mortality

Age-dependent mortality rate (*max_age,* α_1, α_2, β_1, β_2): We followed Hin et al. (2019) and estimated changes in the probability of survival with age using the approach developed by Barlow & Boveng (1991). The following function describing the variation in daily survival with age:

$$Surv_a = e^{-(\alpha_1 e^{-\beta_1 a} + \alpha_2 e^{\beta_2 a})}$$

where *a* is age in days, was fitted to the annual age-specific harbour seal survival rates documented in Sinclair et al. (2020). We used values for a stable population (e.g., Moray Firth, Table 13 of Sinclair et al. 2020) in order to investigate the effects of disturbance on a population that is not food-limited, and for a population increasing at 3-4% per annum using the demographic rates suggested in Table 16 of Sinclair et al. (2020). In the latter case *Rmean* was then adjusted to 1.61 so that the population growth rate was 1.00 to investigate the effects of disturbance on a population that was food-limited. Figure 12 shows the resulting relationship between age and cumulative survival, with maximum age of 30 years (max_age) and

α_1 = 0.0022

β_1 = 0.0019

α_2 = 0.00021

β_2 = 0.0000003

for a stable population and:

α_1 = 0.005

β_1 = 0.0055

α_2 = 0.00013

β_2 = 0.0000000036

for an increasing population.

The life expectancy of each simulated female was calculated by choosing a random number between 0 and 1 and determining the age in days at which cumulative survival equalled this value.

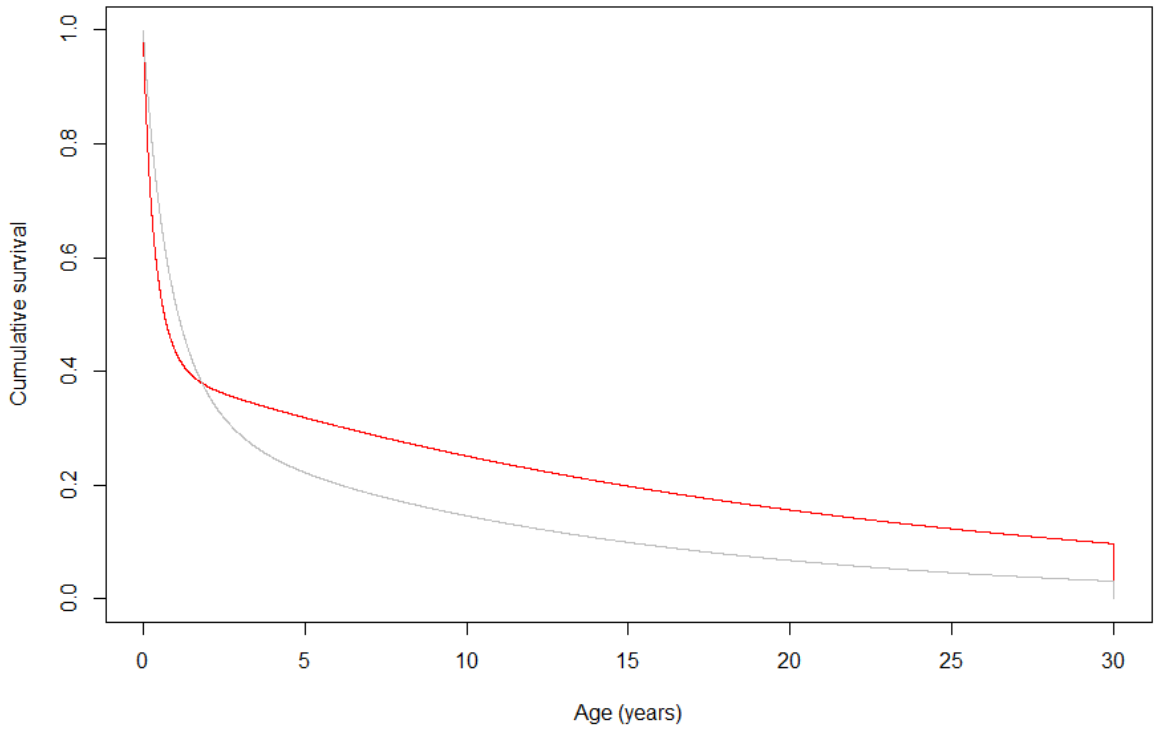

Figure 12. Cumulative survival curve for female harbour seals used in simulations, with annual survival values estimated by Sinclair et al. (2020), where juvenile survival is estimated to 0.79 and adult to 0.92 ('stable population' red line) and 0.86 and 0.96 respectively ('increasing' population, grey line).

We also assumed that there was some mortality of foetuses during pregnancy. In the baseline model mortality over the entire duration of the pregnancy was set at foetal_mortality = 0.1.

Starvation-induced mortality rate (μ_S): No empirical information that could provide a species-specific value of this parameter for harbour seals is available. We used the value of 0.2 proposed by Hin et al. (2019) and used for grey seal DEB.

5.2 Model results – pattern-oriented modelling

The following results are based on 50 simulations for 1000 females each.

5.2.1 Annual changes in mother and pup condition and total body weight

Total body weight and condition of the modelled females are at maximum at the start of lactation and at a minimum at the end of lactation. They increase soon after lactation, as described by Renouf et al. (1993). Bowen et al. (2001) documented that during the initial 80% of lactation, females lose 32.3% of their postpartum body mass and their mean reserve mass at parturition is 43% of the total body mass, which is also the case for the modelled females (Figure 9).

Pup condition is at maximum of around 0.43 at the end of lactation, which corresponds to values reported by Muelbert et al. (2003). The total weight of a pup at 1 year of age is approximately 31 kg, which also corresponds to values reported by Muelbert et al. (2003). The simulated weight of a pup at around 110 days (17 kg) is slightly lower than the 20-30 kg observed by Harding et al. (2005). Two months later simulated total weight is around 23 kg, within the range reported by Harding et al. (2005)(Figure 9 & Figure 13).

Figure 13 shows examples from three different females whose body mass and condition are displayed for three consecutive years. Panel A shows a female who gave birth in three consecutive years; panel B shows a female who skips the third pregnancy; and panel C shows a female whose pup dies before weaning. The body mass and condition of this female return to the pre-parturition level more quickly than for females that nurse their pups until weaning.

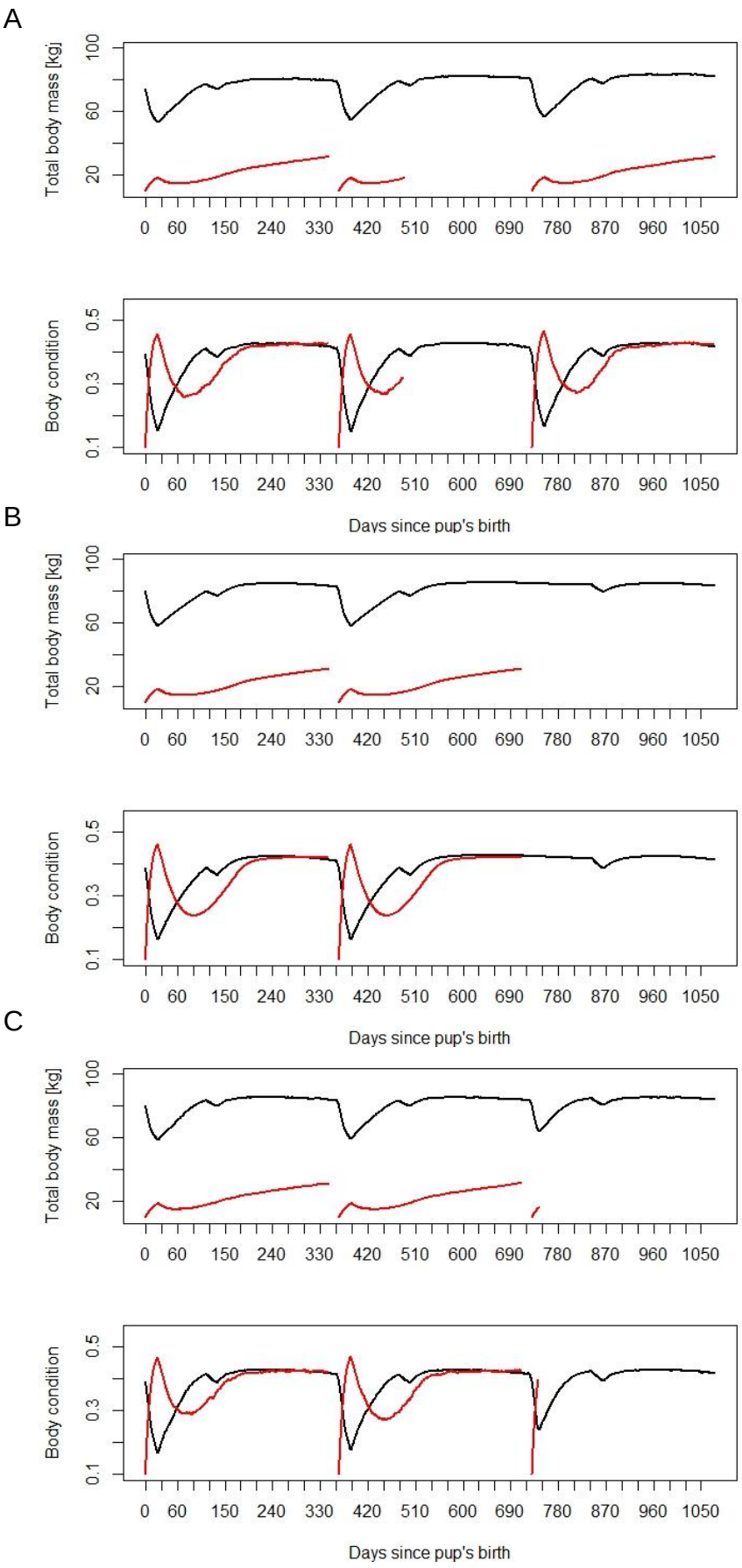

Figure 13 - examples of annual changes total body mass and body condition of

female (black lines) and her offspring (red lines). (a) example of female having pups in three consecutive years, her second pup died soon after post-weaning fast, (b) example of female skipping one breeding year, (c) example of female whose third pup died before the end of lactation. her body mass and condition returned to pre-birth values sooner than females who nurse pups till weaning.

5.2.2 Birth rate: proportion of adult females breeding

The proportion of adult females giving birth to a pup each year (birth rate) showed little variation between simulations and was within the range observed in the wild populations (Figure 14).

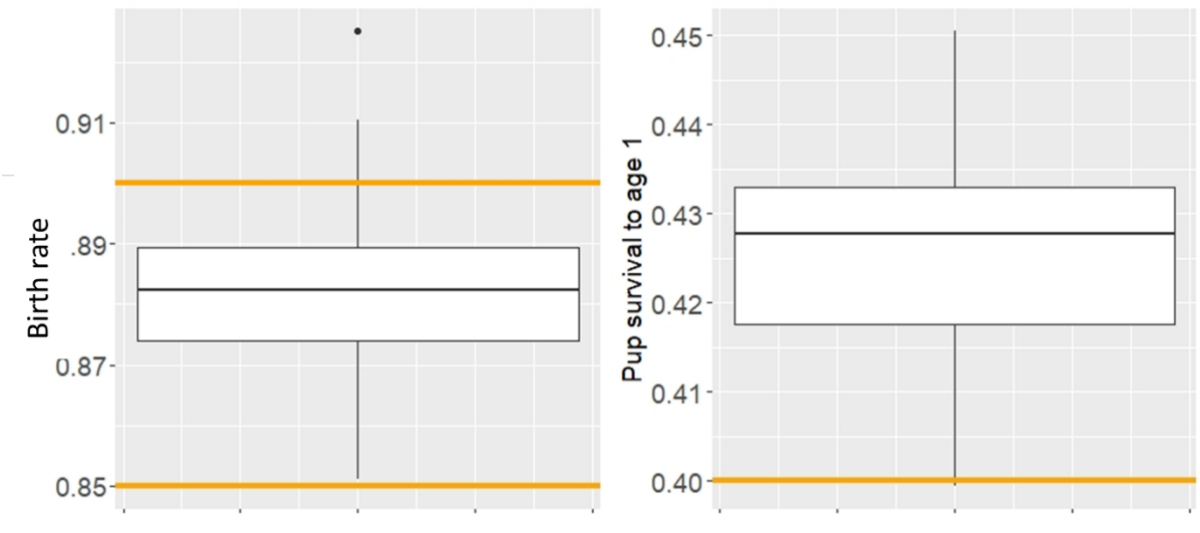

Figure 14. Result of 50 simulations of 1000 females each for two Pattern Oriented Modelling (POM) patterns: Birth rate (left) and Pup survival (right). Orange lines mark range of observed values for UK harbour seal populations (see Table 18 in Sinclair et al. 2020).

5.2.3 Pup survival to age 1

Pup survival to age 1 showed relatively large variation between simulations. It was higher than the value recommended by Sinclair et al. (2020) for stable population (Figure 14).

5.3 Simulating the effect of disturbance

Disturbance was modelled by reducing energy intake by 16% on each day of disturbance. This is based on studies by (Russell et al. 2016) which showed that although seals are displaced from an area when piling occurs, they return within two hours after piling stops. Given the average piling duration is 6 hours, this implies that seals are displaced from an area for 8 hours. We assumed that they can still forage

at 50% of the normal rate while they are displaced. This results in the loss of 4 hours of foraging time (16% of the day). We modelled the effect of 1, 2, 3, 4, 5, 7, 10, 15, 20, 25, 30, 40, 50, and 60 days of disturbance and simulated 4500 11 and 21 year-old females for two values of *Rmean*: *Rmean* = 2.1 for a population that is not limited by food, and *Rmean* = 1.61 for a population that is food-limited (see Section 5.1.7). We chose 11 and 21 years-old females to understand the difference between younger females which may express higher costs of pregnancy. We modelled disturbance scenarios at three different life history stages of females and pups: i) **low impact**: disturbance happens from implantation day to the day on which a female decides whether or not to continue with pregnancy (a period of approximately 5 months); ii) **medium impact**: disturbance occurs between the decision day and parturition (a period of approximately 3 months); iii) **high impact**: disturbance occurs between giving birth and implantation (a period of approximately 4 months). Figure 15 shows these three periods in relation to changes in female body condition. The days on which disturbance occurred within each period were chosen at random.

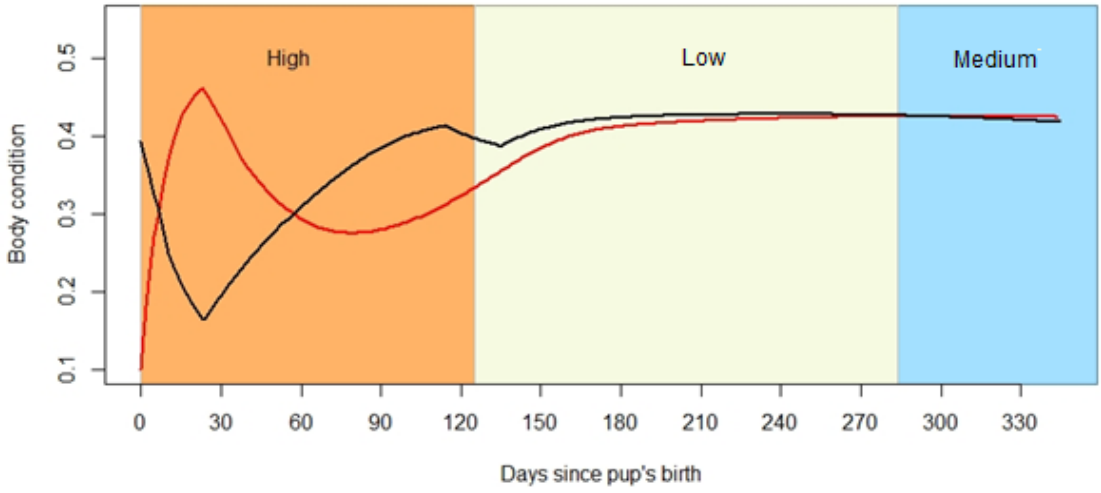

Figure 15. Relationship between body condition of female (black) and her pup (red) and three periods of disturbance: high - from giving birth to implantation; medium – from implantation till decision day whether to continue with pregnancy; and low – from decision day to giving birth

We analysed the effect of disturbance on four vital rates over the course of the year when the disturbance happened: pup survival to age 1, adult mortality, birth rate, and implantation rate.

There was no difference in the effect of disturbance between 11- and 21-years old females. The disturbance had no effect on any of the four vital rates regardless of the duration of disturbance or the disturbance period when food is not a limiting factor (Figure 16, top four panels). When food is a limiting factor, disturbance had the highest effect on pup survival and this effect was most pronounced for the 'High impact' disturbance period. The remaining three vital rates were not affected

regardless of the duration of disturbance or the disturbance period (Figure 16, bottom four panels).

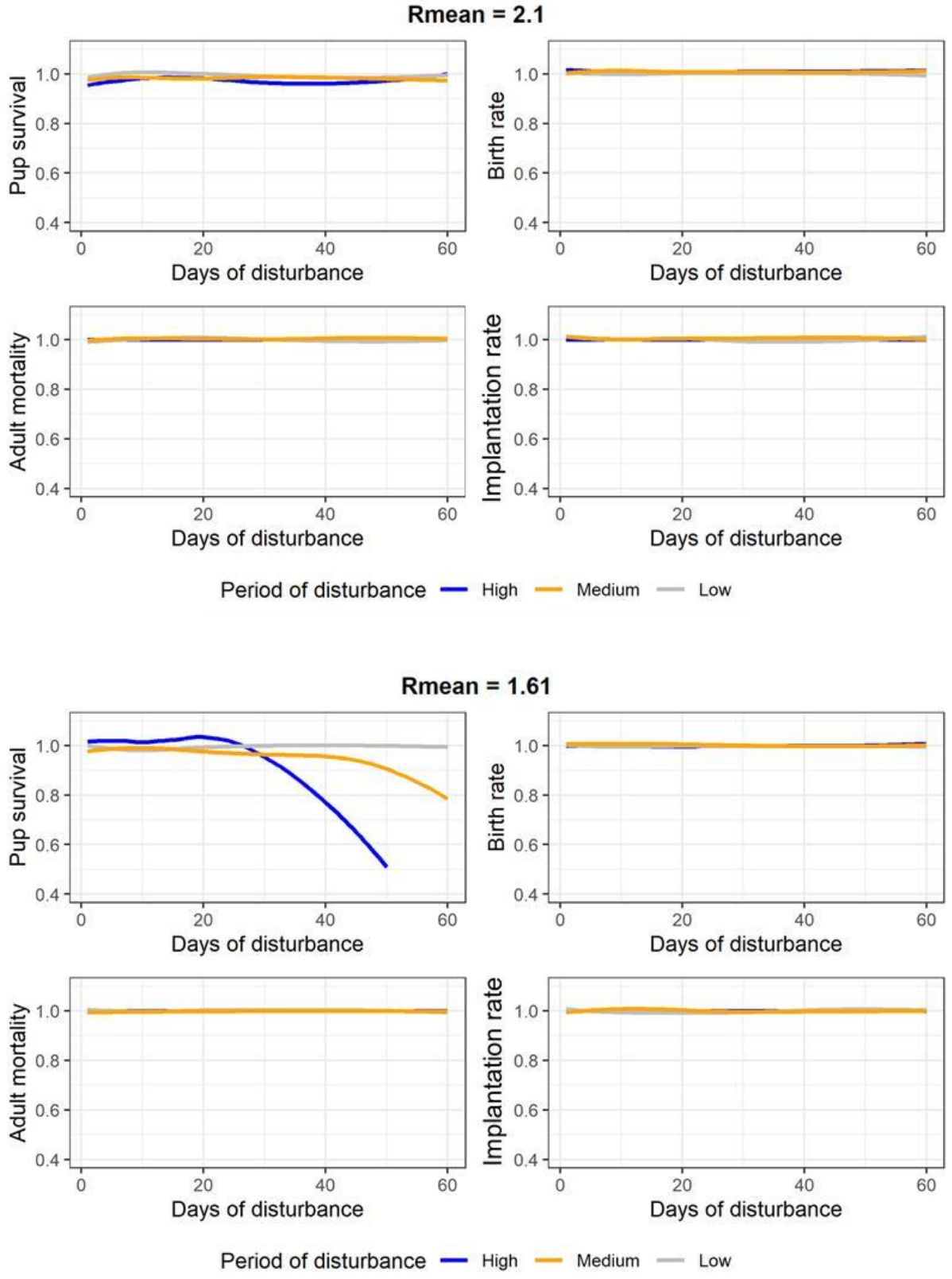

Figure 16. The effect of various durations of disturbance on four vital rates for a harbour seal population that are not food-limited (top panels) and one that is food-

limited (bottom panels) during four different period of disturbance (see figure 15). all values are expressed as proportion change in comparison to no disturbance.

5.4 Sensitivity analysis

The aim of the sensitivity analysis (SA) was to explore the influence of parameter values outside the ranges used in the model simulation on the outputs of the model. SA is frequently based on parameters which either have a large range reported in literature or arbitrary parameters which cannot be directly measured. From the list of all parameters, we tested the effect of varying *K, Tr, σ_M, decision_day* and *R_prop_lactation* (Table 5). We also tested the effect of mu_s and upsilon and results can be presented on demand. Although, there are other parameters used in the model which either have a large range reported in literature or arbitrary parameters which cannot be directly measured, we chose the ones which were not already used in the design phase of model (such as *η)* or parameters, which were directly copied from other species, due to no information in the literature specific for harbour seals (like *ε-, ε_+, Θ_F)*

Table 5. List of parameters, their description, value used in the final model simulation and variation range used in the global sensitivity analysis.

Name of parameter	Description	Value used in the final model simulation	Variation range in the sensitivity analysis
K	Proportion of assimilated energy allocated to growth when energy intake is limited	0.1	± 0.1
T_R	Age at which calf's resource foraging efficiency is 50%	65 days	± 20 days
σ_M (sigma_m)	Field metabolic maintenance scalar	2.3	± 0.2
decision_day	Day of pregnancy when female decides whether or not to continue	160 days	± 40 days
R_prop_lactation	Foraging efficiency during lactation	0.6	± 0.2

We analysed both the effect of varying one parameter at a time and the interaction between them by varying parameters simultaneously. We followed the Design of Experiment methodology first formulated by (Lorscheid et al. 2012) and applied to

individual based models (IBMs) by Thiele et al. (2014). We used a full factorial design of the extreme values of each of the parameters (Table 5), leading to 32 combinations, and we ran one simulation for 500 females for each of these combinations. We then analysed the results using the FrF2 (Groemping 2011) and DoE.base (Groemping 2013) packages in R, following the description by Thiele et al. (2014). We did not run stepwise fitting of a linear regression model to the SA data, as suggested by Thiele et al. (2014), but we based our conclusions on visual analysis of the plots, as discussed below. The results of regression models can be strongly influenced by the sample size, and do not necessarily reflect the actual effect of different parameters (White et al. 2014).

We used the following patterns in SA: mean age of first breeding (Age1stBreed), mean proportion of adult females breeding (Fertility), mean reproduction success defined as proportion of pups which survived to age 1 (PupSurv), mean female condition at parturition (RhoBirth), mean female condition at the end of lactation (RhoEndLact) and mean number of pups which died of starvation (StarvedPups).

5.4.1 Main effect: varying one parameter at the time

The chosen parameters had very little effect on Age1stBreed, Fertility, RhoBirth: these patterns varied little during SA. Sigma_M has the largest effect on the remaining patterns; increasing in Tr resulted in increased pup mortality due to starvation and reducing R_prop_lactation from 0.6 to 0.2 resulted in a decline in RhoEndLact from 0.175 to 0.15 (Figure 17).

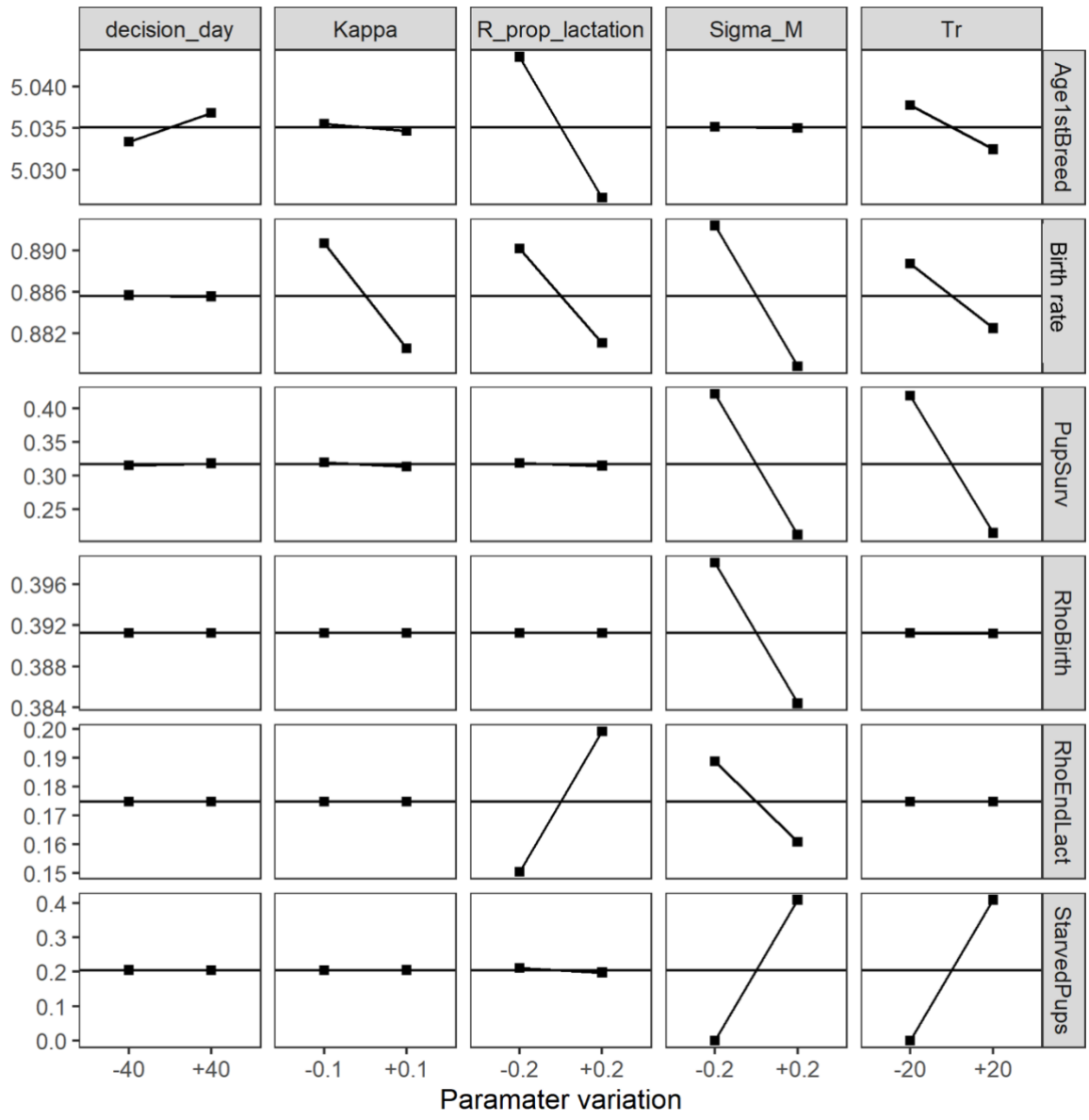

Figure 17. Main effect plots. Parameters in columns and outputs (patterns) in rows. Horizontal lines (without rectangles) in rows visualise mean values. Right rectangle higher than left rectangle indicates a main effect with a positive sign and vice versa. Rectangles on the same output value (y-axis) indicate no main effect.

5.4.2 Interaction effect: varying two parameters at the time

Simultaneous increase in Sigma_M and Tr resulted in large increase in the number of pups that died from starvation. The reduction in RhoEndLact was larger when females foraged little during lactation than when only energy expenditure (Sigma_M) was increased (Figure 18). Varying remaining combinations of parameters had little effect on model results.

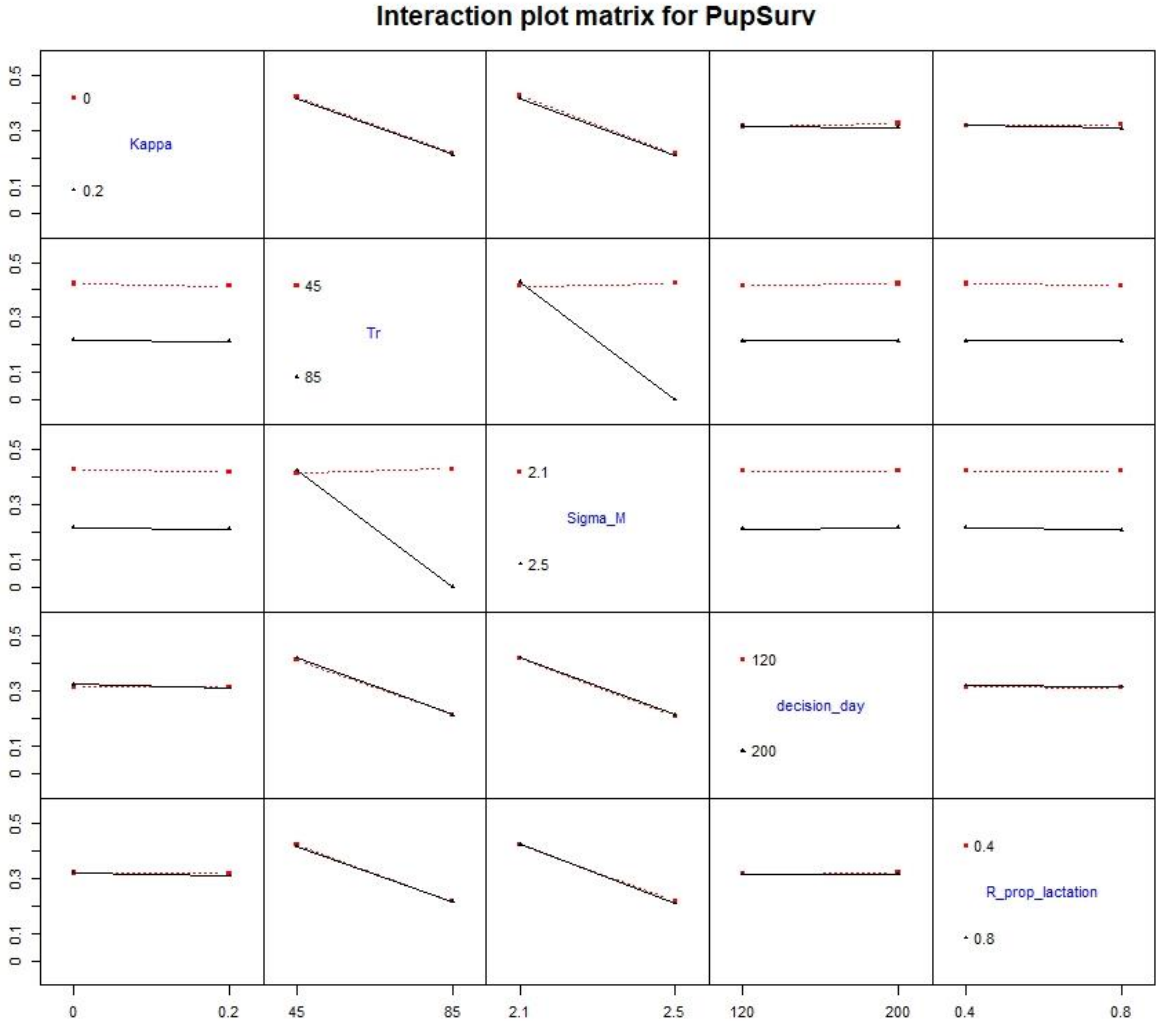
Interaction plot matrix for PupSurv
Kappa
0
0.2
Tr
45
85
Sigma_M
2.1
2.5
decision_day
120
200
R_prop_lactation
0.4
0.8
0
0.1
0.3
0.5
0
0.2
45
85
2.1
2.5
120
200
0.4
0.8

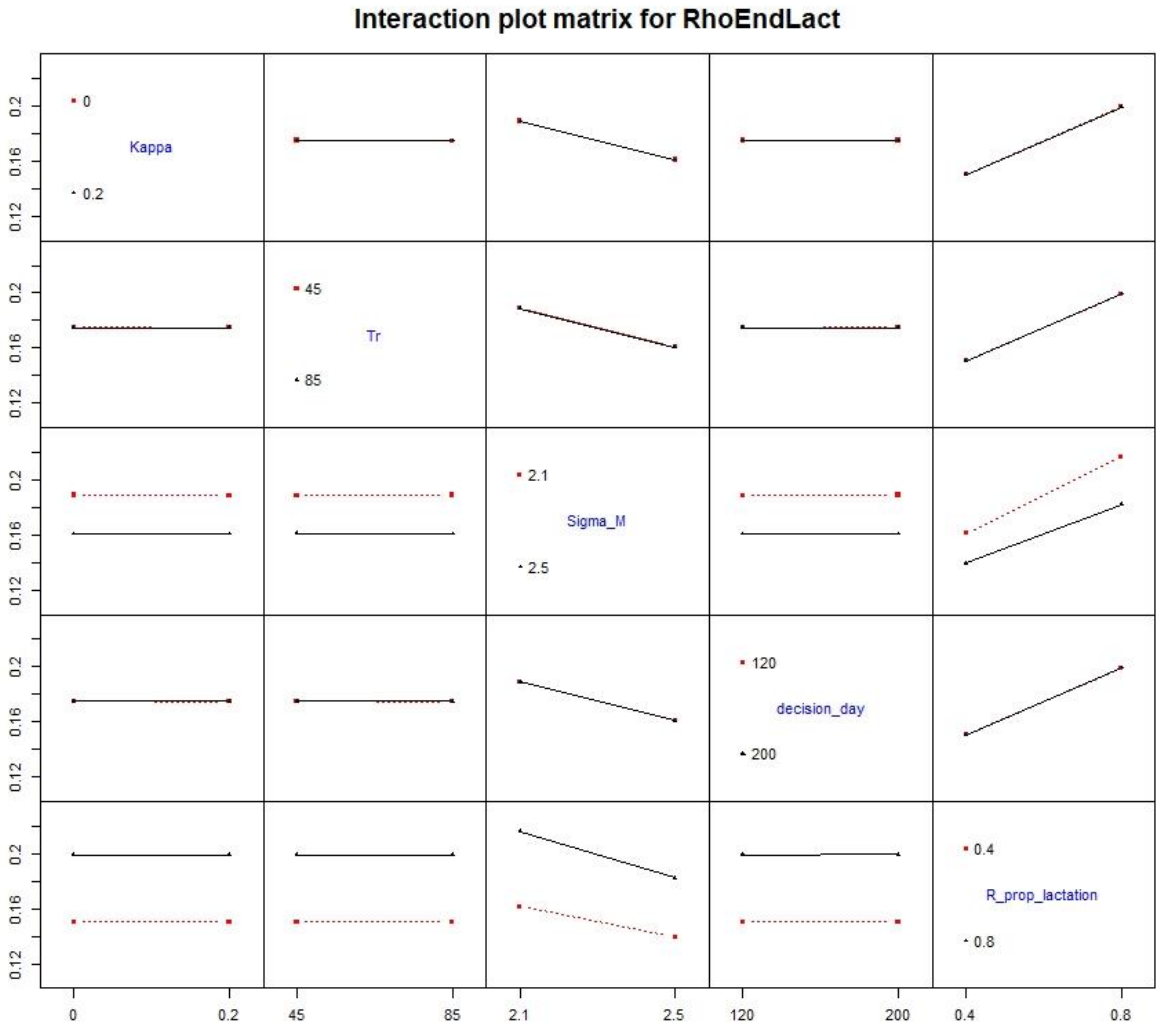

Figure 18. Interaction effect plots for two patterns: Pup survival (top set of panels) and condition at the end of lactation (Rhoendlact, bottom set of panels). The two-way interaction effect plots indicate interaction effects if the lines for a factor combination are not parallel. The less parallel the lines are, the higher is the expected interaction effect.

6 Grey seal DEB model

6.1 Model parameters

Table 6 shows the parameter values used in most of the simulations described in this chapter. Details of how these values were derived are outlined below.

Table 6. Parameter values used in the grey seal DEB model.

Parameter names	Code name	Value	Description	Source
Resource density				
R	Rmean	1.63	Annual mean resource density	See text
a_{beta}	a_beta	23.65	Shape parameters of beta distribution defining stochasticity in resource density	See text
b_{beta}	b_beta	19.35		See text
	amplitude	0.1	Parameter defining the amplitude of seasonal variation in resource density	See text
	offset	184 days	Parameter determining when during the year *Rmean* has its maximum value	See text
Timing of life history events				

Parameter names	Code name	Value	Description	Source
min_age	min_age	3 years	Minimum age for reproduction	
mean_birthday	mean_birthday	23 November	Mean pupping date for Farne Islands grey seals	Boyd (1984)
T_P	Tp	240 days	Gestation period	Hall and Russell (2018)
T_L	Tl	18 days	Age at weaning (duration of lactation)	Hall and Russell (2018)
T_R	Tr	100 days	Age at which calf's resource foraging efficiency is 50%	See text
max_age	max_age	40 years	Maximum age	Hall and Russell (2018)
	max_age_calf	345 days	Maximum modelled age of pup	
moult_duration	moult_duration	20 days	Duration of moult	
Reserves				
ρ	rho	0.5	Target body condition for adults	Pomeroy et al. (1999), Lang et al. (2011) (
ρ_c	rho_C	0.7	Target body condition for pups	Pomeroy et al. (1999)
θ_F	Theta_F	0.2	Relative cost of maintaining reserves	Hin et al. (2019)
Growth				

Parameter names	Code name	Value	Description	Source
L_0	L0	89.8 cm	Length at birth	
L_∞	Linf	184 cm	Female maximum length	
k	k	0.0005	Modified von Bertalanffy growth function: growth rate parameters	
x_0	x0	-58.04		
b	b	0.27	Von Bertalanffy growth function: length at age zero	McLaren (1993)
ω1	omega1	$1.5x10^{-4}$ kg/cm	Structural mass-length scaling constant	Hauksson (2007)
ω2	omega2	2.575	Structural mass-length scaling exponent	Hauksson (2007)
Energetic rates				
σ_M	Sigma_M	2.5	Field metabolic maintenance scalar	Sparling and Fedak (2004)
σ_G	Sigma_G	30 MJ/kg	Energetic cost per unit structural mass	Derived using the approach of Hin et al. (2019)
ε	epsi	25.8 MJ/kg	Energy density of reserve tissue	Reilly et al. (1996)
ε-	epsi_minus	23.2 MJ/kg	Catabolic efficiency of	

Parameter names	Code name	Value	Description	Source
			reserves conversion	
ε+	epsi_plus	35.5 MJ/kg	Anabolic efficiency of reserve conversion	
ε_{+pups}	epsi_plus_pups	28.5 MJ/kg	Anabolic efficiency of reserve conversion for pups	
μ_s	mu_s	0.2	Starvation mortality scalar	Hin et al. (2019)
η	eta	40	Steepness of assimilation response	See text
ϒ	upsilon	1.62	Shape parameter for effect of age on resource foraging efficiency	See text
K	Kappa	0.8	Proportion of the daily assimilated energy allocated to growth	See text
	moult_reduction	0.5	Reduction in resource assimilation during moult	Paterson et al. (2012)
	moult_duration	20 days	Duration of moult	
Pregnancy				

Parameter names	Code name	Value	Description	Source
fert_success	fert_success	1	Probability that implantation will occur	See text
decision_day	decision_day	200	Day of pregnancy when female decides whether or not to continue	See text
Lactation				
φ_L	phi_L	8.85	Lactation scalar	See text
σ_L	Sigma_L	0.86	Efficiency of conversion of mother's reserves to calf tissue	Lockyer (1993)
T_N	Tc	17 days	Pup age at which female begins to reduce milk supply	See text
lact_feed	lact_feed	N/A	Day of lactation when female starts foraging	
R_prop_lactation	R_prop_lactation	N/A	Female foraging efficiency during lactation	
ξ_M	xi_m	2	Non-linearity in female body condition-milk provisioning relation	See text

Parameter names	Code name	Value	Description	Source
pw_fast	pw_fast	21 days	Duration of post-weaning fast	
Mortality				
foetal_mortality	foetal_mortality	0.0	Background foetal mortality	
α_1	alpha1	0.007	Coefficients of age-dependant mortality curve	Thomas et al. (2019)
α_2	alpha2	1.3×10^{-4}		
β_1	beta1	0.01		
β_2	beta2	10^{-7}		
ρ_S	rho_s	0.1	Starvation body condition threshold	See text
μ_s	mu_s	0.2	Starvation mortality scalar	See text
Disturbance				
$Dist_{dur}$	days.of.disturbance		Number of days on which disturbance occurs	See text for values
$Dist_{start}$	first_day		First day of disturbance period	See text for values
$Dist_{end}$	Last_day		Last day of disturbance period	See text for values
$Dist_{effect}$	disturbance.effect	0.25	Reduction in resource density caused by disturbance	
Age_{Dist}	age.affected		Age threshold defining which age class of	See text

Parameter names	Code name	Value	Description	Source
			simulated animals is affected by the disturbance	

6.1.1 Resources

Resource density (*R*) The observed variations in the body condition of female grey seals in the UK over the course of the year suggest that resource density varies seasonally. For example, (Boyd, 1984) found that female grey seals did not increase their weight from the end of lactation until the moult, approximately 4 months later, and Hall and McConnell (2007) found that grey seals pups did not increase their weight over the same calendar period. These results suggest that resource density is relatively low during this period. Presumably, resource density increases thereafter so that reproducing females can accumulate the reserves they need to fuel lactation. We therefore assumed that resource density varies cyclically over the year, with maximum resource density occurring at around the mid-point of pregnancy. For animals with a birthday of around 23 November, this would equate to a peak in resource density in mid-August and a minimum value in mid-February. The predicted pattern of resource density for such animals is shown in Figure 19.

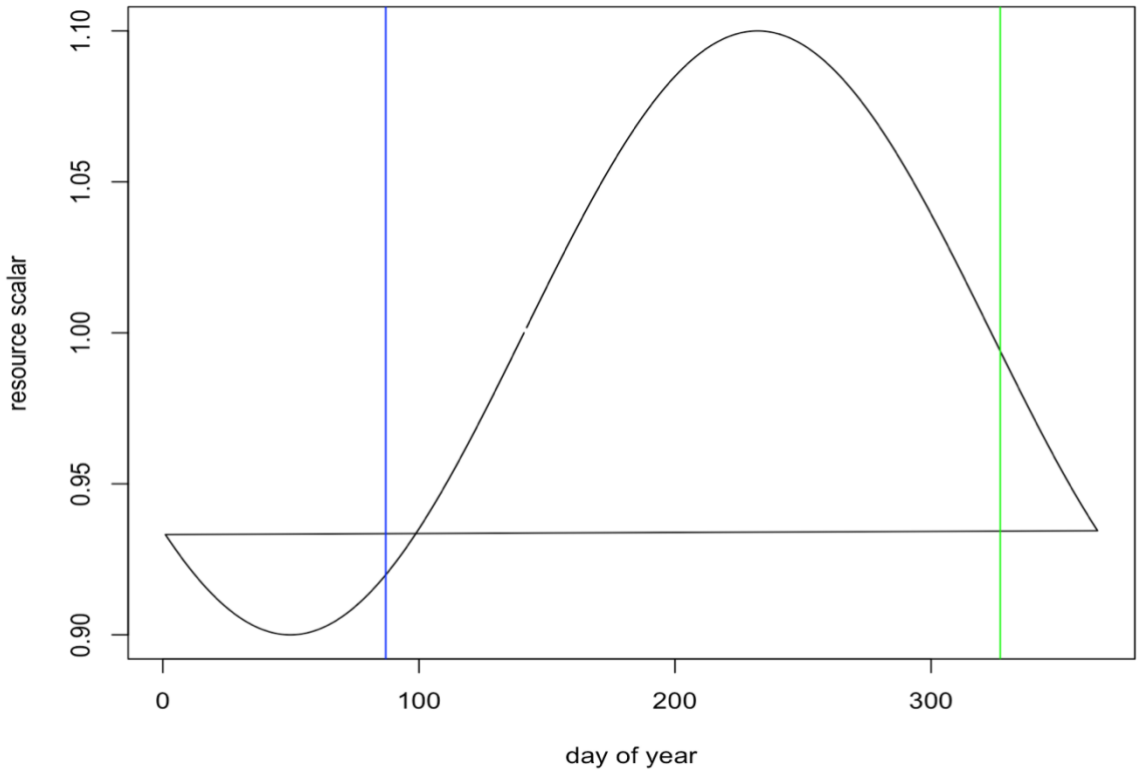

Figure 19. Modelled variation in resource density over the course of the year for a female whose mean pupping date (indicated by the vertical green line) is 23 November. The vertical blue line indicates the day on which implantation occurs.

For each simulation, mean resource density was set to a value that resulted in a population growth rate close to the value of 1.01 reported for the UK grey seal population (Sinclair et al. 2020).

6.1.2 Timing of life history events

We used a mean pupping date for each modelled population and assigned a specific birth date for each simulated female. These dates were symmetrically distributed around the mean pupping date. Simulations were started at the start of the 2nd year of life so that we could include the effects of resource density on the survival of a female's pups to age 1 year in the calculation of individual fitness.

All females that were at least 3 years old were assumed to become pregnant each year, with implantation occurring 125 days (= 365 - gestation period) after that individual's birthday.

Gestation period (T_P) We used a value of 240 days (~ eight months) as suggested by Hall and Russell (2018).

Lactation period/age at weaning (T_L) We used the value of 18 days for age at weaning suggested by Hall and Russell (2018).

6.1.3 Reserves and growth

Reserve threshold (ρ) (Boyd 1984) measured the total body weight and sculp (skin + blubber) weight of 72 adult female grey seals collected from the Farne Islands over the course of a year. Mean core weight (body weight – sculp weight) did not vary over the year, once the weight of any foetus was accounted for. Total body weight was at a minimum at the end of lactation and did not begin to increase until after implantation of the embryo; thereafter it increased to a maximum in mid-August, when sculp weight was around 42% of total body weight. Pomeroy et al. (1999) documented a mean decline in weight of 67 kg over the course of lactation for females whose mean weight at the start of lactation was 185 kg. Lang et al. (2011) estimated that lipid made up 31-34% of the total mass of Canadian grey seal females 3 days post-partum. We calculated that the equivalent post-partum values were 33-36% lipid. Hanson et al. (2019) found that lipid made up only 27% of the post-partum mass of UK grey seals. However, these animals lost significant amounts of protein during lactation, whereas the Canadian animals lost very little. This

suggests that, at least for UK grey seals, tissue other than blubber is also used as reserves. We therefore set ρ to a value of 0.5.

Reserve threshold for pups (ρ_C) The mean weight of grey seal pups at North Rona increased from around 16 kg at birth to around 43.5 kg at weaning (Pomeroy et al. 1999). We assumed that almost all of this increase was in reserve tissue, since the increase in core tissue predicted from our modification of McLaren's (1993) growth curve was only ~ 1 kg. This suggests that ρ at weaning is around 0.65, and we used a slightly higher value (0.7) as the target level for pups.

Figure 20 shows predicted variation in the total body mass of a female and her calf over the course of 1 year using these values.

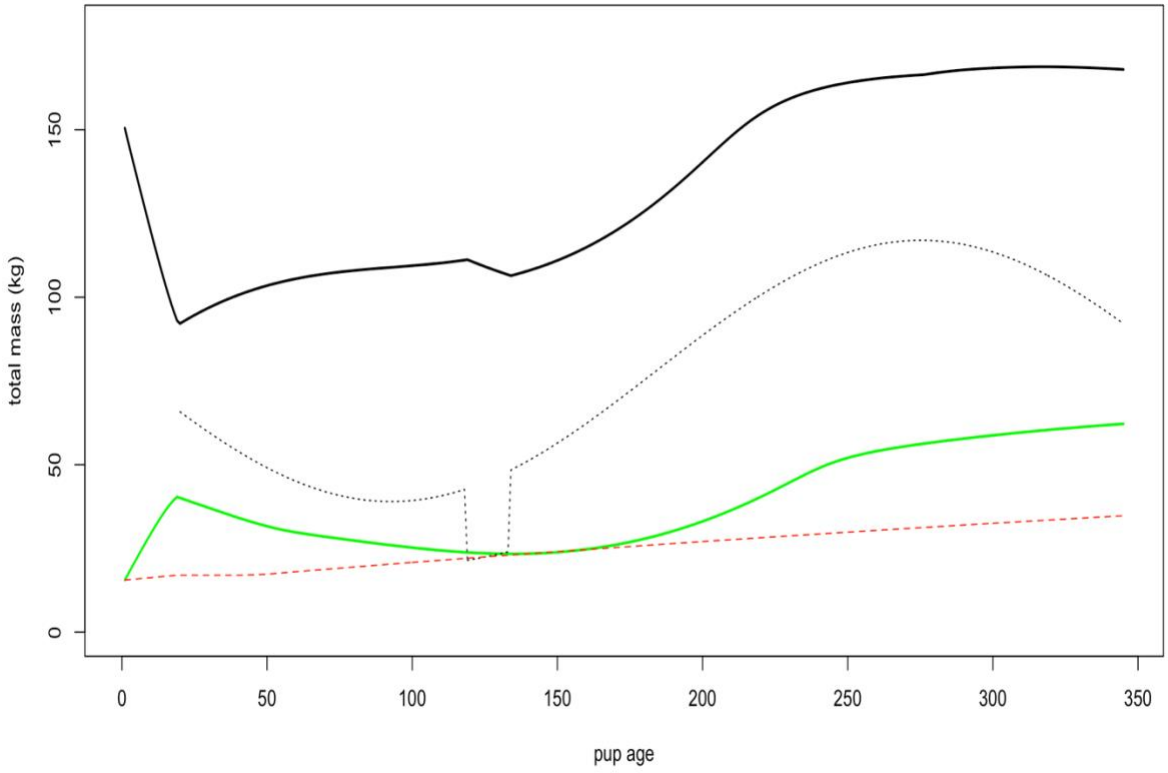

Figure 20. Predicted variation in total body weight of a female grey seal (solid black line) and her pup (solid green line) over 1 year. Cyclical variation in resource density over this period is indicated by the dotted black line (the dip around day 120 indicates the effect of the moult – when females spend more time hauled out - on energy assimilation). The red dotted line indicates the threshold mass below which pups may experience starvation-related mortality.

Relative cost of maintaining reserves (Θ_F) We were unable to find any published data that would allow a value specific to grey seals to be calculated for this parameter. We therefore used the value of 0.2 assumed by Hin et al. (2019).

Structural length and structural mass *(L_0, $L\infty$, ω_1, ω_2, k, x_0,)* (McLaren, 1993) fitted this modified Von Bertalanffy growth curve to data from 527 female grey seals sampled at the Farne Islands:

$$L_a = L\infty\left(1 - e^{-(k(a+x_0)}\right)^b$$

where *a* is age in days, k = 0.182/365, b = 0.27 and x_0 = (- 0.59 x 365). The estimated size at birth (L_0) from this equation is 99.3 cm, which is within the range of 90-105 cm reported by Bonner (1981). However, when combined with the formula used below to estimate structural mass, the estimated mass at birth is 21 kg, much higher than the values reported by Pomeroy et al. (1999). Resetting x_0 to (– 0.4 x 365) provided a more realistic estimate of 16.1 kg for birth weight, and a value of 89.8 cm for L_0.

We modelled foetal growth in terms of T_P and L_0 as:

$$L_{af} = af.L_0/T_p$$

Where *af* is foetal age in days.

Hauksson (2007) estimated the following relationship between structural length and mass for grey seals from Iceland:

$$S_a = 0.0001933L_a^{2.575}$$

However, mass in this equation includes some reserve tissue. We therefore modified Hauksson's (2007) equation to:

$$S_a = 0.00015L_a^{2.575}$$

which, when combined with estimates of F_a from the DEB model, gave a predicted mean post-partum mass for mature females of 181.5 kg, close to the values reported by Hanson et al. (2019).

Modelling growth (*K*) The model developed by Hin et al. (2019) assumes that growth in length and core mass continues unabated, regardless of energy intake. This is clearly not the case in grey seals. For example, the weight-at-age of yearling grey seals is highly variable (Hall and McConnell 2007), presumably as a result of variations in foraging success among individuals. We, therefore, assumed that growth in grey seals may be reduced if energy intake is less than the combined costs of metabolism, growth and reproductive activities (pregnancy and lactation). We modelled these circumstances using a modification of the Kappa rule which is a fundamental component of classic DEB models (Kooijman 2010). We assumed that

an individual will allocate a proportion of the assimilated energy (I_t) it acquires on a particular day to growth (including growth of the foetus, because this is treated as part of the female's core mass), up to a maximum of (1-*K*).I_t . If this amount of energy is less than the energy required for growth, the growth rate of the female and her foetus is reduced accordingly. The balance of the energy intake is allocated to metabolism. If this is insufficient to cover all of the costs of metabolism, reserves must be metabolised. Values of $K < 0.5$ indicate that growth is prioritised over metabolism. Because there is no empirical information that can be used to estimate a value for *K* we explored the implications of a wide range of values for this parameter. Mean reproductive success (total number of female offspring born to a female that survived to age 1 year) increased as *K* approached 1, implying that individuals adopting this trait would come to dominate in any population. Most simulations were conducted with a value of 0.8 for *K*. However, in Chapter 7 we explore the implications of values of *K* between 0.7 and 0.9.

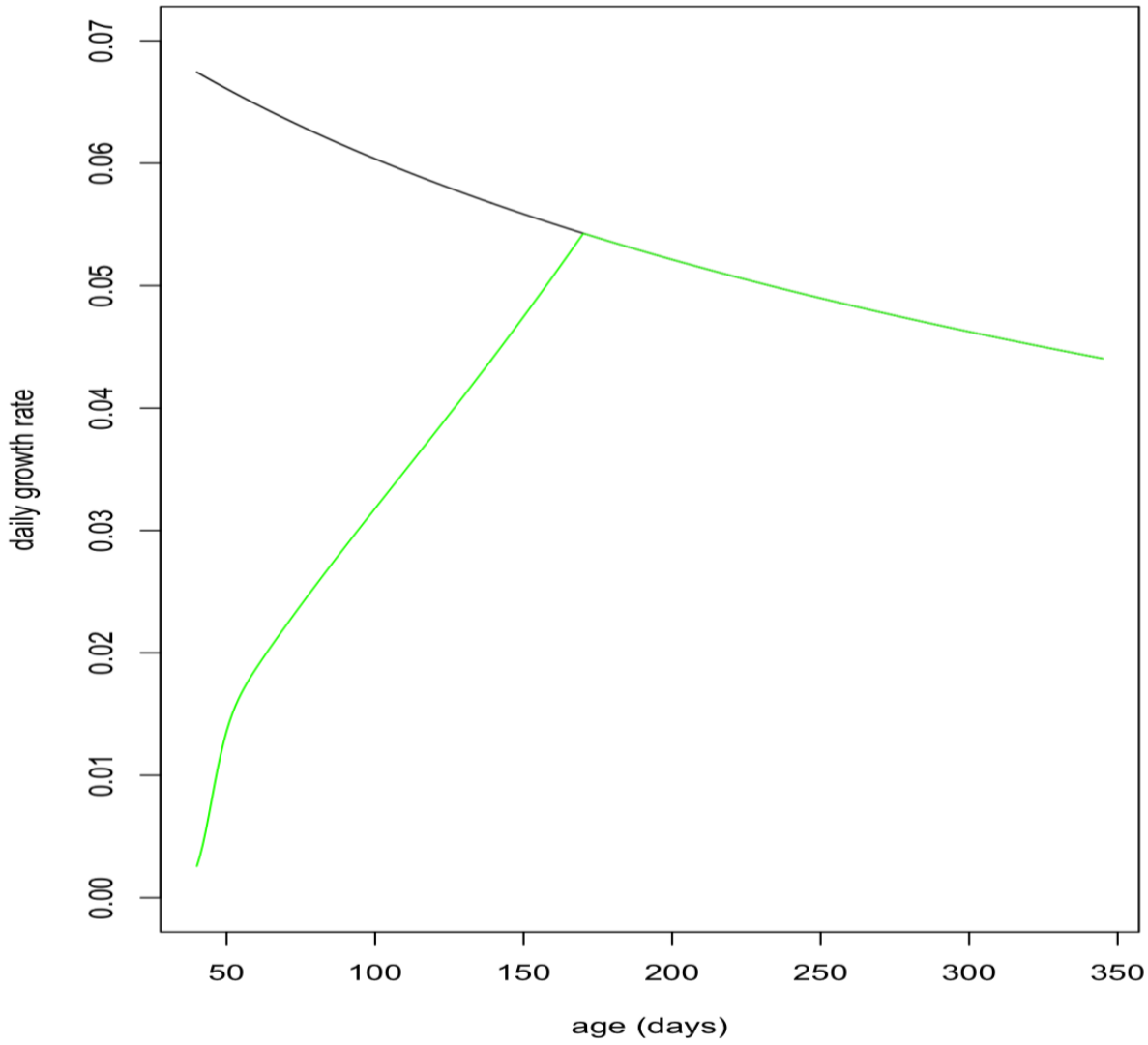

Figure 21. The effect of the Kappa rule on calf growth in kg/day. The black line shows daily growth as predicted by the underlying growth curve and the green line shows realised growth with Kappa=0.8. The reduced level of growth during the first

160 days of life is a consequence of the relatively low feeding efficiency of young animals who are unable to assimilate enough energy to cover the combined costs of maintenance and growth.

Field metabolic maintenance scalar (σ_M) Sparling et al. (2006) measured the RMR of captive adult and juvenile grey seals based on oxygen consumption and estimated that this was, on average, 1.95x that predicted by Kleiber's equation. Sparling and Fedak (2004) measured the Diving Metabolic Rate (DMR) of captive grey seals and found that this was 1.7x the RMR predicted by Kleiber's equation. They note that predictions of FMR of 2-3x the Kleiber value "*might be higher than they are in reality*". Most simulations were carried out using a value of 2.5x Kleiber for the entire life history of simulated animals because Reilly et al. (1996) estimated that the FMR of lactating female grey seals was 2.3x Kleiber, and Paterson et al. (2019) estimated that the FMR of moulting phocid seals was also 2.3x Kleiber. However, in Chapter 7 we explore the implications of higher and lower values for this parameter.

Energetic cost per unit structural mass (σ_G) We calculated growth efficiency using the same approach as Hin et al. (2019) and an energy density for foetal tissue of 6.5 MJ/kg (the mean of the values for new-born harp and grey seal pups reported by Worthy and Lavigne (1987)). This produced a value of 25 MJ/kg for σ_G.

Catabolic and anabolic efficiency of reserve conversion (ε_-, ε_+, ε_{+pups}) Results from studies of the weight loss of fasting pinnipeds, described in more detail in Harwood et al. (2019), indicate that the energy density of phocid reserve tissue is 20-25 MJ/kg. In the absence of any direct measurements of these parameters for adult grey seals, we followed Hin et al. (2019) and used a range of values that were 90% of the energy density of reserve tissue for ε_- and 40% higher for ε_+. Pups convert the lipid rich milk supplied by their mothers to reserve tissue and this process is probably more efficient than the conversion of normal food. We calculated the cost of this process from Reilly et al.'s (1996) estimate that the mean daily energy expenditure of grey seal pups is 13.5 MJ. This includes the costs of metabolism, growth in core tissue and accumulation of reserves. We calculated the mean costs of metabolism and core growth using the DEB model and subtracted these costs from 13.5 MJ to estimate the additional costs of accumulating reserves, which was 2.67 MJ/kg. This suggests that ε_+ for pups is 11-13% higher than the energy density of reserves.

Steepness of assimilation response (η) We were unable to find any data in the literature that could be used to set a feasible range for this parameter. We explored the implications of values between 5 and 40 and found that mean reproductive success was maximized when η = 40.

Effect of age on resource foraging efficiency (Y, $T_{R,\,pw\_fast}$): Grey pups undertake a post-weaning fast of approximately 21 days (Noren et al. 2008). After this, they continue to lose weight for the next 3 months (Hall and McConnell 2007) but regain their initial weight around the age of 6 months. We assumed that foraging

efficiency was 0 up to the age of 39 days (T_L + 21) and experimented with various combinations of T_R and Y to see if we could duplicate Hall and McConnell's (2007) observations while still ensuring that female feeding efficiency was close to 100% by the time they were 5 years old.

Moult duration and reduction in foraging during moult: To take account of the fact that seals spend more time hauled out when they are moulting (Paterson et al., 2012), and are therefore likely to acquire less energy, we reduced foraging efficiency by 50% for 10 days before and after implantation (Figure 22 shows the resulting variation in foraging efficiency over the first 5 years of life).

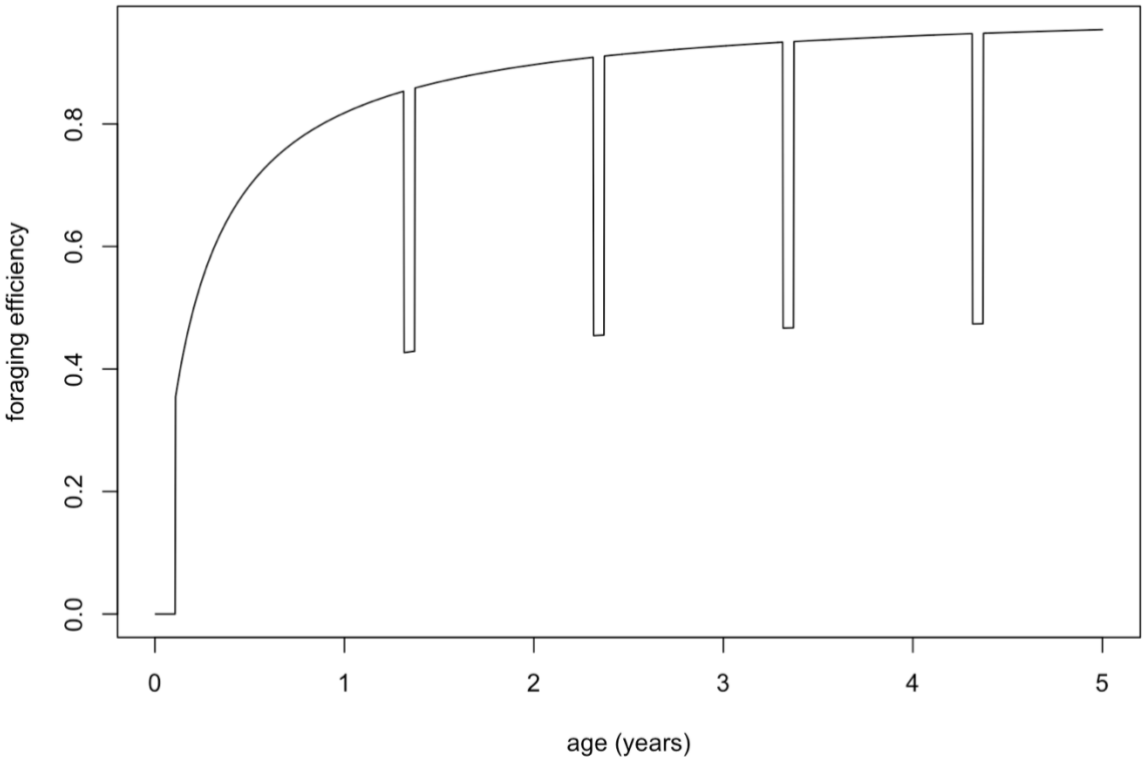

Figure 22. Predicted variation in foraging efficiency with age, showing the reduction in efficiency during the annual moult, which begins in the second year of life

6.1.4 Pregnancy

Pregnancy threshold (*decision_day*) Smout et al. (2019) documented a relationship between a female grey seal's mass at the end of lactation and the likelihood of giving birth in the following breeding season. The threshold mass that resulted in a 0.5 probability of giving birth was lower if prey abundance was greater than average in the subsequent year. The relationship is:

$$P\{\text{pupping}\}_{t+1} = \exp(a_p + b_b \varepsilon_t W_{j,t})/(1 + \exp(a_p + b_b \varepsilon_t W_{j,t}))$$

where $W_{j,t}$ is female mass at weaning in year t. Because $M_{j,t+1} = \delta \varepsilon_t W_{j,t}$ this can be rewritten as:

$P\{pupping\}_{t+1} = \exp(a_p + (b_b/\delta)M_{j,t+1})/(1 + \exp(a_p + (b_b/\delta)M_{j,t+1}))$

where $M_{j,t+1}$ is predicted female post-partum mass in year $(t+1)$, β indicates mass loss during lactation (0.65 at the two colonies studied by Smout et al. 2019), with a tight 95% credible interval), δ is mass gain during pregnancy (estimated as 1.4 at both colonies) and ε_t is a year effect related to sandeel density or the strength of the North Atlantic Oscillation. Figure 23 shows how resource density affects age-specific birth rates using this relationship.

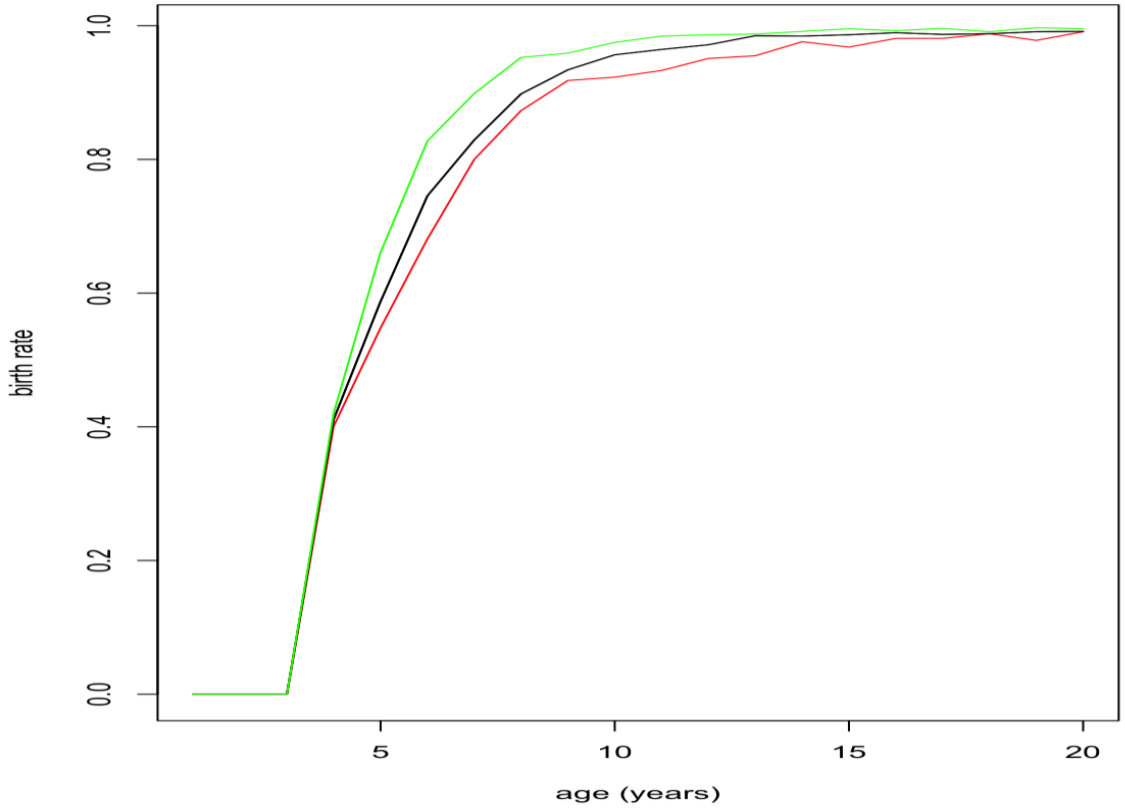

Figure 23. Predicted variation in birth rate with age at three different resources densities (*Rmean* = 1.6 in red, *Rmean* = 1.63 in black, *Rmean* = 1.7 in green). Each curve is based on simulations for 2000 females.

Given that changes in body mass from the end of lactation until implantation are relatively small (Boyd 1984), the decision to give birth to a pup is probably made some time during pregnancy, rather than at implantation. However, the exact time at which females should make this decision is not entirely obvious and we considered the implications of a making that choice at a number of different points during pregnancy.

6.1.5 Lactation

Efficiency of conversion of mother's reserves to calf/pup tissue (σ_L): Lang et al. (2011) estimated that approximately 70% of the energy obtained by grey seal pups from milk was converted into tissue. However, this "storage efficiency" includes the costs of maintenance. We therefore used the value of 0.86 from Hin et al. (2019).

Effect of calf/pup age on milk assimilation (T_C , ξ_C) There appears to be little variation in the amount of milk provided to the calf over the duration of lactation, suggesting that T_C should be close to T_L. We chose values of (T_L *-1*) days and 0.95 for these parameters.

Effect of female body condition on milk provisioning (ξ_M) Although it would be possible to estimate an appropriate value for this parameter from the raw data generated by Pomeroy et al. (1999) and Bowen et al. (2006), those data are not presented in the relevant papers thus precluding this analysis. Because females are "anticipating" a large reduction in their body condition during lactation we explored the implications of a range of values and found that ξ_M = 2 best reproduced observed changes in milk delivery.

Lactation scalar (Φ_L) All of a grey seal pup's energy requirements during the lactation period must be supplied by milk. As noted above, Reilly et al. (1996) estimated that grey seal pups expend 13.5 MJ/day during lactation. If pups achieve their target body condition of 0.7 at the end of lactation they will have gained 31 kg. Using this value in Hin et al.'s (2019) formula gives Φ_L = 8.85 if ε = 25.8 MJ/kg.

6.1.6 Mortality

Age-dependent mortality rate We followed the approach used by Hin et al. (2019) and estimated changes in the probability of survival with age using the approach developed by Barlow & Boveng (1991). The following function describing the variation in daily survival with age:

$$Surv_a = e^{-(\alpha_1 e^{-\beta_1 a} + \alpha_2 e^{\beta_2 a})}$$

where *a* is age in days, was fitted to the annual age-specific grey seal survival rates estimated by Thomas et al. (2019). Their population model includes a density-dependent term for first-year survival, and we used the maximum value (0.478) because they assumed density-dependence operates via reduced prey availability. This value is very close to the product of survival from birth to weaning of 0.831 reported by Pomeroy et al. (1999) for grey seal pups at North Rona and the estimate of survival from weaning to age 1 obtained by Hall et al. (2001). Figure 24 shows the resulting relationship between age and cumulative survival, with:

α_1 = 0.007

β_1 = 0.01

α_2 = 0.00013

β_2 = 0.000001

and a maximum age of 40 years. The life expectancy of each simulated female was calculated by choosing a random number between 0 and 1 and determining the age in days at which cumulative survival equalled this value.

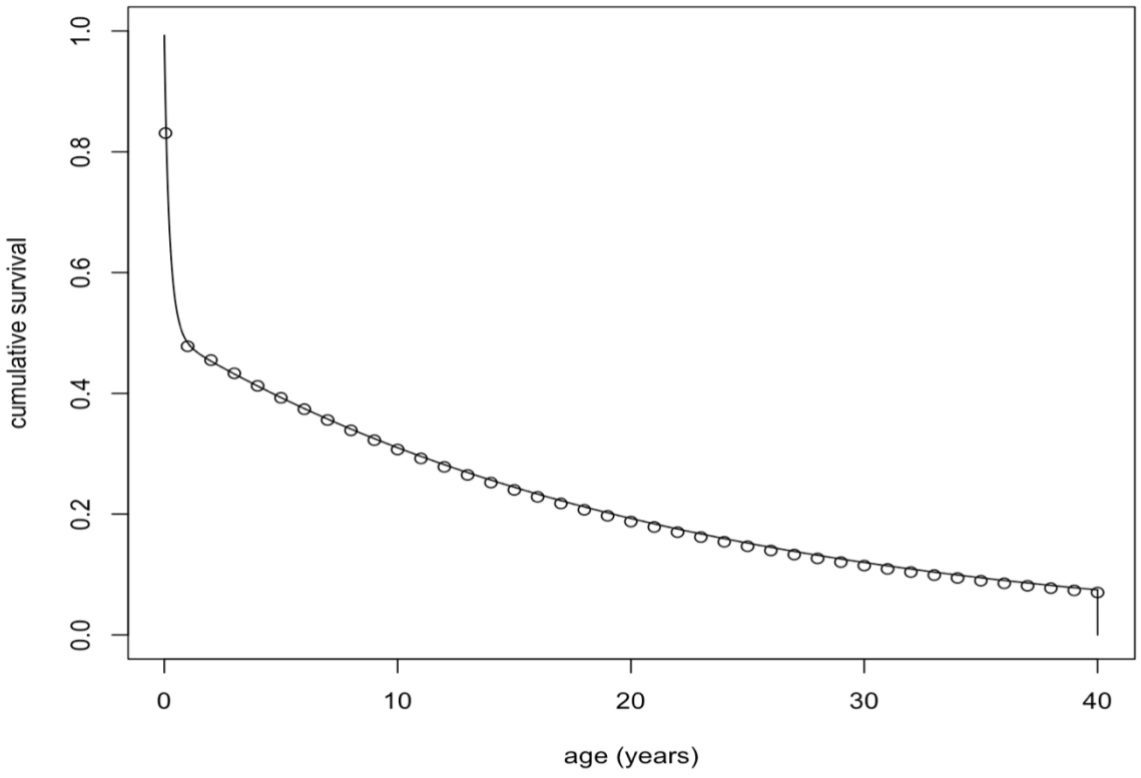

Figure 24. Cumulative survival curve for female grey seals used in simulations, with annual survival values estimated by Thomas et al. (2019) shown by open circles.

Starvation body condition threshold *(ρ_s)* The body condition of female grey seals declines to around 0.15 at the end of lactation, which would suggest a value of 0.1 for ρ_s. However, the implications of other values for this parameter are explored in Chapter 7.

Starvation-induced mortality rate (μ_s) No empirical information that could provide a species-specific value of this parameter for grey seals is available. As a starting point for exploratory modelling we used the value of 0.2 proposed by Hin et al. (2019) but we also explore the implications of other values.

6.2 Model results – pattern-oriented modelling

We compared the DEB models outputs with information from Hall and McConnell (2007), Hanson et al. (2019) and Smout et al. (2019) on the total mass and body condition of calves and adult females at different stages of their life cycle.

Hall and McConnell (2007) found that grey seal pups from the Isle of May lost mass and total body fat during the first 5-6 months of life after leaving the breeding colony, but pups that survived beyond 6 months regained their lost mass. Simulated animals showed a similar pattern of change in total weight and body condition, losing 30% of their weight and most of their reserves in the first 6 months of life. They recovered all of this lost weight over the subsequent 6 months and were 33% heavier than when they left the breeding colony by their first birthday. However, their body condition was substantially higher at this age than the 12% total body fat observed by Hall and McConnell (2007). This suggests that the target body condition for young animals may be lower than for adults.

Hanson et al. (2019) measured changes in the mass of lactating female grey seals at two UK colonies (North Rona and the Isle of May) over a number of years. They found that, on average, the mass of females at the end of lactation was 66% of their post-partum mass. This is very similar to the average change in mass over the course of lactation estimated by Smout et al. (2019) using the same data but a different analytical approach (see below). The mass of simulated grey seal females at the end of lactation was 69% of their post-partum mass, suggesting that the DEB model may underestimate the costs of lactation. This is reflected in the fact that the average weaned weight of simulated pups (32 kg) was lower than the mean weight of weaned pups from the Isle of May colony (~45 kg) studied by Bennett et al. (2007). However, it is not clear whether the pups in Bennett et al.'s (2007) study were a representative sample of all weaned pups.

The model used by Smout et al. (2019) to estimate the effects of female weight at the end of lactation on the probability of giving birth in the following year, described in Section 4.1, also provided an estimate of the average increase in weight over the same period. This was determined by the product of the two parameters δ and ε_t. δ was estimated to be 1.4 at the Isle of May and 1.34 at North Rona which varied from year to year but, from Figures 3 and 4 of Smout et al. (2019) it appears to have averaged around 1.09 for Isle of May seals and 1.12 for North Rona seals, resulting in an average predicted post-partum mass that was 1.5 x mass at weaning in the previous year. The equivalent value from the DEB model was 1.45.

6.3 Simulating the effect of disturbance

Disturbance was simulated by reducing resource density by a proportion $Dist_{effect}$ on the days on which disturbance was predicted to occur. This has the effect of reducing assimilated energy by the same amount. We modelled the effect of increasing numbers of days of disturbance in the following periods of the annual cycle:

- from the date on which pups are weaned to the day of embryonic implantation (equivalent to the “high” impact period used for harbour seals);
- from implantation to the day on which a decision whether or not to continue a pregnancy is made (equivalent to the “low” impact period used for harbour seals); and
- from this decision day to the mean birthday (equivalent to the “medium” impact period used for harbour seals).

The disturbance effect parameter ($Dist_{effect}$) was set to either 0.14 or 0.25, based on the values derived from direct observations of tagged harbour seals and harbour porpoises respectively.

We investigated the effects of disturbance on pup survival and birth rate for 1,000 mature adults (20 years of age), and on 1,000 10 year-old females to assess the consequences of the relatively higher cost of pregnancy and lactation for smaller individuals.

6.3.1 Weaning to implantation

Disturbance in this period (equivalent to December to late March for Farne Islands’ seals) had no effect on birth rate. However, the survival of pups born to fully-grown females (>20 years old) declined steadily with increasing levels of disturbance (Figure 25) and was 0 if disturbance exceeded 60 days if $Dist_{effect}$ =0.14 and if it exceeded 40 days with $Dist_{effect} = 0.25$. Disturbance had a similar effect on the survival of pups born to younger females, but pup survival was reduced to 0 if disturbance exceeded 15 days, because the undisturbed survival of their pups was lower. For these females there was also a small effect on birth rate, which was reduced by 5% if disturbance exceeded 50 days.

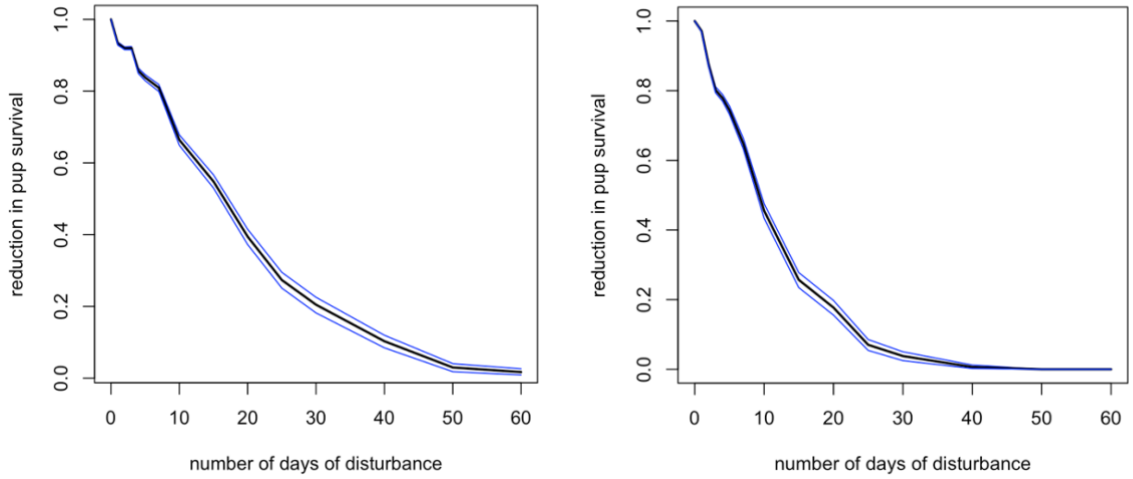

Figure 25. Effect of disturbance between the end of the pupping season and the day of implantation on the survival of pups born to 21 year old females. The black line is the mean, and the blue lines enclose 90% of 10,000 bootstrapped estimates. Left-hand panel: disturbance effect = 0.14; right-hand panel: disturbance effect = 0.25.

6.3.2 Implantation to “decision day”

Disturbance during this period (equivalent to late March to the end of August for Farne Islands’ seals) had no effect on birth rate for mature females, but it did result in a reduction in pup survival (Figure 26). However, the reduction was slightly less than that caused by disturbance in the immediate post-weaning period.

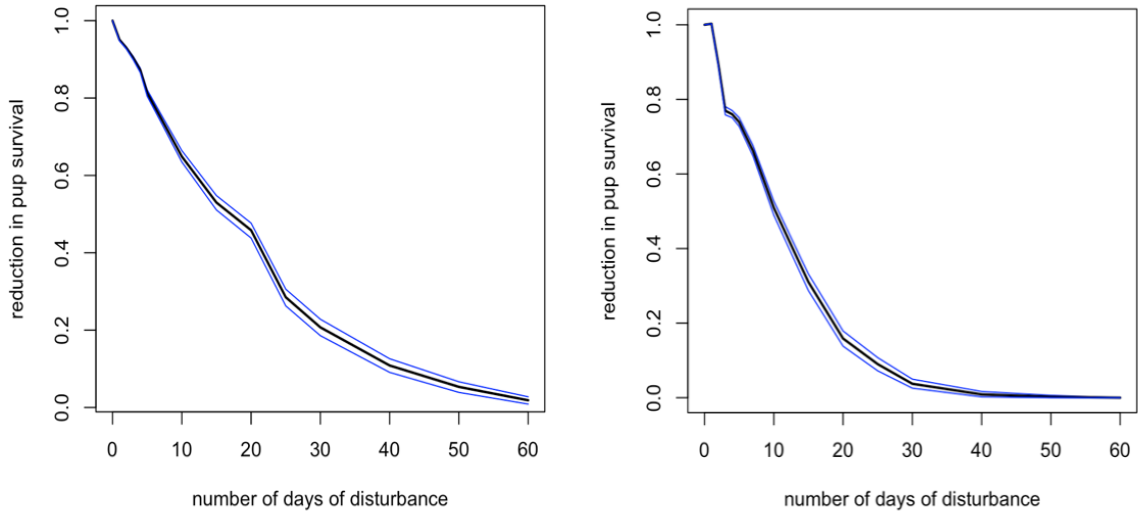

Figure 26. Effect of disturbance between the day of implantation and the day on which females decide whether or not they will continue their pregnancy on the

survival of pups born to 21 year old females. The black line is the mean, and the blue lines enclose 90% of 10,000 bootstrapped estimates. Left-hand panel: disturbance effect = 0.14; right-hand panel: disturbance effect = 0.25.

Disturbance during this period also has a small effect on the birth rate of younger females (Figure 27), but the population consequences of this will be trivial because of the high mortality rate experienced by pups born to these females.

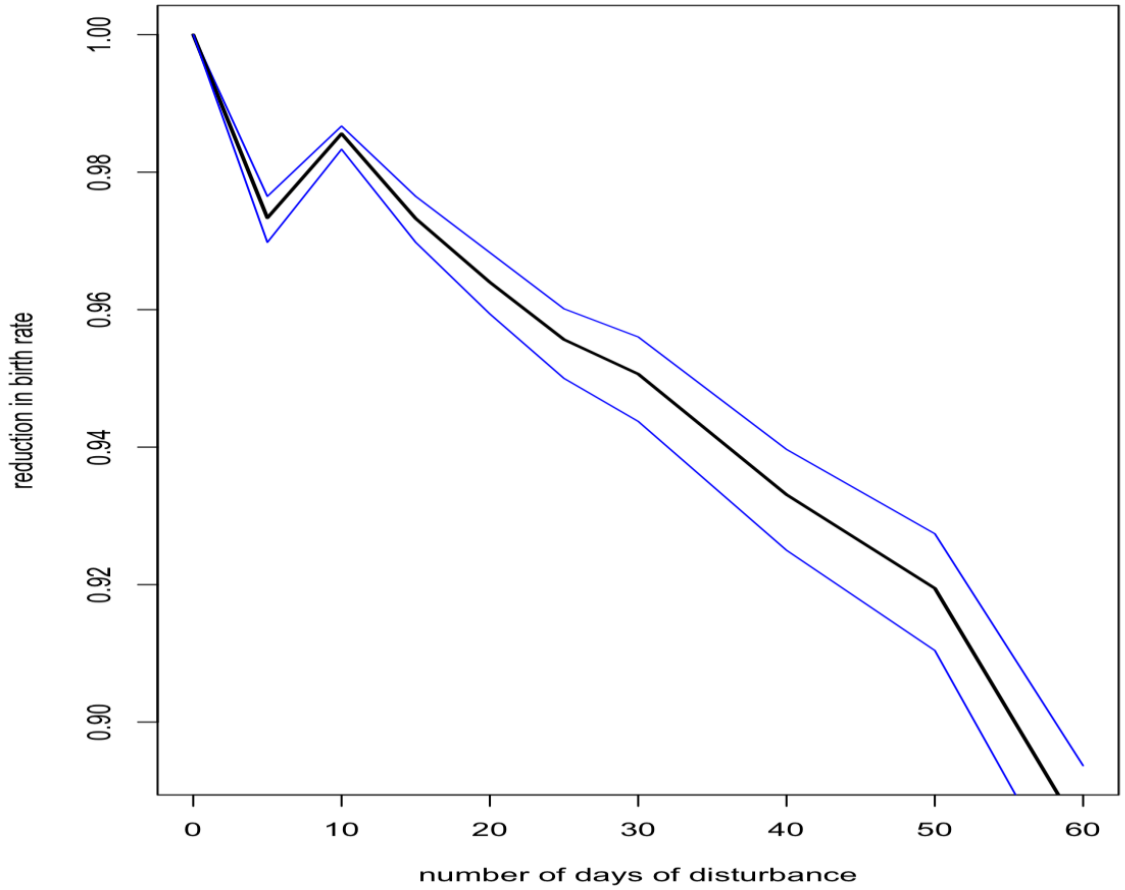

Figure 27. Effect of disturbance between the day of implantation and the day on which females decide whether or not they will continue their pregnancy and the birth rate of 10 year old females. The black line is the mean, and the blue lines enclose 90% of 10,000 bootstrapped estimates.

6.3.3 “Decision day” to birth of pup

The main effect of disturbance at this time (August to mid-November for Farne Islands’ grey seals) is to reduce the body condition of females at parturition. As a result, their pups are weaned at a lower mass and this affects their subsequent survival, as shown in Figure 28. Pup survival generally declines to zero if the number of days of disturbance exceeds 40 days. However, this would require disturbance to occur on every day during this period.

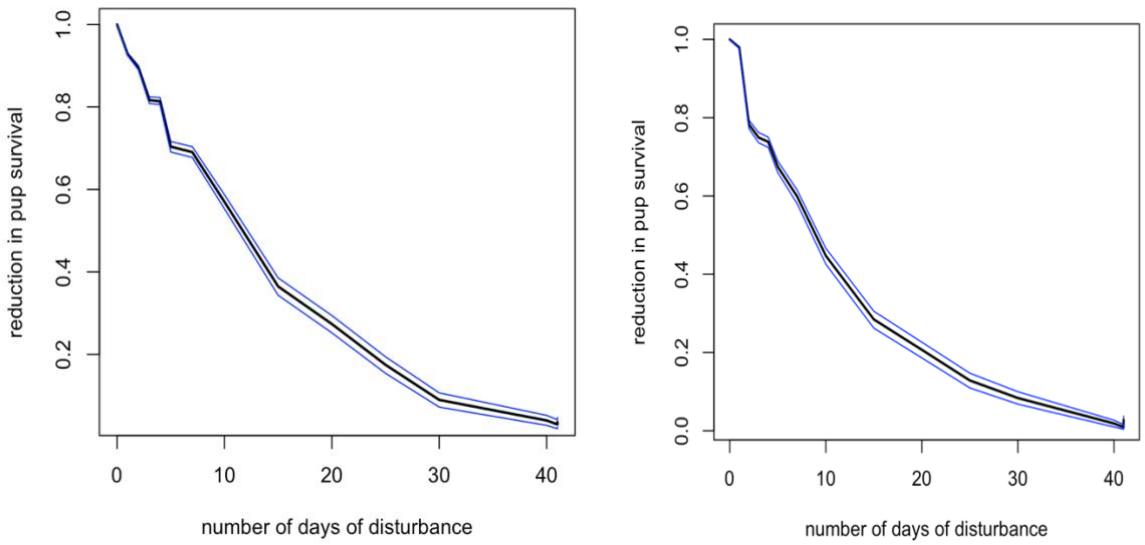

Figure 28. Effect of disturbance between the day on which females decide whether or not they will continue their pregnancy and the mean date on which those pups are born on the survival of pups born to 21 year old females. The black line is the mean, and the blue lines enclose 90% of 10,000 bootstrapped estimates. Left-hand panel: disturbance effect = 0.14; right-hand panel: disturbance effect = 0.25.

7 Bottlenose dolphin in the NE Atlantic DEB model

7.1 Model parameters

Table 7 shows the baseline parameter values used in the model. Details of how these values were derived are outlined below.

Table 7. Parameter values used in the bottlenose dolphin DEB model.

Parameter names	Code name	Value	Description	Source
Resource density				
R	Rmean	3.54	Annual mean resource density	See text
a_{beta}	a_beta	23.65	Shape parameters of beta distribution defining stochasticity in	See text
b_{beta}	b_beta	19.35		See text

Parameter names	Code name	Value	Description	Source
			resource density	
	amplitude	0.1	Parameter defining the amplitude of seasonal variation in resource density	See text
	offset	0 days	Parameter determining when during the year *Rmean* has its maximum value	See text
Timing of life history events				
min_age	min_age	5 years	Minimum age for reproduction	
mean_birth day	mean_birthday	15 July	Mean calving date for Moray Firth	Cheney et al. (2019)
T_P	Tp	365 days	Gestation period	Perrin & Reilly (1984)
T_L	Tl	1095 days	Age at weaning (duration of lactation)	See text
T_R	Tr	412 days	Age at which calf's resource foraging efficiency is 50%	See text
max_age	max_age	65 years	Maximum age	Wells & Scott (2018)

Parameter names	Code name	Value	Description	Source
	max_age_calf	1075 days	Maximum modelled age of calf	
Reserves				
ρ	rho	0.34	Target body condition for adults	See text
θ_F	Theta_F	0.2	Relative cost of maintaining reserves	Hin et al. (2019)
Growth				
L_0	L0	165.4 cm	Length at birth	B.Cheney (pers.comm.)
L_∞	Linf	343.3 cm	Female maximum length	
b	b	-0.69545	5-parameter log-logistic dose-response curve developed by Finney (1979).	
ee	c	0.1		
M	M	5.38968		
ω1	omega1	$(1-\rho_S)*10^{-5.03}$ kg/cm	Structural mass-length scaling constant	Lower 95% quantile from Hart et al. (2013)
ω2	omega2	3.01	Structural mass-length scaling exponent	
Energetic rates				
σ_M	Sigma_M	4.5	Field metabolic maintenance scalar	Field measurements fin winter from Bejarano et al. (2017)

Parameter names	Code name	Value	Description	Source
σ_G	Sigma_G	30 MJ/kg	Energetic cost per unit structural mass	Derived using the approach of Hin et al. (2019)
ε	epsi	25.8 MJ/kg	Energy density of reserve tissue	
ε-	epsi_minus	23.2 MJ/kg	Catabolic efficiency of reserves conversion	
ε+	epsi_plus	35.5 MJ/kg	Anabolic efficiency of reserve conversion	Reilly et al. (1996)
μ_s	mu_s	0.2	Starvation mortality scalar	Hin et al. (2019)
η	eta	20	Steepness of assimilation response	See text
ϒ	upsilon	0.95	Shape parameter for effect of age on resource foraging efficiency	See text
K	Kappa	0.5	Proportion of the daily assimilated energy allocated to growth	See text
Pregnancy				
fert_success	fert_success	0.714	Probability that implantation will occur	O'Brien & Robeck (2012)

Parameter names	Code name	Value	Description	Source
$F_{neonate}$	F_neonate	0.8* $F_{neonate}$ kg	Threshold for pregnancy	See text
Lactation				
φ_L	phi_L	5.4	Lactation scalar	See text
σ_L	Sigma_L	0.86	Efficiency of conversion of mother's reserves to calf tissue	Lockyer (1993)
T_N	Tn	183 days	Calf age at which female begins to reduce milk supply	See text
ξc	xi_c	0.2	Non-linearity in milk assimilation-calf age relation	See text
ξ_M	xi_m	2	Non-linearity in female body condition-milk provisioning relation	See text
Mortality				
foetal_mortality	foetal_mortality	0.14	Background foetal mortality	
α_1	alpha1	0.00039	Coefficients of age-dependant mortality curve	Thomas et al. (2019)
α_2	alpha2	1.5×10^{-4}		
β_1	beta1	0.005		
β_2	beta2	0.5×10^{-8}		
ρ_S	rho_s	0.1	Starvation body condition threshold	See text

Parameter names	Code name	Value	Description	Source
μ_s	mu_s	0.2	Starvation mortality scalar	See text
Disturbance				
$Dist_{dur}$	days.of.disturbance		Number of days on which disturbance occurs	See text for values
$Dist_{start}$	first_day		First day of disturbance period	See text for values
$Dist_{end}$	Last_day		Last day of disturbance period	See text for values
$Dist_{effect}$	disturbance.effect	0.25	Reduction in resource density caused by disturbance	See text
Age_{Dist}	age.affected		Age threshold defining which age class of simulated animals is affected by the disturbance	See text

7.1.1 Resources

Resource density (*Rmean*) The strong seasonality in births observed in the Moray Firth bottlenose dolphin population (Cheney et al. 2018) suggests that resource density varies through the year and that ovulation is timed to optimize the lifetime reproductive success of females. We therefore experimented with the patterns of seasonal variation in *Rmean* shown in Figure 29 and identified which pattern resulted in the greatest reproductive success. Individual females had much higher reproductive success when *Rmean* varied according to the pattern illustrated in green in Figure 29, with a maximum value around 14 October (mid-way through the period when lactating females are provided all of their calves energy requirements),

across a range of parameter values. We therefore used this pattern in all our simulations, although we investigated the effect of different values for the amplitude of the cycle.

In the original Hin et al. (2019) model, *Rmean* is assumed to be constant or to vary smoothly over the course of the year. However, in reality, the resource density encountered by an individual is likely to vary from day to day. This stochasticity in resource density can be modelled by multiplying *Rmean* for each day by a number drawn at random from a beta distribution with mean=1 and a 90% confidence interval of 0.5-1.5. Extreme values for this multiplier could be as low as 0.1 or as high as 2.4. We assumed that calves encountered the same resource density as their mothers on each day.

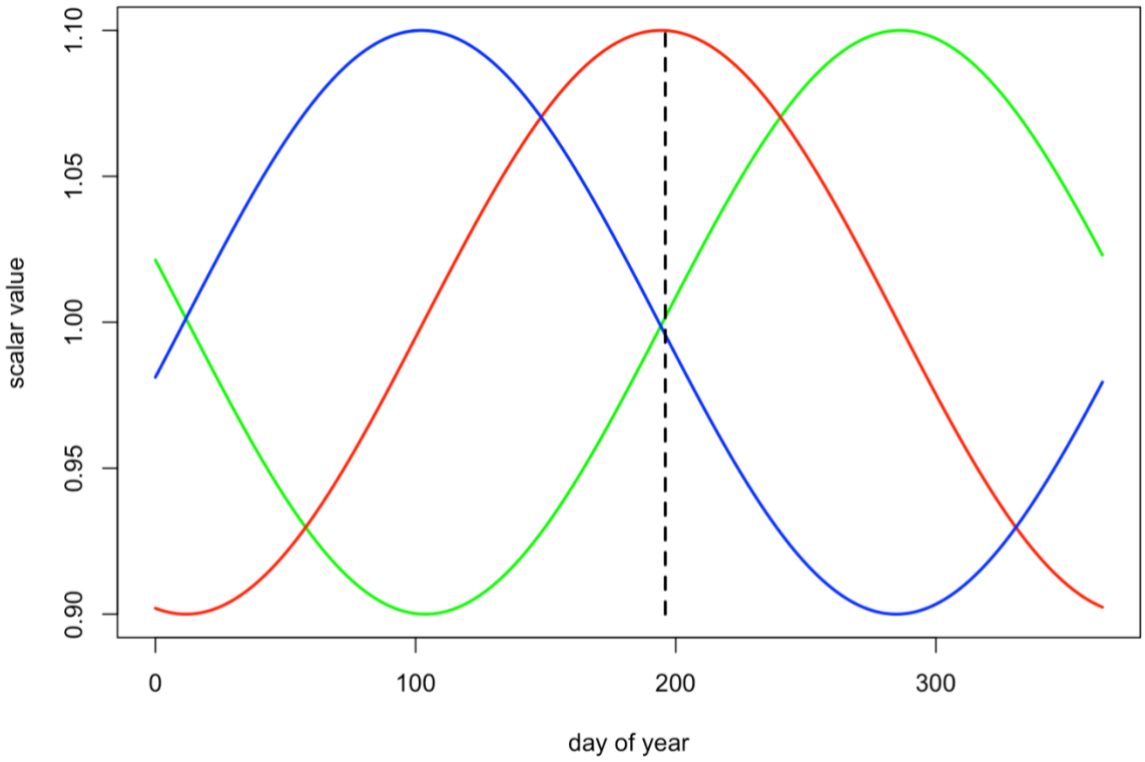

Figure 29. Seasonal patterns of variation in resource density that were evaluated. The vertical dotted line indicates the mean birth date for calves in the Moray Firth. Blue = maximum resource density on 14 April, red = maximum resource density on 15 July, green = maximum resource density on 15 October.

7.1.2 Timing of life history events

Cheney et al. (2018) detected a clear peak in first sightings of bottlenose dolphin calves in the Moray Firth between 1 June and 30 September. We therefore assumed that sexually mature female bottlenose dolphins ovulate every year, unless they have a young calf (in our simulations this is defined as a calf that is less than (T_L-T_p) days old). For simplicity, we assumed that each female ovulates on her birthday,

which was randomly chosen from a normal distribution with a mean equivalent to 15 July (the modal date on which calves in the Moray Firth were estimated to be born (see Figure 4 in Cheney et al. 2018) and a standard deviation of 10 days, which resulted in 99% of births occurring in a 50 day period centred on the mean birth day.

Gestation period (T_P) This is generally considered to be 365 days (Perrin and Reilly 1984), although slightly longer periods (up to 395 days) have been recorded in captive animals (O'Brien and Robeck 2012). We used 365 days.

Lactation period/age at weaning (T_L) Perrin and Reilly (1984) report an average age at weaning of 18-20 months. The oldest nursing calf presented in Table 7 in Perrin and Reilly (1984) was 38 months. A similar range (14-37 months) was recorded for captive animals by Kastelein et al. (2002). However, Grellier et al. (2003) reported that mother-calf pairs in the Moray Firth remain associated for 3 to "at least 8" years. We therefore investigated a range of values from 550 days (18 months) to 1095 days (3 years). Figure 30 shows that a 550 day lactation period maximizes lifetime reproductive success at high values of resource density (*Rmean*), but lifetime reproductive success declines sharply as *Rmean* is reduced because newly-weaned calves (which are relatively small) cannot maintain their weight, even if their body condition at weaning is close to ρ. At lower values of *Rmean*, a 730 day lactation period becomes optimal but reproductive success declines sharply as *Rmean* is reduced, because of low post-weaning survival. In both cases, calf survival remains high across the entire range of *Rmean* values. At even lower values of *Rmean*, a 1095 day lactation period becomes optimal, but in this case it is calf survival rather than post-weaning survival that decreases as *Rmean* is reduced. We conducted most simulations with a lactation duration of 1095 days because this allows a population to persist over a wide range of resource densities and the effects of changes in resource density on demographic rates are similar to those observed in the wild (i.e., a reduction in calf survival with decreasing prey availability or increasing population size).

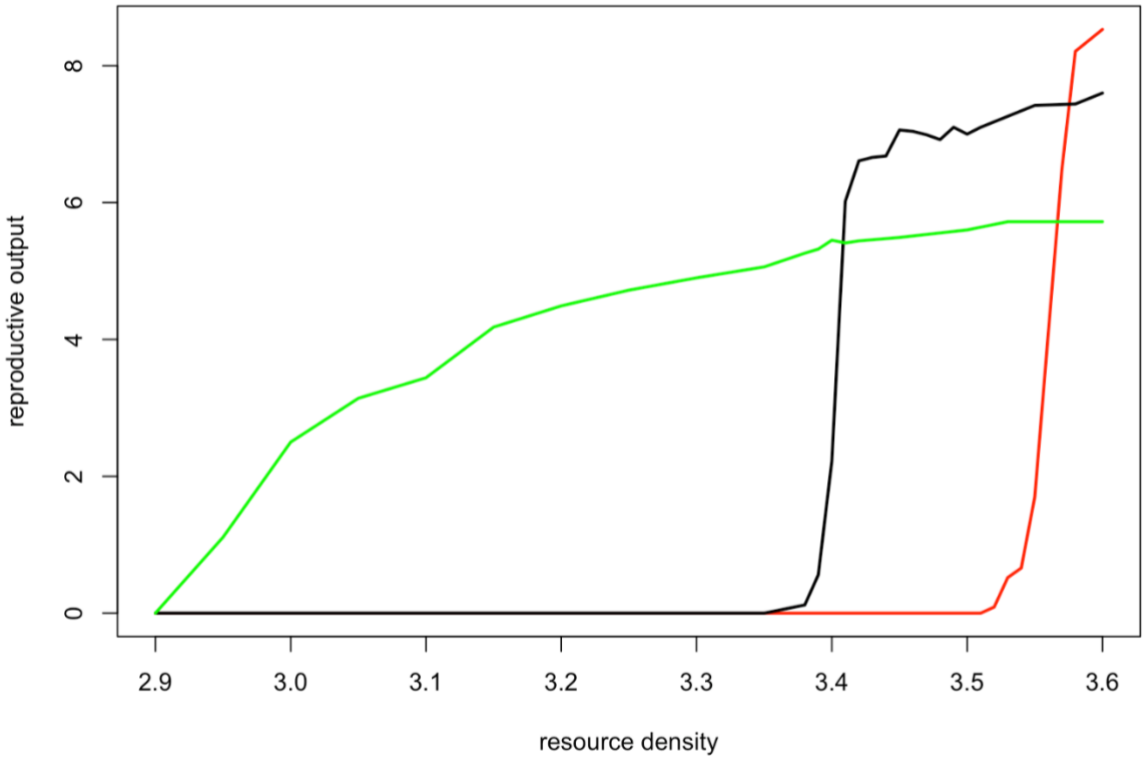

Figure 30. The relationship between resource density (*Rmean*) and lifetime reproductive success for a female that survives to the maximum age of 65 years. The green line shows the relationship for a lactation duration (TL) of 1095, the black line is for TL = 730, and the red line for TL = 550 days.

7.1.3 Reserves and growth

Reserve threshold (ρ) Bottlenose dolphins have a relatively thin blubber layer (thoracic blubber thickness 12-18 mm, based on Figure 2 of Noren and Wells 2009), with an almost two-fold increase in estimated blubber mass between summer and winter for animals older than 2 years (Figure 3 in Noren and Wells 2009). This suggests that blubber's main role in this species is to provide insulation rather than to act as an energy store.

An alternative measure of reserve size can be derived from the difference in mass of dolphins of the same length. In an extensive analysis of measurements from bottlenose dolphins in Sarasota Bay, Florida, Hart et al. (2013) fitted a set of equations for predicting mass from length; we used their upper 95% quantile relationship between length and mass to estimate the target body condition by assuming that the difference in mass between the estimates from this relationship and the calculated value of S_a at the same age represented reserve tissue. This gave a value of 0.34 for ρ.

Relative cost of maintaining reserves (Θ_F) We were unable to find any published data that would allow a value specific to bottlenose dolphins to be calculated for this

parameter. We, therefore, suggest using the value of 0.2 assumed by Hin et al. (2019).

Structural length and structural mass *(L_0, L_∞, ω_1, ω_2, b, c , M)* Most published growth curves for bottlenose dolphins (e.g., Stolen et al. 2002, Neuenhoff et al. 2011, Bejarano et al. 2017) are not appropriate for UK bottlenose dolphin populations because the maximum length obtained by UK animals is substantially greater than observed elsewhere. However, Cheney et al. (2018) fitted a version of Richard's (1959) growth curve using the 5-parameter log-logistic dose-response curve developed by Finney (1979) to field measurements of known-age Moray Firth bottlenose dolphins using laser-photogrammetry, calibrated with data from stranded animals. This has the form:

$$L_a = L_0 + (L_\infty - L_0)/\left[1 - e^{b(\log(a)-c)}\right]^M$$

where L_a is length at age a (in years); L_∞ is asymptotic length; L_0 is length at birth; b and c are free parameters that adjust the slope and inflection point of the curve; and M describes the position of the inflection point relative to the asymptote. The fitted values (B. Cheney, pers. comm.) were

L_0 = 165.4 cm

L_∞ = 343.3 cm

b = -0.695

c = - 2.303

M = 5.390

In order to estimate core body mass from length we used the results of an analysis by Hart et al. (2013) of the relationship between mass and length based on an extensive set of measurements from bottlenose dolphins in Sarasota Bay, Florida. They suggested that animals which fell outside the lower 95% quantile of their relationship could be identified as emaciated. The appropriate formula is:

$$emaciated\ mass_a = 10^{-5.03}.L_a^{3.01}$$

where *mass* is total mass at age *a* in days. This threshold corresponds closely with the mass:length ratio for emaciation suggested by Ridgway and Fenner (1982) based on data from 144 common bottlenose dolphins (from the Atlantic). We assumed that the body condition of these emaciated animals was at the threshold for 95

starvation-related mortality (i.e., that reserves constituted ρ_s x 100% of their body mass). Thus:

$$S_a = (1 - \rho_s).emaciated\ mass_a = (1 - \rho_s).10^{-5.03}.L_a^{3.01}$$

We assumed growth in foetal length was linear from conception to birth and used the same mass to length relationship as for adults.

Modelling growth (*K*) The model developed by Hin et al. (2019) assumes that growth in length and core mass continues unabated, regardless of energy intake. This is clearly not the case in many marine mammals. We, therefore, assumed that growth may be reduced if energy intake is less than the combined costs of metabolism, growth and reproductive activities (pregnancy and lactation). We modelled these circumstances using a modification of the kappa rule, which is a fundamental component of classic DEB models (Kooijman 2010). We assumed that an individual will allocate a proportion of the assimilated energy (I_t) it acquires on a particular day to growth (including growth of the foetus, because this is treated as part of the female's core mass), up to a maximum of (1-*K*).I_t . If this amount of energy is less than the energy required for growth, the growth rate of the female and her foetus is reduced accordingly. The balance of the energy intake is allocated to metabolism. If this is insufficient to cover all of the costs of metabolism, reserves must be metabolised. Values of $K < 0.5$ indicate that growth is prioritised over metabolism. In the baseline calculation we used a value of 0.5, but the implications of other values should be explored. We also assumed that the costs of lactation are given absolute priority over those of growth. One consequence of this approach to modelling growth is that pregnant females who experience reduced energy intake may give birth to smaller calves than those that are able to meet their total energy requirements every day.

7.1.4 Energetic rates

Field metabolic maintenance scalar (σ_M) Bejarano et al. (2017) considered three different approaches for calculating the daily FMR of bottlenose dolphins, primarily based on data collected in Sarasota Bay, Florida. These were: estimates based on the amount of energy consumed per day as a proportion of body mass for captive animals; a simple multiple of the RMR estimated from the Kleiber equation (i.e. σ_M); and direct measurements of daily FMR (expressed in MJ/kg) from free-ranging animals in summer and winter. Direct measurements of FMR in summer were 40% more than those made in winter. Summer water temperatures in the shallow waters of Sarasota Bay (mean 29.7℃) (Noren and Wells 2009) are much higher than those

likely to be encountered by bottlenose dolphins in UK waters, and so we believe that the winter values are more appropriate for these populations. These winter field measurements predicted a daily FMR that was 4.5 – 6x (depending on the value used for metabolic mass - *MMa*) the value derived from the Kleiber equation. We used values from this range, although most simulations were conducted with a value of 4.5.

Energetic cost per unit structural mass (σ_G) We were unable to find any published estimates of the energy density of lean bottlenose dolphin tissue. We, therefore, used the value of 30 MJ/kg that Hin et al. (2019) derived for pilot whales.

Catabolic and anabolic efficiency of reserve conversion (ε^-, ε^+,) In our simulations we assumed the same values for these parameters as those used for non-pups in the grey seal DEB. These are the same values as those used by Hin et al. (2019) for long-finned pilot whales.

Steepness of assimilation response (η) We were unable to find any data in the literature that could be used to set a feasible range for this parameter. We explored the implications of values between 5 and 25 and found that predicted changes in body weight and reproductive success were relatively insensitive to the value of this parameter. We, therefore, carried out most simulations with a value of 20.

Effect of age on resource foraging efficiency (Y, T_R): The majority of information on this parameter comes from studies of calves born in captivity. These animals are reported to begin feeding at age 6-18 months (Cockcroft and Ross 1990, Peddemors et al. 1992, Kastelein et al. 2002). Mann and Smuts (1999) record that bottlenose dolphin calves in the Shark Bay, Australia population that are >3 months old "frequently" chase small fish and trap them at the water surface (a behaviour they call "snack foraging"), with the earliest observation of this behaviour occurring at 3 weeks. The quantity of food consumed by the calves studied by Kastelein et al. (2002) increased linearly over time, and stabilised before they were weaned. The latter effect is probably an artefact of captivity, because fish will be more difficult to catch in the wild. We initially set $\gamma = 3$, and $T_R = 0.75*T_L$ for T_L = 550 and 730 days, and T_R = 412 days when T_L = 1095 days. This resulted in females providing 50% of their calves' energy requirements at about the same time that the calf's foraging efficiency was 0.5.

7.1.5 Pregnancy

Pregnancy threshold ($F_{neonate}$): The pregnancy threshold determines when females become pregnant for the first time, and also how quickly they can become pregnant after the birth of a calf. Initially, we followed Hin et al. (2019) and assumed that a female can only become pregnant if her energy reserves at the time of ovulation are sufficient to cover the additional costs of foetal growth. However, the resulting levels of reserves at parturition were more than sufficient to allow all females to raise a calf successfully. We, therefore, reduced the pregnancy threshold to 0.8x $F_{neonate}$. Under this assumption, the calves of small females (i.e., those aged 6 to 10) suffered relatively high levels of starvation-related mortality (Figure 31), as observed by Cheney et al. (2018), whereas older females usually raised their calves successfully.

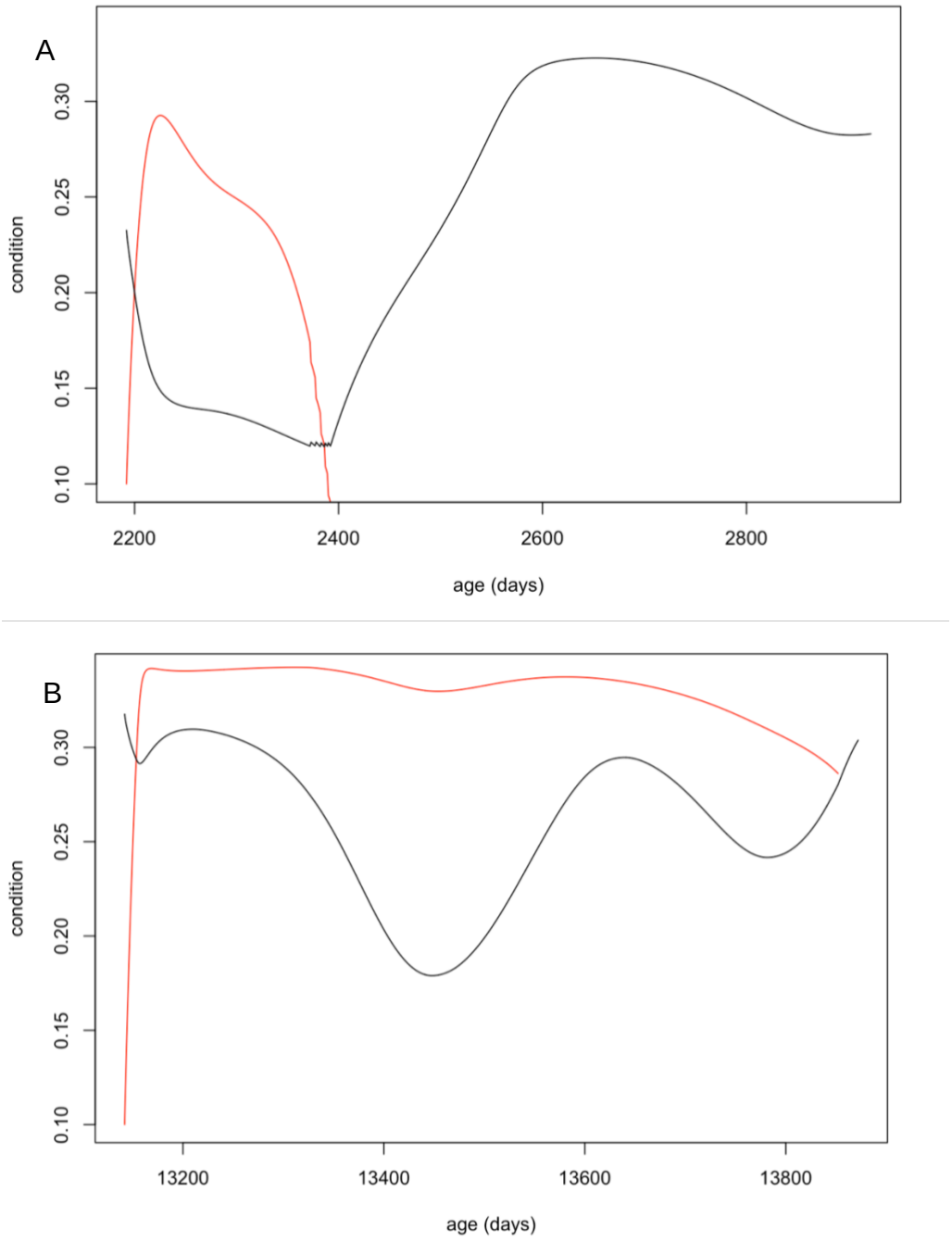

Figure 31. Predicted changes in body condition of a female (black line) and her calf (red line) over the course of lactation. A. If the female is 6 years old when the calf is born. B. If the female is 36 years old. The strong cycles in female condition reflect the seasonal variations in resource density.

Probability that implantation will occur (*fert_success*) O'Brien & Robeck (2012) reported that only 71.4% of 119 documented reproductive cycles among captive bottlenose dolphins resulted in a conception, and we used this as the probability that a female whose body condition exceeded the pregnancy threshold would actually

conceive in a particular year. Combined with the assumed values for foetal and calf mortality (see below), this resulted in an inter-birth interval of 2-6 years (c.f. 3.94 – 4.93 years; Arso Civil, et al 2017).

7.1.6 Lactation

Efficiency of conversion of mother's reserves to calf/pup tissue (σ_L): In the absence of any direct measurements of the relevant efficiencies for bottlenose dolphins, we used the value of 0.86 for long-finned pilot whales from Hin et al. (2019).

Effect of calf/pup age on milk assimilation (ξ_C, T_N): Most data on these parameters comes from captive animals. Most of the lactating females studied by Kastelein et al. (2002) dramatically increased their food intake shortly after parturition, and then slowly decreased it (although food intake remained above the maintenance level until calves were weaned). In contrast, the food intake levels of the four captive, lactating females studied by Reddy et al. (1994) remained at the same high level for 18 months. Milk assimilation in the DEB model is affected by both the calf's age and its body condition. As a result, calves that begin foraging early are predicted to demand less milk from their mothers than those that have not begun to forage. Thus, predicted milk assimilation may begin to decline before the calf is T_C days old. We experimented with values of T_N around 6 months and ξ_C = 0.2 (i.e., an almost linear decline in milk assimilation after age T_N).

Effect of female body condition on milk provisioning (ξ_M) The relatively high mortality of young calves observed by Cheney et al. (2019), and the known longevity of bottlenose dolphins (e.g., Wells & Scott 2018 report that females in Sarasota Bay can live to more than 67 years) suggest that females may be reluctant to compromise their own survival by continuing to provide milk to their calves when their own body condition is low. We, therefore, used relatively low values of this parameter, in the range 2-3.

Lactation scalar (Φ_L) We calculated the total costs of calf growth and calf metabolism up to the age of 6 months (the period during which females are assumed to be providing 100% of their calf's energy needs) and assumed that the calf's body condition was close to ρ throughout this period. This gave a value of 5.4 for Φ_L . This resulted in the daily energy requirements of a lactating female in the first 6 months of lactation being 55-65% (depending on the female's age) higher than a non-lactating female of the same age. This is very similar to the range of values used by Bejarano et al. (2017).

7.1.7 Mortality

Age-dependent mortality rate We followed the approach used by Hin et al. (2019) and estimated changes in the probability of survival with age using the approach developed by Barlow & Boveng (1991). The following function describing the variation in daily survival with age:

$$Surv_a = e^{-(\alpha_1 e^{-\beta_1 a} + \alpha_2 e^{\beta_2 a})}$$

where *a* is age in days, was fitted to the annual age-specific survival rates for bottlenose dolphin survival rates recommended by Sinclair et al. (2020) for the Moray Firth population. Figure 32 shows the resulting relationship between age and cumulative survival, with

α_1 = 0.00039

β_1 = 0.005

α_2 = 0.15×10^{-3}

β_2 = 0.5×10^{-8}

and a maximum age of 65 years (as in Wells & Scott 2018). The life expectancy of each simulated female was calculated by choosing a random number between 0 and 1 and determining the age in days at which cumulative survival equalled this value.

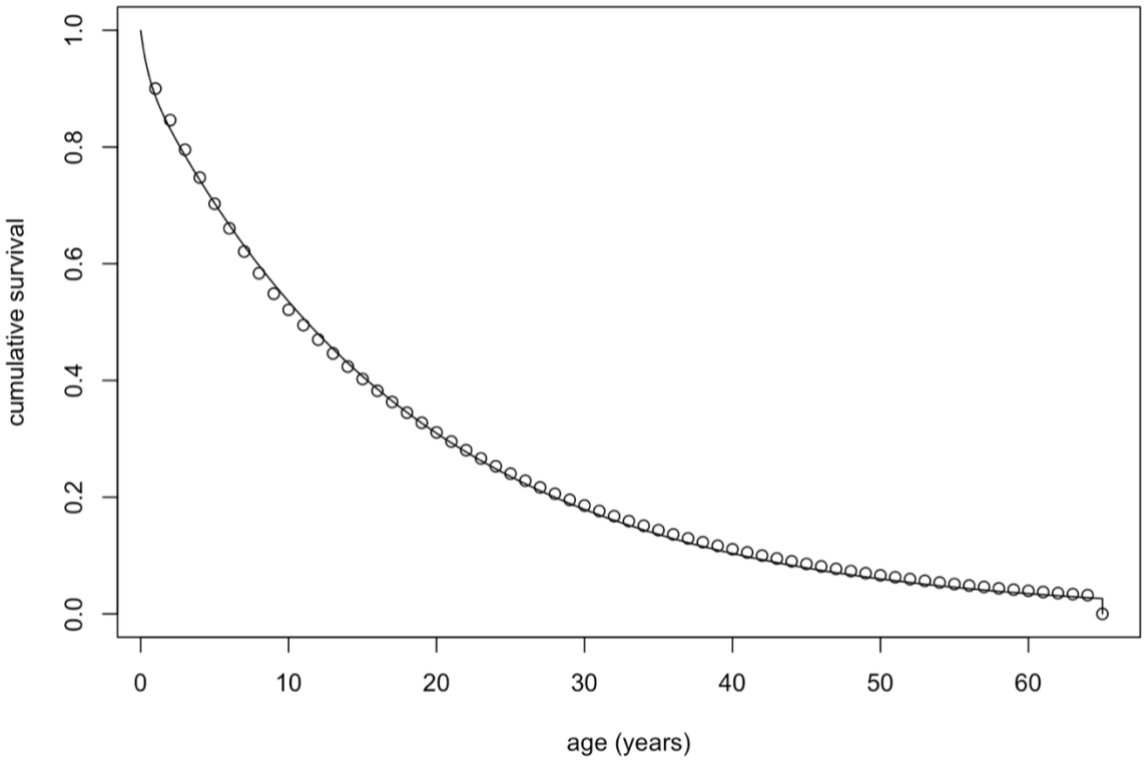

Figure 32. Cumulative survival curve for female bottlenose dolphins used in simulations, with annual survival rates recommended by Sinclair et al. (2020) for the Moray Firth population shown by open circles.

Foetal mortality O'Brien & Robeck (2012) reported that 85.9% of 85 documented pregnancy among captive bottlenose dolphins resulted in a live birth. We, therefore, assumed that the background foetal mortality (i.e., mortality not related to the mother's condition) over the entire duration of the pregnancy was 14%.

Starvation body condition threshold *(ρ_S)* As noted above, we were unable to find any empirical information on ρ_S. Instead, S_a is back-calculated from the mass-length relationship for emaciated animals and the assumed value for ρ_S. We investigated the implications of a range of values centred on $\rho_S = 0.1$.

Starvation-induced mortality rate (μ_S) No empirical information that could provide a species-specific value of this parameter for bottlenose dolphins is available. As a starting point for exploratory modelling, we used the value of 0.2 proposed by Hin et al. (2019).

7.2 Model results – pattern-oriented modelling

Using the default parameter values in Table 7, in particular a lactation duration of 1095 days, and a resource density of 3.2 results in a population growth rate of 0.99 (i.e., a 1% decline in abundance per year). Annual calf survival is 0.41 and the median inter-calf interval is 3.3 years (range 2-6 years). The highest population growth rate that can be achieved with this lactation duration is 1.018 (an annual increase in abundance of approximately 2%), identical to the mean growth rate presented in Table 4 of Sinclair et al. (2020). Annual calf survival is 0.72 and the median inter-calf interval is 3.8 years (range 2-10 years). These demographic characteristics closely match those reported by Cheney et al. (2018) and Arso Civil (2018).

7.3 Simulating the effect of disturbance

We simulated the effects of different numbers of days of disturbance within a single year on the vital rates of 1,000 females using the default parameter values shown in Table 7. Disturbance was simulated by reducing resource density by a proportion $Dist_{effect}$ on the days on which disturbance was predicted to occur. This has the effect of reducing assimilated energy by the same amount.

The condition of calves and lactating females is predicted to be at its lowest level in the first 8-12 months of lactation, as resource density increases from its lowest value in the annual cycle (Figure 33). This corresponds to the period from April – mid-July, and it seems likely that any disturbance at this time could affect both calf and adult survival. In addition, this is the time when females are building up reserves in advance of ovulation and a reduction in body condition could result in failure to implant.

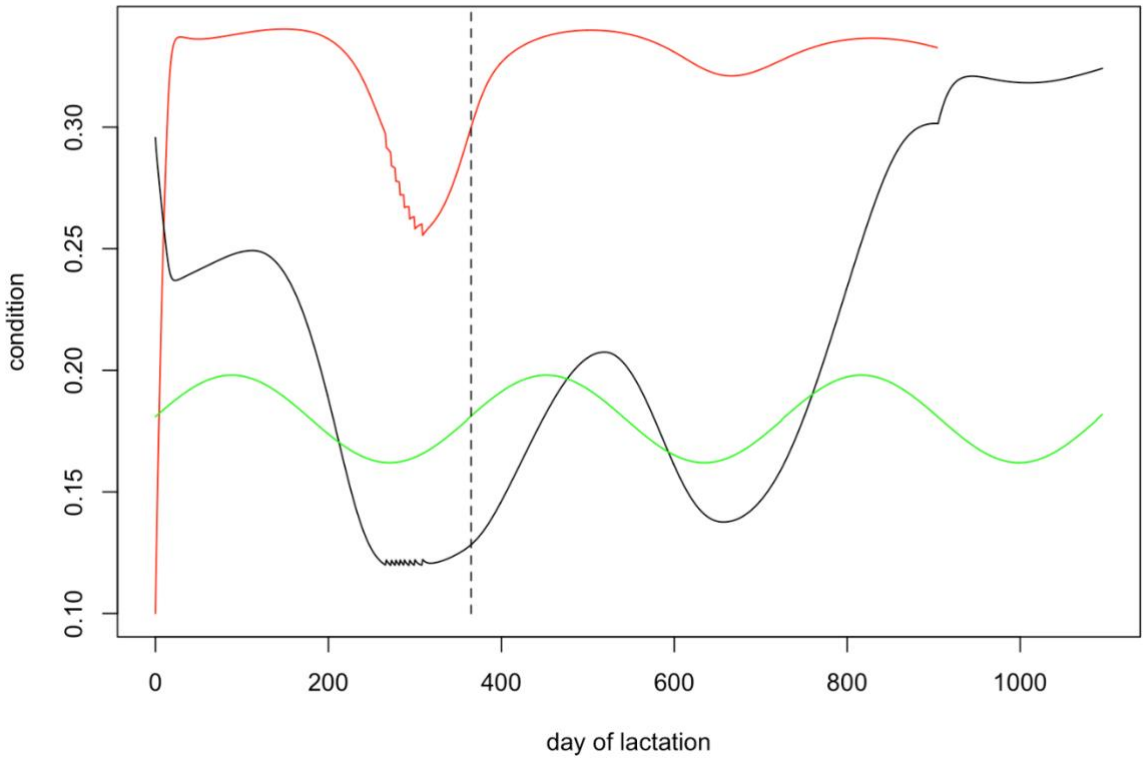

Figure 33. Predicted variation in the body condition of a female (black line) and her calf (red line) over the course of lactation for a population increasing at 2% per annum. The vertical dotted line represents the mean calving date in the Moray Firth (assumed to be 15 July). The green line represents an index of resource density (*Rmean*).

We therefore compared the effects of disturbance in three 4-month periods: May-August, September – December and January – April for young (7 years old) and mature (36 years old) females.

7.3.1 Disturbance between 1 May and 31 August

Disturbance that reduced foraging success by 25% during this period had no significant effect on any vital rate for mature or young females. Figure 34 shows the variations in calf survival from the start of the disturbance period to weaning with the number of days of disturbance.

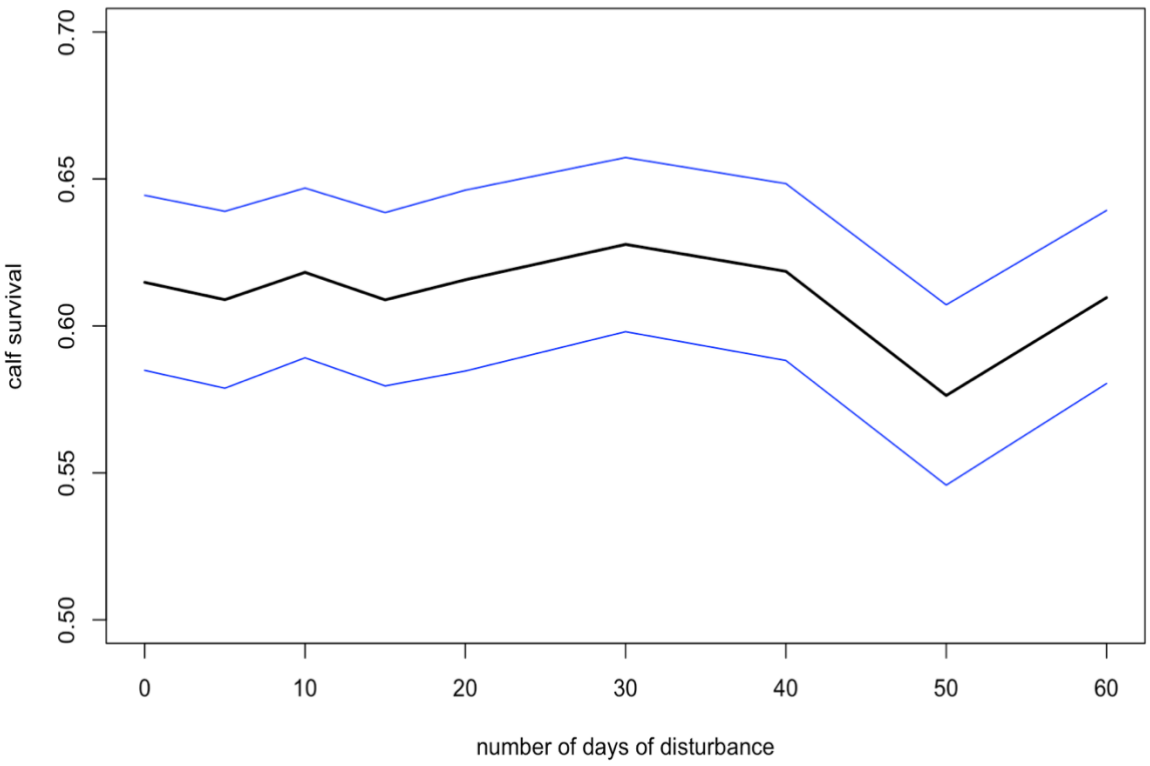

Figure 34. Effect of disturbance between 1 May and 31 August on the survival of all calves of mature females that were alive at the start of the disturbance period. The black line is the mean, and the blue lines enclose 90% of 10,000 bootstrapped estimates.

7.3.2 Disturbance between 1 September and 31 December

Disturbance that reduced foraging success by 25% during this period had no significant effect on any vital rate for mature or young females.

7.3.3 Disturbance between 1 January and 30 April

Disturbance that reduced foraging success by 25% during this period had no significant effect on any vital rate for mature or young females.

8 Common minke whale DEB

8.1 Model parameters

Table 8 shows the parameter values used in most of the minke whale simulations described in this Chapter. Details of how these values were derived are outlined below.

Table 8. Parameter values used in the minke whale DEB model.

Parameter names	Code name	Value	Description	Source
Resource density				
R	Rmean	2.315	Annual mean resource density	See text
a_{beta}	a_beta	8.08	Shape parameters of beta distribution defining stochasticity in resource density	See text
b_{beta}	b_beta	24.25		See text
	amplitude	0.5	Parameter defining the amplitude of seasonal variation in resource density	See text
	offset	105 days	Parameter determining when during the year *Rmean* has its maximum value	See text
Timing of life history events				
min_age	min_age	6 years	Minimum age for reproduction	Christensen (1981)

Parameter names	Code name	Value	Description	Source
mean_birthday	mean_birthday	15 November	Mean pupping date for NE Atlantic stock	Hauksson et al (2011)
T_P	Tp	330 days	Gestation period	See text
T_L	Tl	150 days	Age at weaning (duration of lactation)	See text
T_R	Tr	150 days	Age at which calf's resource foraging efficiency is 50%	See text
max_age	max_age	50 years	Maximum age	
	max_age_calf	345 days	Maximum modelled age of calf	
Reserves				
ρ	rho	0.3	Target body condition for adults	See text
θ_F	Theta_F	0.2	Relative cost of maintaining reserves	Hin et al. (2019)
Growth				
	Lb	247 cm	Length at birth	Hauksson et al. (2011)
L_0	L0	415 cm	Length at weaning	
L_∞	Linf	907 cm	Female maximum length	
b	b	- 0.000389	Von Bertalanffy exponent	Christensen (1981)

Parameter names	Code name	Value	Description	Source
ω1	omega1	$3.62x10^{-5}$ (kg/cm	Structural mass-length scaling constant	Hauksson et al. (2011)
ω2	omega2	2.758	Structural mass-length scaling exponent	
Energetic rates				
σ_M	Sigma_M	2.5	Field metabolic maintenance scalar	
σ_G	Sigma_G	30 MJ/kg	Energetic cost per unit structural mass	Derived using the approach of Hin et al. (2019)
ε	epsi	27.5 MJ/kg	Energy density of reserve tissue	
ε-	epsi_minus	24.75 MJ/kg	Catabolic efficiency of reserves conversion	
ε+	epsi_plus	34.03 MJ/kg	Anabolic efficiency of reserve conversion	Reilly et al. (1996)
μ_s	mu_s	0.2	Starvation mortality scalar	Hin et al. (2019)
η	eta	20	Steepness of assimilation response	See text
ϒ	upsilon	2.5	Shape parameter for effect of age on resource	See text

Parameter names	Code name	Value	Description	Source
			foraging efficiency	
K	Kappa	0 for calves & juveniles 0.5 for all other age classes	Proportion of the daily assimilated energy allocated to growth	See text
Pregnancy				
fert_success	fert_success	0.9	Probability that implantation will occur	Hauksson et al (2011)
$F_{neonate}$	F_neonate		Reserves required to cover costs of pregnancy and lactation	See text
	F_neo_multiplier	0.9	Fraction of F_neonate used as actual threshold	
Lactation				
φ_L	phi_L	5.4	Lactation scalar	See text
σ_L	Sigma_L	0.86	Efficiency of conversion of mother's reserves to calf tissue	Lockyer (1993)
T_N	Tn	135 days	Calf age at which female begins to reduce milk supply	See text
ξc	xi_c	0.2	Non-linearity in milk	See text

Parameter names	Code name	Value	Description	Source
			assimilation-calf age relation	
ξ_M	xi_m	6	Non-linearity in female body condition-milk provisioning relation	See text
Mortality				
foetal_mortality	foetal_mortality	0.0	Background foetal mortality	See text
α_1	alpha1	0.00045	Coefficients of age-dependant mortality curve	Sinclair et al. (2020)
α_2	alpha2	0.943×10^{-4}		
β_1	beta1	0.0004		
β_2	beta2	1.1×10^{-6}		
ρ_S	rho_s	0.1	Starvation body condition threshold	See text
μ_s	mu_s	0.2	Starvation mortality scalar	See text
Disturbance				
$Dist_{dur}$	days.of.disturbance		Number of days on which disturbance occurs	See text for values
$Dist_{start}$	first_day		First day of disturbance period	See text for values
$Dist_{end}$	Last_day		Last day of disturbance period	See text for values
$Dist_{effect}$	disturbance.effect	0.25	Reduction in resource	See text

Parameter names	Code name	Value	Description	Source
			density caused by disturbance	
Age_{Dist}	age.affected		Age threshold defining which age class of simulated animals is affected by the disturbance	See text

8.1.1 Resources

Resource density (*Rmean*) Northeast Atlantic minke whales are believed to spend the summer on prey-rich feeding areas in northern latitudes and migrate south in winter to areas with much lower prey density. We modelled this variation by allowing resource density to vary seasonally following the sinusoidal curve shown in Figure 35. This predicts maximum resource density will occur around mid-July and that resource density may be effectively zero at some time during the winter.

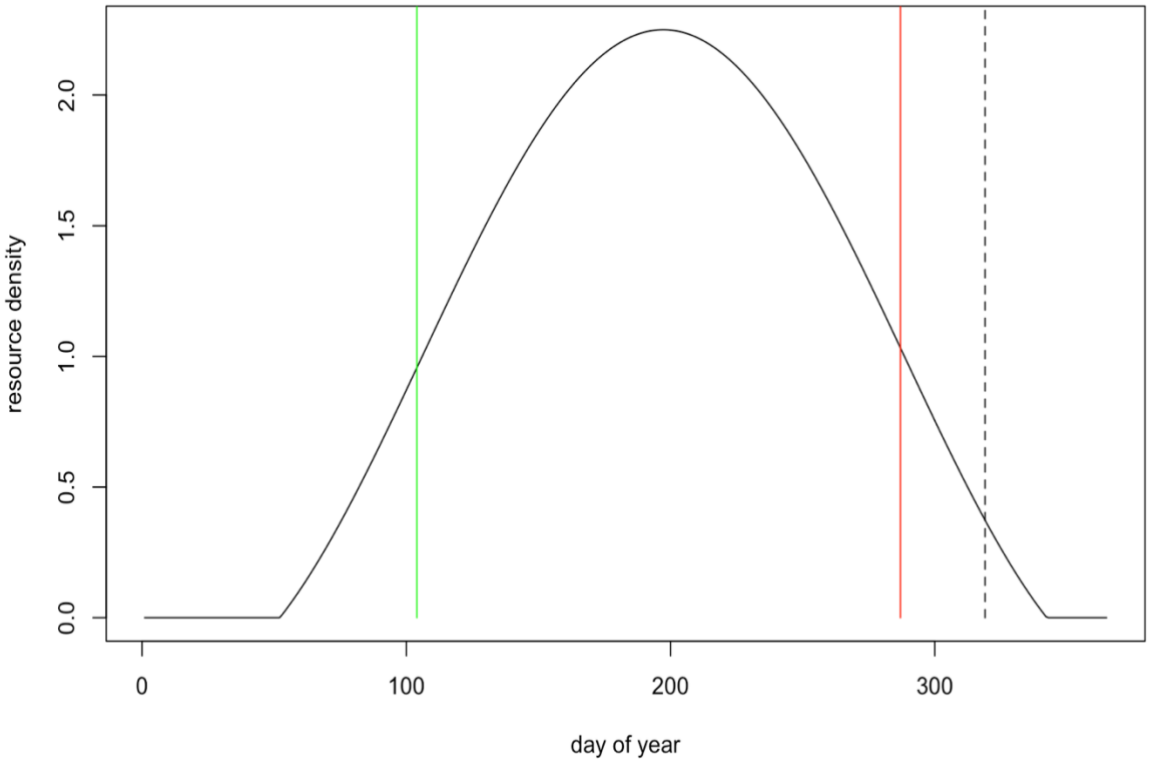

Figure 35. Seasonal pattern of variation in resource density that was used in simulations. The vertical dotted line indicates the mean birth date for calves in the Northeast Atlantic stock, the vertical green line represents the date of arrival on the feeding grounds and the vertical red line the date of departure.

The duration of this period of zero resource density, and the difference in mean resource density between summer and winter, is determined by the amplitude of the sinusoidal variation, as shown in Figure 36.

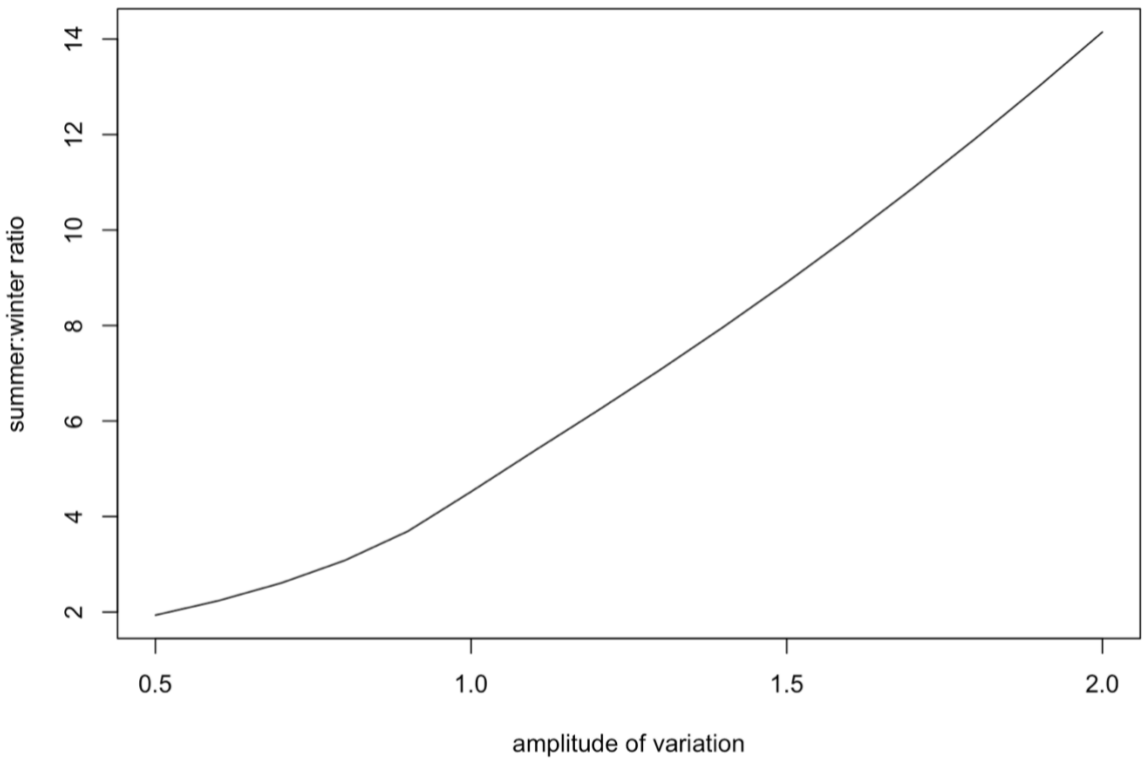

Figure 36. Effect of the amplitude of the variation in resource density on the ratio of mean resource density in summer to mean resource density in winter.

Although it is often assumed that baleen whales do little if any feeding during the winter period, this is almost certainly not the case for Northeast Atlantic minke whales. The values for energy expenditure and energy acquisition in Table 1 of Nordøy et al. (1995) indicate that the energetic content of the reserves accumulated over the summer are only sufficient to cover field metabolic costs for 55 days of fasting in the case of adult females (mean length 8 m) and 64 days in the case of growing animals (mean length of 7 m). Therefore, these animals must be feeding for some of the time during the winter. We therefore set the amplitude of variation to a relatively low value (0.5, equivalent to a 2x difference in resource density between summer and winter) in our initial simulations.

In the original Hin et al. (2019) model resource density is assumed to be constant or to vary smoothly over the course of the year. However, in reality, the resource density encountered by an individual is likely to vary from day to day. This stochasticity in resource density can be modelled by multiplying *Rmean* for each day by a number drawn at random from a beta distribution with mean=1 and a 90% confidence interval of 0.5-1.5. Extreme values for this multiplier could be as low as 0.1 or as high as 2.4.

We assumed that calves encountered the same resource density as their mothers on each day during lactation.

8.1.2 Timing of life history events

Following Christensen (1981) we assumed that females had to be at least 7 m long before they could ovulate. The mean birthday for all calves was set at mid-November, as suggested by Hauksson et al. (2011).

Gestation period (T_P) This is 10 months (~300 days) according to Perrin et al. (2018). However, a value of 330 days is more consistent with observed lengths at birth (see below).

Lactation period/age at weaning (T_L) This is 5-6 months according to Perrin et al. (2018). However, Nordøy et al. (1995) and Jonsgård (1951) report that minke whales spend 6 months in Northeast Atlantic waters each year and that calves are not normally seen with these animals. Given the reported annual breeding cycle of minke whales, this suggests that lactation must last less than 6 months and we used a value of 150 days.

8.1.3 Reserves and growth

Reserve threshold (ρ) Nordøy et al. (1995) provided detailed information on changes in the mass and energy density of blubber, muscle and intra-abdominal fat for immature and adult Northeast Atlantic minke whales, from the time they arrive on the feeding grounds (around 14 April) until their departure 183 days later. We combined this with our calculations of the structural mass of animals of different lengths from the growth curve described below to estimate changes in body condition over the course of this period. The blubber mass and muscle mass of all individuals increased over the course of the summer, as did the energy density of these tissues (Nordøy et al. 1995). Nordøy et al. (1995) report that an 800 cm long whale increases its energy reserves by 151 MJ/day over the course of the summer, and we calculated that the average energy density of these tissues was 26 MJ/kg. The total energy accumulated in reserve tissue by an 800 cm long animal over the 183-day summer period is therefore equivalent to 1440 kg, resulting in a body condition of 0.28. However, some animals achieved a greater mass gain than this, and we therefore set ρ at 0.3.

Relative cost of maintaining reserves (Θ_F) We were unable to find any published data that would allow a value specific to minke whales to be calculated for this parameter. We, therefore, suggest using the value of 0.2 assumed by Hin et al. (2019).

Structural length and structural mass *(L_0, L_∞, ω_1, ω_2)* A number of von Bertalanffy growth curves have been published for the Central and Northeast Atlantic minke whale stocks (Christensen 1981, Olsen and Sunde 2002, Hauksson et al. 2011), but the youngest animals in the samples used to fit these curves are usually at least 2 years old. None of the growth curves provide estimates of length at birth that are in the range 240-270 cm reported by Perrin et al. (2018), and only the Christensen (1981) growth curve is consistent with Jonsgård (1951) suggestion that length at weaning is about 450 cm.

Hauksson et al. (2011) fitted the following growth curve for minke whale foetuses, based on animals sampled at the Icelandic whaling station:

$$L_t = 0.002 * t^{2.022}$$

where *t* is the Julian days. Figure 2 of Christiansen et al. (2014) shows a similar pattern of foetal growth, probably because it is – at least in part - based on the same sample of animals. Hauksson et al's (2011) curve predicts a length at birth of 204 cm if foetal growth begins on 1 January and gestation last 300 days, and 247 cm if gestation lasts 330 days. Only the latter value is consistent with the various estimates of length at birth for the Northeast Atlantic minke whale stock documented in Christensen (1981), supporting our assumption that T_P = 330 days.

We estimated foetal weight at age using the following formula derived by Hauksson et al. (2011) from the same sample:

$$S_a = 0.00003682.L_a^{2.758}$$

We assumed that growth in length was linear from birth to age T_L (with a predicted length of 415 cm at this age) and then used Christensen (1981) growth curve

$$L_a = 907.0 - (907.0 - 415)e^{-0.000389a}$$

(re-parameterised to match the formulation used by Hin et al. 2019) from this age onwards. Structural mass at age (S_a) was calculated from L_a using Hauksson et al.'s (2011) formula for foetuses.

Modelling growth (*K*) The model developed by Hin et al. (2019) assumes that growth in length and core mass continues unabated, regardless of energy intake. This is clearly not the case in many marine mammals. We therefore assumed that growth may be reduced if energy intake is less than the combined costs of metabolism, growth and reproductive activities (pregnancy and lactation). We

modelled these circumstances using a modification of the kappa rule, which is a fundamental component of classic DEB models (Kooijman 2010). We assumed that an individual will allocate a proportion of the assimilated energy (I_t) it acquires on a particular day to growth (including growth of the foetus, because this is treated as part of the female's core mass), up to a maximum of (1-K).I_t. If this amount of energy is less than the energy required for growth, the growth rate of the female and her foetus is reduced accordingly. The balance of the energy intake is allocated to metabolism. If this is insufficient to cover all of the costs of metabolism, reserves must be metabolised. Values of $K < 0.5$ indicate that growth is prioritised over metabolism.

Following Christiansen et al. (2013) we set K to zero for immature animals, which are believed to prioritise growth above all else. Conversely, we assumed that nursing calves would prioritise reserves over growth, because adequate reserves are crucial to their survival in the post-weaning period. We experimented with a range of values of K for adult females.

8.1.4 Energetic rates

Field metabolic maintenance scalar (σ_M) Blix and Folkow (1995) estimated the average energy expenditure of 6 free-ranging, tagged minke whales to be 80 kJ/kg/day, based on their respiration rate. Folkow et al. (2000) used this value to calculate that a 5,900 kg adult minke whale would expend 472 MJ/day. This is equivalent to using a scalar of 1.7-2.5, depending on what assumptions are made about the values of ρ and Θ_F. We used a value of 2.5 in both summer and winter to account for the potential increase in metabolic rate when animals are in warmer waters during the winter, as appears to be the case for baleen whales (Villegas-Amtmann et al. 2017).

Energetic cost per unit structural mass (σ_G) We calculated growth efficiency using the same approach as Hin et al. (2019), with a mass at birth of 144 kg (based on a length at birth of 247 cm) and an energy density of 3.8 MJ/kg for the tissue of minke whale foetuses estimated by Nordøy et al. (1995). This produced a value of 33 MJ/kg for σ_G.

Catabolic and anabolic efficiency of reserve conversion (ε-, ε+,) Nordøy et al. (1995) estimated that the energy density of minke whale blubber on arrival at the summer feeding grounds was 27.5 MJ/kg, very similar to the mean energy density of the tissues accumulated over the summer. Allowing for a 90% efficiency of catabolism, we assumed ε- = 24.75 MJ/kg.

In the absence of any direct measurements of $\varepsilon+$ for minke whales, we followed Hin et al. (2019) and used a value for $\varepsilon+$ that was 40% higher than $\varepsilon-$ (i.e., 34.65 MJ/kg).

Steepness of assimilation response (η) We were unable to find any data in the literature that could be used to set a feasible range for this parameter. We explored the implications of values between 5 and 25 and found that predicted changes in body weight and reproductive success were relatively insensitive to the value of this parameter. We therefore carried out most simulations with a value of 20.

Effect of age on resource foraging efficiency (Y, T_R): We could find no information that could be used to estimate these parameters in the literature. Initially, we assumed that calves are 50% efficient at foraging when they are weaned.

8.1.5 Pregnancy

Pregnancy threshold ($F_{neonate}$): Jonsgård (1951) observed that most adult females on the feeding grounds were pregnant, suggesting that minke whales have a one-year reproductive cycle. Christiansen et al. (2014) observation that female minke whales on the Icelandic feeding grounds that were in poor condition (as measured by their blubber volume) had smaller foetuses suggests that females respond to reduced energy intake in summer by reducing their investment in their offspring rather than by terminating a pregnancy. However, there is a high risk of starvation-related mortality if females attempt to complete lactation when they have insufficient energy reserves. We, therefore, experimented with a range of value for $F_{neonate}$ on day 300 of pregnancy. This is equivalent to 15 October in the Northeast Atlantic and represents the date at which most females leave the feeding grounds. We calculated the amount of energy a female would require to complete her pregnancy and provide her calf with 100% of its energy requirements during the lactation period. We then examined the consequences of setting a threshold for continuing a pregnancy that was a fraction of this value. Female fitness, measured by lifetime reproductive success at a particular value of *Rmean*, increased as the magnitude of the threshold was increased from 0.8* $F_{neonate}$ to 0.9* $F_{neonate}$, but there was little increase beyond this value. We, therefore, carried out all subsequent simulations with a threshold of 0.9* $F_{neonate}$.

Probability that implantation will occur (*fert_success*) The probability of successful implantation was set at 0.88 based on the ovulation rate reported by Hauksson et al. (2011).

8.1.6 Lactation

Efficiency of conversion of mother's reserves to calf/pup tissue (σ_L): In the absence of any direct measurements of the relevant efficiencies for minke whales, we suggest using the value of 0.86 that was used by Hin et al. (2019).

Effect of calf/pup age on milk assimilation (ξ_C, T_N): It is generally assumed that resource density is low on the breeding grounds and that females will provide almost all of their calves' energy requirements up to the age at weaning. We therefore set $T_C = 0.9*T_L$.

Effect of female body condition on milk provisioning (ξ_M) Because calves are weaned on the breeding grounds or during migration to the summer feeding grounds, lactating females that are in poor condition at this time will be close to the starvation threshold and may struggle to recover their depleted reserves. We therefore assumed a "conservative" strategy in which females began reducing milk supply relatively rapidly as their condition declined (i.e., a value of $\xi_M \geq 5$, see Figure 6). Values of $\xi_M > 5$ resulted in increased levels of adult female mortality, without any obvious improvement in fitness. We therefore carried out all simulations with $\xi_M = 5$.

Lactation scalar (Φ_L) We calculated the total costs of calf growth and calf metabolism during the period when females are assumed to be providing 100% of their calf's energy needs and assumed that the calf's body condition was close to ρ throughout this period.

8.1.7 Mortality

Age-dependent mortality rate We followed the approach used by Hin et al. (2019) and estimated changes in the probability of survival with age using the method developed by Barlow & Boveng (1991). The following function describing the variation in daily survival with age:

$$Surv_a = e^{-(\alpha_1 e^{-\beta_1 a} + \alpha_2 e^{\beta_2 a})}$$

where *a* is age in days, was fitted to the annual age-specific minke whale survival rates from Taylor et al. (2007). We used a maximum age of 50 years, based on the fact that the oldest female in a sample of 288 whales examined by Hauksson et al.

(2011) was 42 years old and that Taylor et al. (2007) propose a maximum age of 51 years. The resulting fitted values were:

$\alpha_1 = 0.00045$

$\beta_1 = 0.0004$

$\alpha_2 = 0.943 \times 10^{-4}$

$\beta_2 = 1.1 \times 10^{-6}$

Figure 37 shows the fitted curve. Combined with a pregnancy rate of 0.9, these survival rates generate a population growth rate of 1.05. The life expectancy of each simulated female was calculated by choosing a random number between 0 and 1 and determining the age in days at which cumulative survival equalled this value.

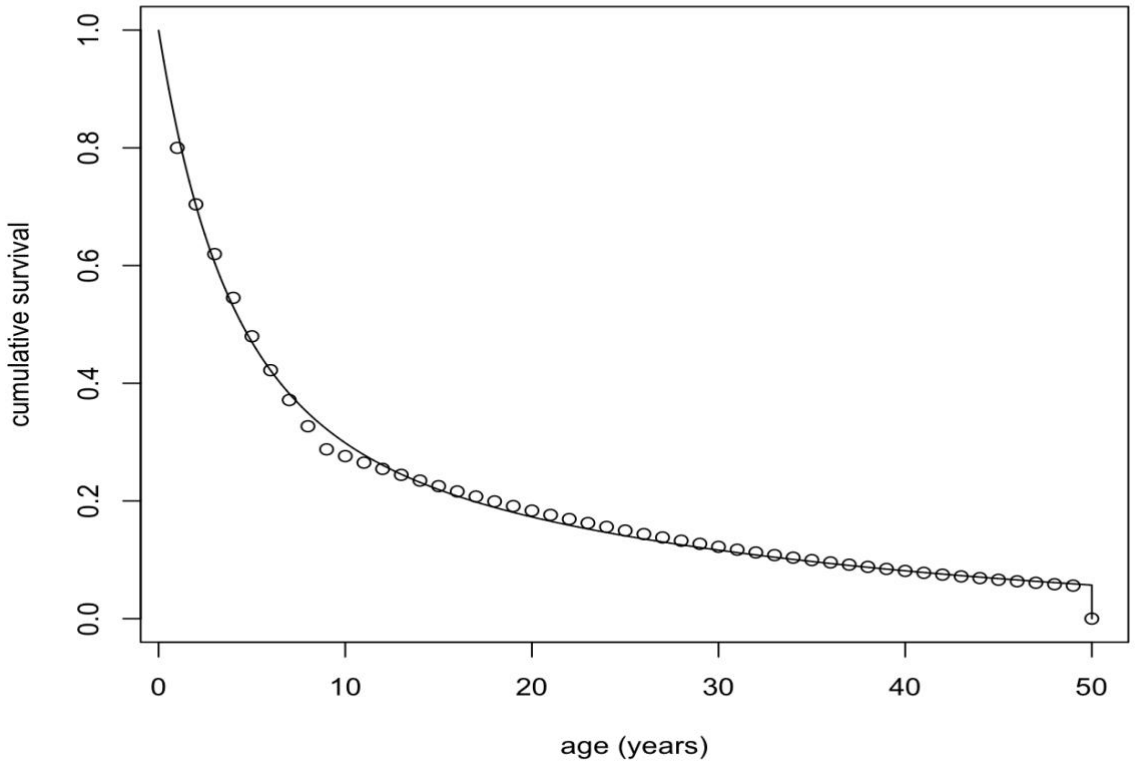

Figure 37. Cumulative survival curve for female minke whales used in simulations, with annual survival rates Taylor et al (2007) shown by open circles.

Foetal mortality In the absence of any empirical information on foetal mortality, this parameter was assumed to be zero.

Starvation body condition threshold *(ρ_s)* We combined information on body composition from Nordøy et al. (1995) with estimates of structural body mass at different lengths from our growth to estimate that the mean body condition of sub-adult and adult animals on arrival at the feeding grounds was 0.12, based on the ratio of blubber mass to total mass. Adult females arriving on the feeding grounds will have just finished lactation and migration from their breeding grounds, so a body condition of 0.12 should represent a typical minimum level in their annual cycle. This suggests that 0.1 is an appropriate value for ρ_s.

Starvation-induced mortality rate (μ_s) No empirical information that could provide a species-specific value of this parameter for minke whales is available. As a starting point for exploratory modelling, we used the value of 0.2 proposed by Hin et al. (2019).

8.2 Model results – pattern-oriented modelling

We used three additional sources of information to investigate the performance of the minke whale DEB model.

Nordøy et al. (1995) documented the relationship between female length and blubber mass in animals killed at the start (average catch date 19 May) and end (average catch date 9 September) of the Norwegian whaling season and found that the slope of the regression relating these two variables was higher in animals taken at the beginning of the whaling season; the DEB model generated similar outputs (Figure 38).

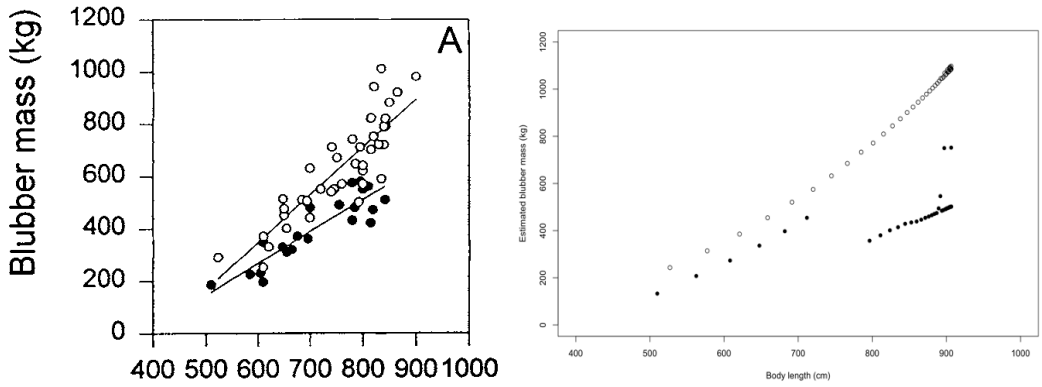

Figure 38. The left panel shows Figure 1(A) from Nordøy et al. (1995) showing the relationship between blubber mass and body length for females killed early in the whaling season (solid dots) and those killed at the end of the season. The right panel figure shows the equivalent outputs from the minke whale deb model.

Christiansen et al. (2013) found that the total blubber volume of pregnant and mature female minke whales killed in the Icelandic whale hunt increased over the course of the whaling season, while the blubber volume of immature animals did not (Figure 39). Again, the DEB model predicted very similar changes.

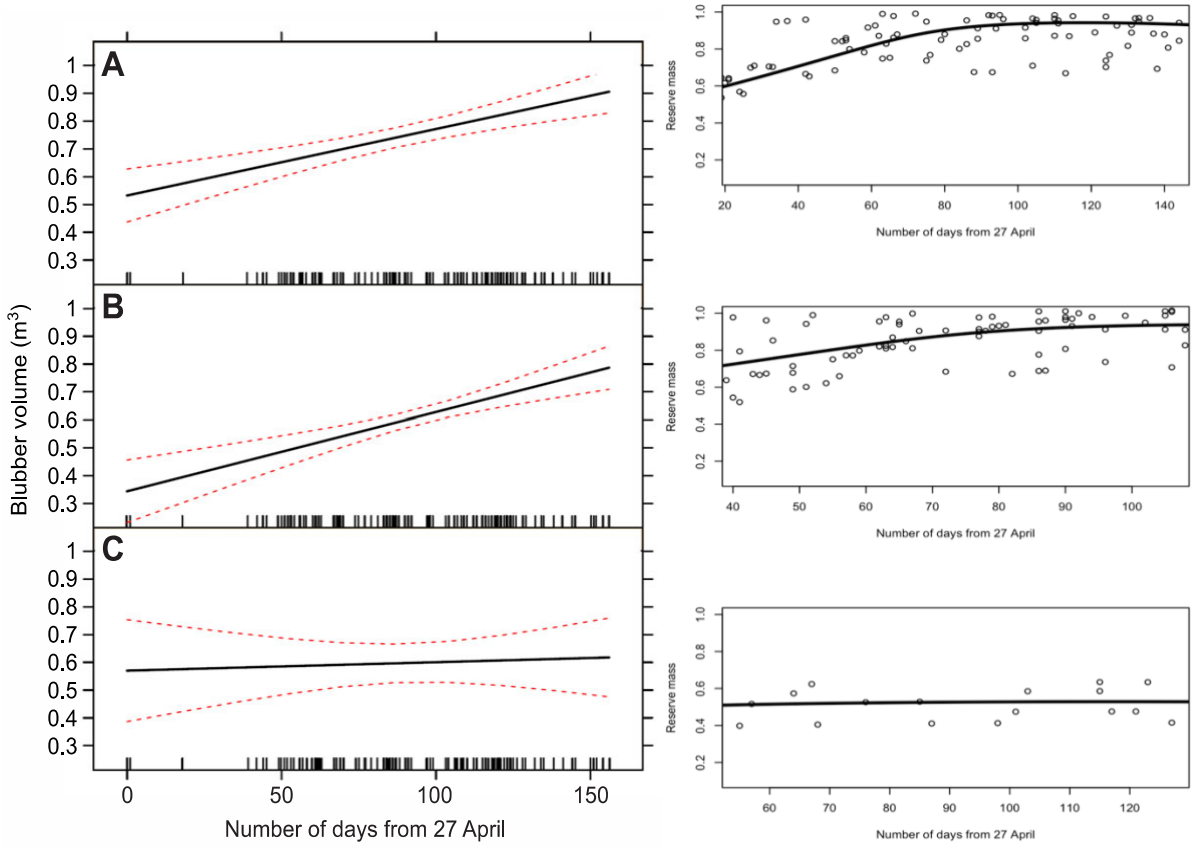

Figure 39 – The left panel shows Figure 2 from Christiansen et al. (2013) showing changes in blubber volume over the course of the Icelandic whaling season for pregnant (panel A), mature (panel B) and immature (panel C) minke whales. The right panel shows the equivalent outputs from the deb model.

Christiansen et al. (2014) used the same information to show that pregnant females that were in poor body condition (with a lower-than-expected blubber volume at a particular date in the whaling season) had foetuses that were substantially shorter than females that were in average or good condition. We were unable to duplicate this relationship in the DEB model, partly because all simulated females within a particular simulation experienced exactly the same resource density at a particular time of year, and therefore had similar blubber mass. Reducing *Rmean* to simulate the effects of low resource density for all whales did result in slightly smaller foetuses, but the main effect was to increase starvation-related mortality of females during the lactation period. This suggests that Christiansen et al.'s (2014) observations were the result of short-term variations in energy intake among individuals within a year, a process we were unable to capture in the DEB model.

8.3 Simulating the effect of disturbance

We assumed that common minke whales would only experience disturbance in UK waters during the summer months. Although there is some information on the response of minke whales to military sonars (Kvadsheim et al. 2017, Durbach et al. 2021), there is no equivalent information on the response of minke whales to piling noise. We initially assumed a similar response to that observed in harbour porpoises, with a 25% reduction in foraging efficiency on days when animals were exposed to this kind of noise, but disturbance on this scale had very little effect on vital rates. The following results assume that disturbance results in a 50% reduction in foraging efficiency.

Disturbance had a small effect on calf survival if it was spread randomly across the entire summer (Figure 40), but no effect if it was confined to the first three months of the summer (mid-April to mid-July).

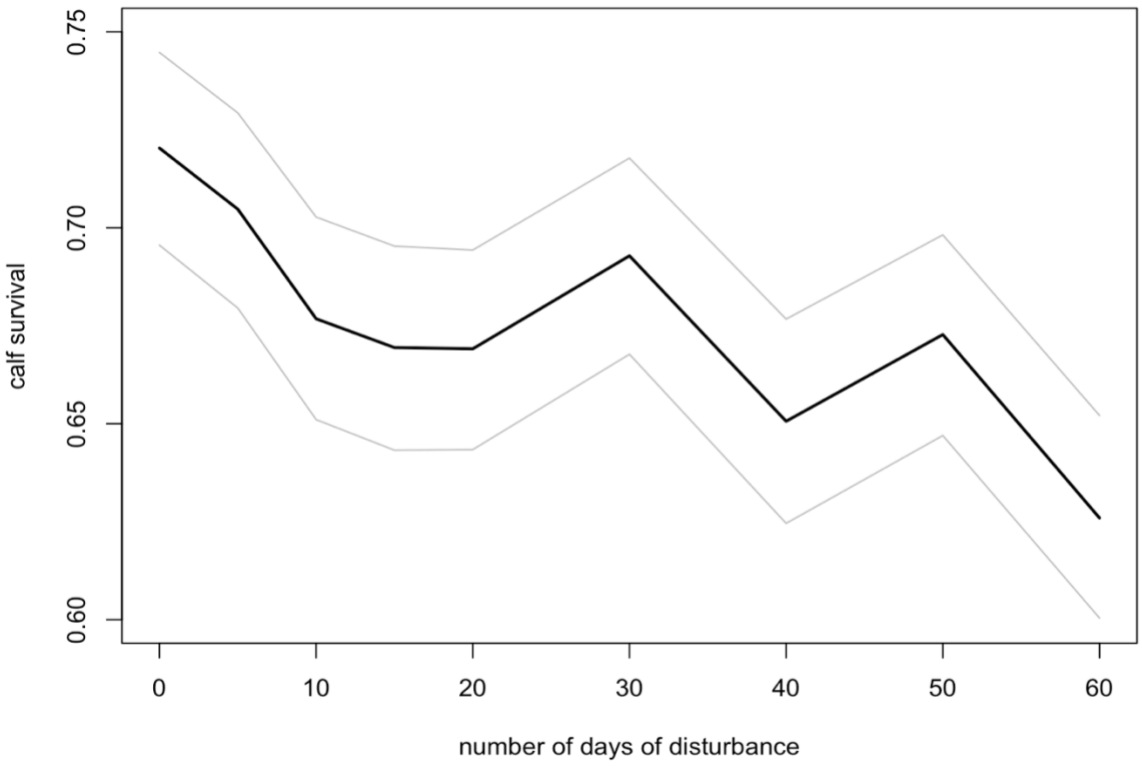

Figure 40. Effect of disturbance random distributed across the summer period (mid-April to mid-October) on the survival of minke whale calves. The grey lines indicate the 95% credible interval based on 10,000 bootstrap calculations.

However, there was a greater effect on calf survival if disturbance was confined to the period mid-July to mid-October (Figure 41). The effect was greatest on the calves of younger females (<25 years old), whose survival was reduced by 80%.

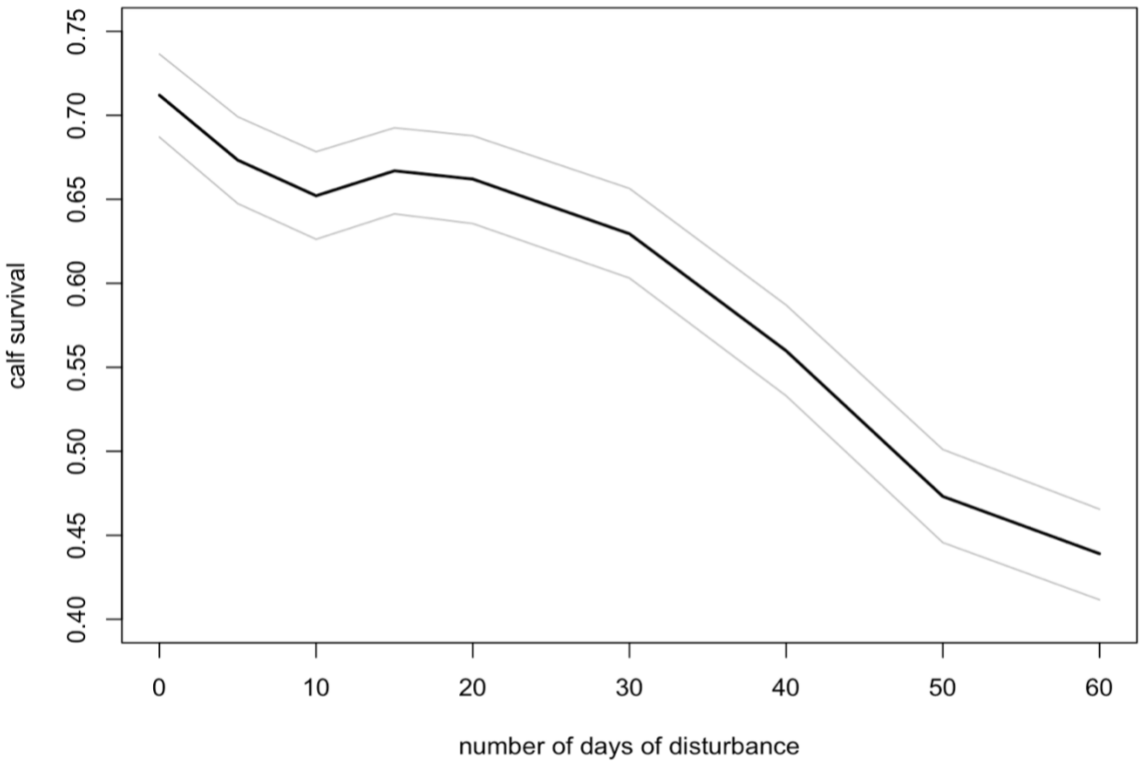

Figure 41. Effect of disturbance randomly distributed across the last three months of the summer feeding period (mid-July to mid-October) on the survival of minke whale calves. The grey lines indicate the 95% credible interval based on 10,000 bootstrap calculations.

Figure 42 shows the changes in maternal and calf condition that cause this additional calf mortality.

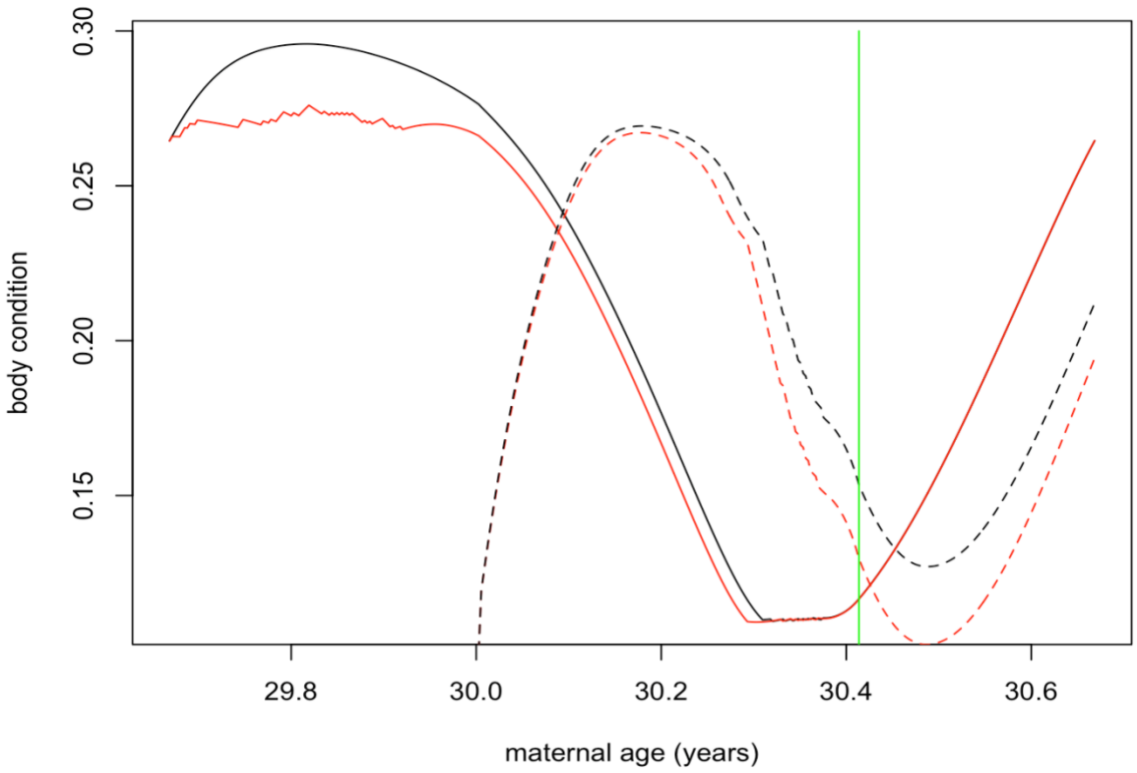

Figure 42. Changes in maternal (solid) and calf (dashed) body condition for an undisturbed (black) female minke whale, and one subject to 60 days of disturbance at the end of the summer (red) that reduces foraging success by 50%. The vertical green line is the day on which the calf is weaned.

9 Accounting for uncertainty in DEB models

9.1 Sources of uncertainty

The DEB models developed in this report require values for more than 30 parameters and it is important that model outputs take account of the uncertainties that are associated with these values. In many cases (e.g., the parameters that determine mass at age, and age-specific survival) these values are estimated from empirical data and the uncertainty associated with them is primarily a result of measurement and sampling error, and among-individual variation. There are standard procedures for quantifying the effects of these uncertainties, such as sampling at random from the statistical distributions associated with the parameter estimates, and we have not investigated these sources of uncertainty in this report. However, it would be valuable to investigate the extent to which the uncertainty is a

result of among-individual variation. If most of the uncertainty is due to individual variation, different resampled values should be applied to individuals rather than all members of the simulated population and this is likely to affect the sensitivity of model outputs to this uncertainty.

Although estimates of FMR are available for many species, these estimates are often highly variable within a species and we did attempt to find a reliable approach to account for this uncertainty (see next sections). A similar issue will arise if no empirical estimate of a potentially measurable parameter is available for the species that is being modelled and values have to be "borrowed" from other, better studied species that have a similar life history strategy.

Finally, there is a suite of parameters that control the rules that determine the decisions made by simulated individuals about how to allocate surplus assimilated energy to growth or reserves, how foraging efficiency increases with age, when females should abandon a pregnancy or calf because their reserves are too small, and how reserves levels affect the risk of individual mortality. It is very difficult (and sometimes impossible) to determine the rules (if any) that free-living animals are actually implementing. We intended to build on an Office of Naval Research (ONR) supported effort on *"Advancing PCOD efforts through a marine mammal bioenergetics workshop"* which aimed to review the current state of knowledge of both modelling (building on Pirotta et al. 2018a) and data needs to support the development of bioenergetic models via a series of mini reviews of key bioenergetic topics (metabolic rates, reproductive energetics, growth and energy intake). The outputs of that workshop will appear in the Conservation Physiology Special Issue in 2022.

It became clear from our sensitivity analyses of the different DEB models that there are strong interactions between some of the subjective parameters which would make it very difficult for experts to assess the likely biological implications of particular combinations of parameter values. With the above points in mind, we chose to use Approximate Bayesian computation rather than expert elicitation. This allowed us to identify biologically plausible combinations of values for these parameters that are consistent with what is known about the population characteristics of the species being modelled. In the next sections, we use this approach to identify a plausible parameter space for the grey seal DEB model, and sample from this space to investigate the effects of uncertainty in these parameters on the predicted effects of disturbance on one vital rate (pup survival).

9.2 Quantifying uncertainty

We applied Approximate Bayesian Computation (ABC) parameterisation to establish plausible distributions for each of the parameters listed in Table 9. The ABC technique consist in (i) simulating the model a very large number of times with parameter values drawn from prior distribution, (ii) comparing the simulation outputs to observational data and (iii) retaining those parameter combinations that were consistent with observations (Jabot et al. 2013).

The potential range of values for each of the parameters listed in Table 9is vast and simply sampling from these ranges would result in an impossible computational task. We therefore did a preliminary manual screening of potential values to identify those that resulted in relatively high values of mean lifetime reproductive success (a measure of individual fitness) at a particular value of *Rmean*. We reasoned that genotypes that resulted in traits that replicated the rules implied by those parameter combinations would have a strong selective advantage and would rapidly dominate the population. The resulting plausible ranges were used to define the limits of the uniform prior distributions for the parameters shown in Table 9.

Table 9. Parameters investigated using Approximate Bayesian Computation, and their prior distributions. Values used in the minke whale DEB model.

Parameter	Description	Prior distribution
κ (Kappa)	Proportion of surplus assimilated energy	Uniform(0.6, 0.9)
Υ (upsilon)	Shape parameter for effect of age on	Uniform(1.4, 1.75)
T_R	Age at which calf's resource foraging	Uniform(70, 120)
μ_S (Mu_s)	Starvation mortality scalar	Uniform(0.1, 0.3)
σ_M	Field Metabolic Rate scalar	Uniform(2, 3)
Rmean	Mean resource density	Uniform(1.3, 2.4)
decision_day	Day of pregnancy when female decides	Uniform(160, 200)
ρ_S (rho_s)	Starvation body condition threshold	Uniform(0.05,

We applied ABC in a stepwise fashion. In the first step we ran 20,000 simulations, each involving 1500 females (which we had previously established as the minimum number of simulated animals necessary to obtain a reliable and unbiased estimate of mean lifetime reproductive output and population growth rate) using the prior distributions listed in Table 10. The main aim of this first step was to identify parameters which are strongly correlated. Once correlation between parameters was established, we ran an additional 60,000 simulations using the same prior distribution for all non-correlated parameters and drawing values of the correlated parameters from the relationship established in step 1. We developed a set of

rejection criteria based on available estimates of the population characteristics of UK grey seal populations, as described in Thomas et al. (2019) and Smout et al. (2019).

Table 10. Rejection criteria used in Approximate Bayesian Computational Analysis

Pattern	Rejection criteria	Used in step
Annual population growth rate	<0.985 or >1.035	1 & 2
Median birth rate	> 0.8	1 & 2
Female starvation mortality	< 0.2	1 & 2
Pup survival	<0.14 or >0.22	2

The first step revealed that there is a strong correlation between *Rmean* and sigma_M (Figure 43) and the established relationship between these two parameters was used in the second step.

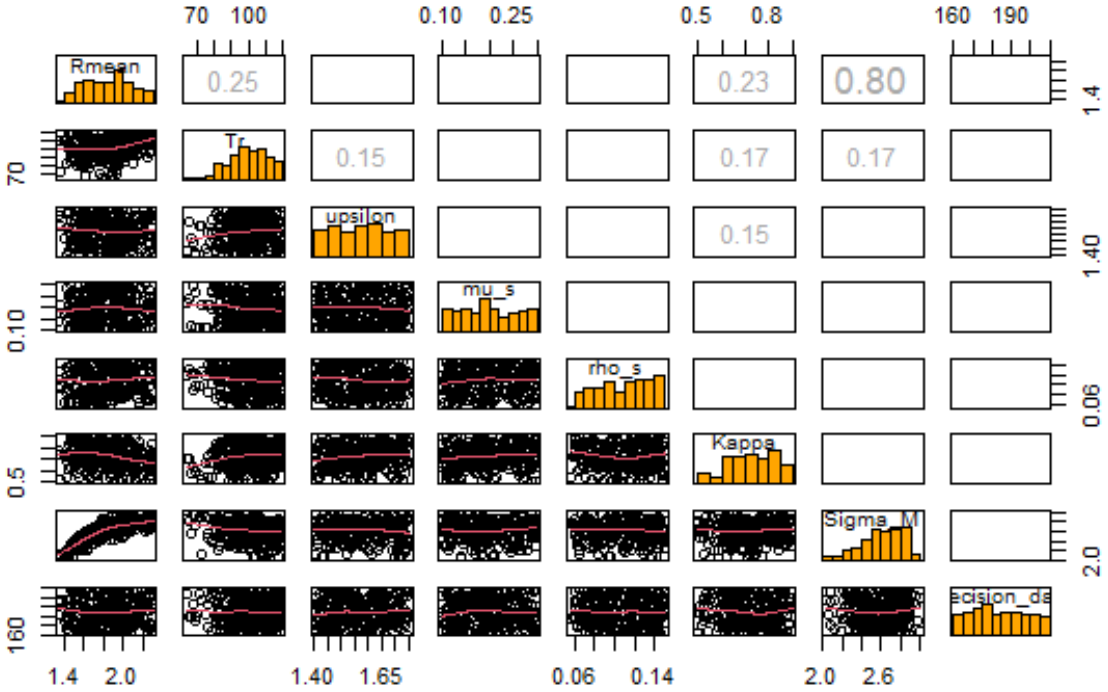

Figure 43. Pairwise plot showing correlation between parameters (grey numbers, only correlation with significance level <0.05 are shown) and their posterior distributions (yellow histograms). See Table 9 for parameter definitions

The 60,000 simulations in step 2, resulted in 519 parameter combinations fulfilling all the criteria listed in Table 10. The prior and posterior distribution of these parameters is shown in Figure 44. These 519 combinations were then used to investigate the effect of uncertainty on the predicted relationship between disturbance and vital rates.

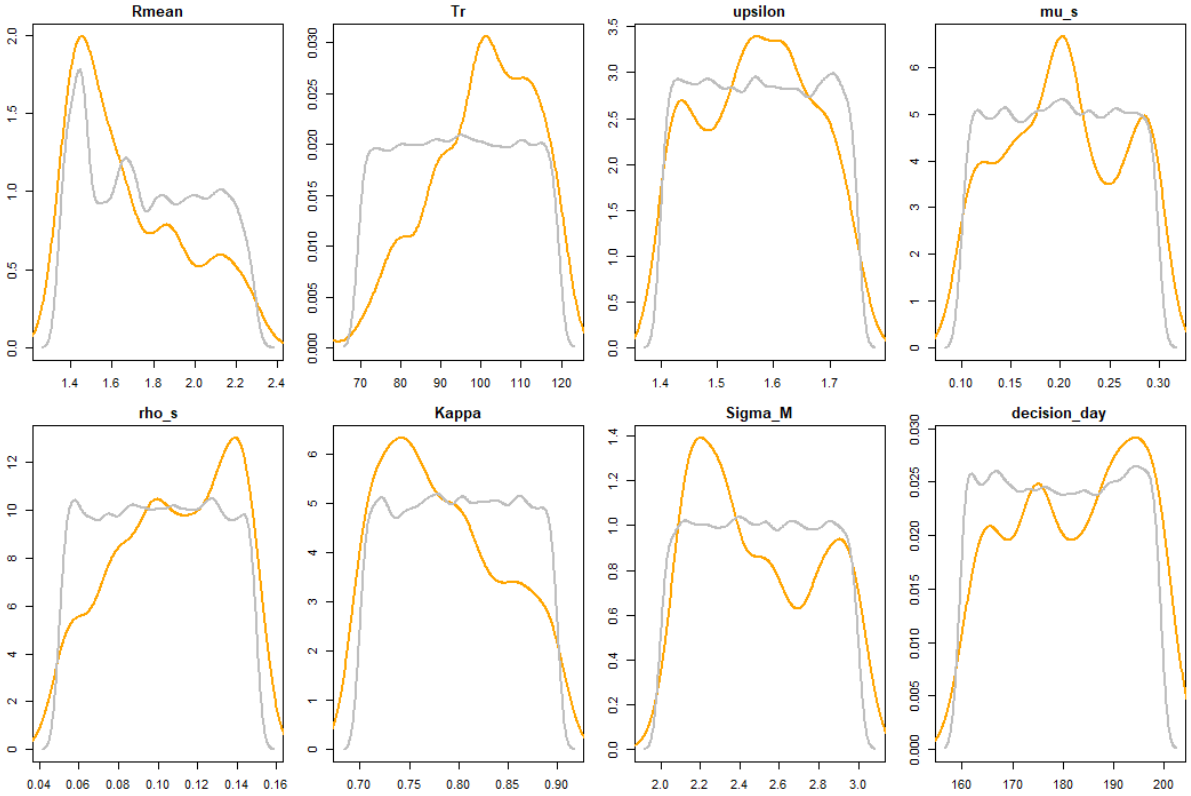

Figure 44. Prior (grey) and posterior (orange) distribution of parameters used in step 2 of the ABC. Note that *Rmean* is a function of Sigma_M and is not, therefore, drawn from a prior distribution but is calculated from the orior value of Sigma_M.

9.3 Effects of uncertainty on the predicted relationship between disturbance and vital rates.

Figure 45 shows the predicted effects of disturbance on calf survival and birth rate for 10-year-old and 21-year-old female grey seals using 100 parameter combinations randomly selected, without replacement from the 519 combinations generated by the ABC analysis. A total of 1500 were simulated for each combination of parameter values and number of days of disturbance, and disturbance was assumed to result in

a 25% reduction in foraging efficiency (equivalent to a cessation of foraging of 6 hours during the day on which disturbance occurred). Few studies have explored this directly. Czapanskiy et al. (2021) describes a 1-hour cessation of foraging to be mild, 2 hours to be moderate and 8 hours to be an extreme response. Disturbances were scheduled to occur on random days within the period from implantation until the female decided whether or not to continue the pregnancy. For seals breeding at the Farne Islands, this is the period from late March to the end of August, which is when piling for offshore wind farms in the North Sea is most likely to occur.

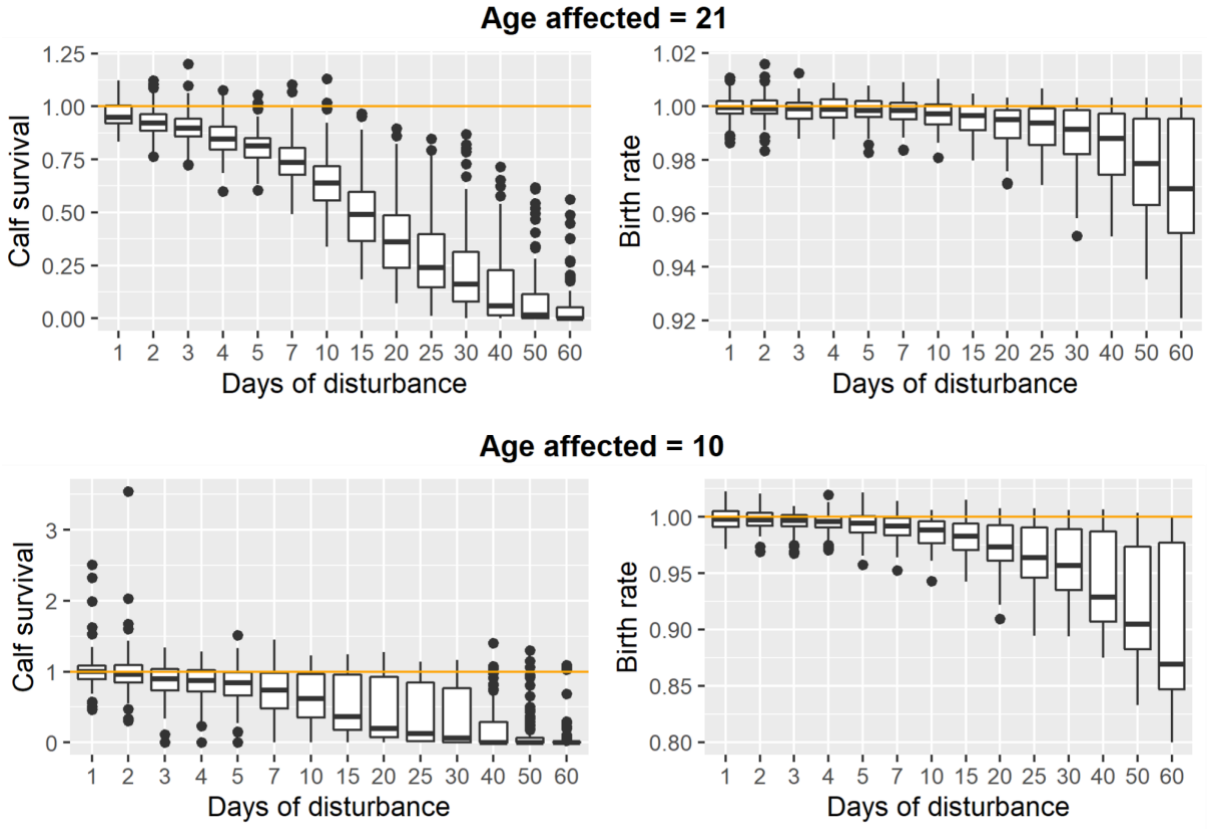

Figure 45. The effect of different number of days of disturbance on calf survival and birth rate for 21year old females (upper two panels) and 10-YEAR-OLD females (lower two panels). The boxplots represent the spread of results from 100 different parameter settings derived from the ABC analysis. All values are expressed as a proportion of the equivalent value from simulations with no disturbance.

In principle, relationships such as those used to produce Figure 45 can be incorporated into iPCoD as an alternative to the “virtual expert” relationships derived from expert elicitation that are currently used. However, it is critical to note that the effect of disturbance (assumed to be 6 hours lost foraging here for indicative purposes only) would need to be carefully considered as relationships will vary depending on the selection of this value.

Some changes to the iPCoD code would be required to take account of the fact that the effects of disturbance predicted by the DEB model are different at different times of year. However, iPCoD requires the user to input a calendar of disturbance events and it records the disturbance history of each simulated individual exposed to these events, so these histories can readily be divided into appropriate sensitive periods.

10 Exploration of animal movement in iPCoD

This part of the study is separate from the DEB model development and the objective was to make a cursory exploration of the other key component impacting assessments of disturbance – the probability of exposure. Here we have explored how animal movement models may be utilised to refine the estimation of exposure histories for iPCoD

10.1 Why simulating movement is important

Currently in iPCoD, estimates of the number of animals of the species under consideration that may be disturbed, is an input number defined by the modeller. Furthermore, the model assumes that all individuals in a population are equally likely to be exposed to disturbance from a particular activity, or that only the members of a local population are likely to be exposed. The real-world situation is likely to be somewhere between these two extremes (see Keen et al. 2021). The use of movement simulation models is, therefore, required to generate more realistic exposure histories.

Here we demonstrate how movement models, for a single species, can be used to provide the kind of information required to improve realism and reduce conservatism in population level assessments.

The Disturbance Effects of Noise on the Harbour Porpoise Population in the North Sea (DEPONS) model is an individual-based model which can be used to predict annual movement patterns for a large number of “virtual” harbour porpoises in the North Sea and Inner Danish Waters. Below we demonstrate how we used DEPONS to estimate the number of days on which each virtual individual is likely to experience disturbance.

10.2 Simulating movement

We used the Inner Danish Waters harbour porpoise version of DEPONS as an example. We ran simulations for 200 individuals over 8 years: 3 years of burn-in period (the period the model needs to be run for before results can be robustly used) and 5 years of actual movement simulations. The duration of burn-in period was defined by observing population stability of the modelled individuals. Coordinates of each tracked individual were outputted in 30-minute time bins. DEPONS allows for tracking individuals from the beginning of the simulations to the death of these

individuals during simulations. Individuals born during simulations are not tracked (see next paragraph for further explanation).

We then defined locations of two disturbance events with contrasting potential effect: ‘high’ (red, Figure 46) where the area of disturbance was superimposed on an observed high density region for porpoises, and ‘low’ (black, Figure 46), where the observed density of animals is low (Sveegaard et al. 2011). In both the high- and low-density regions, disturbance impact radii of 30, 45 and 60 km were superimposed.

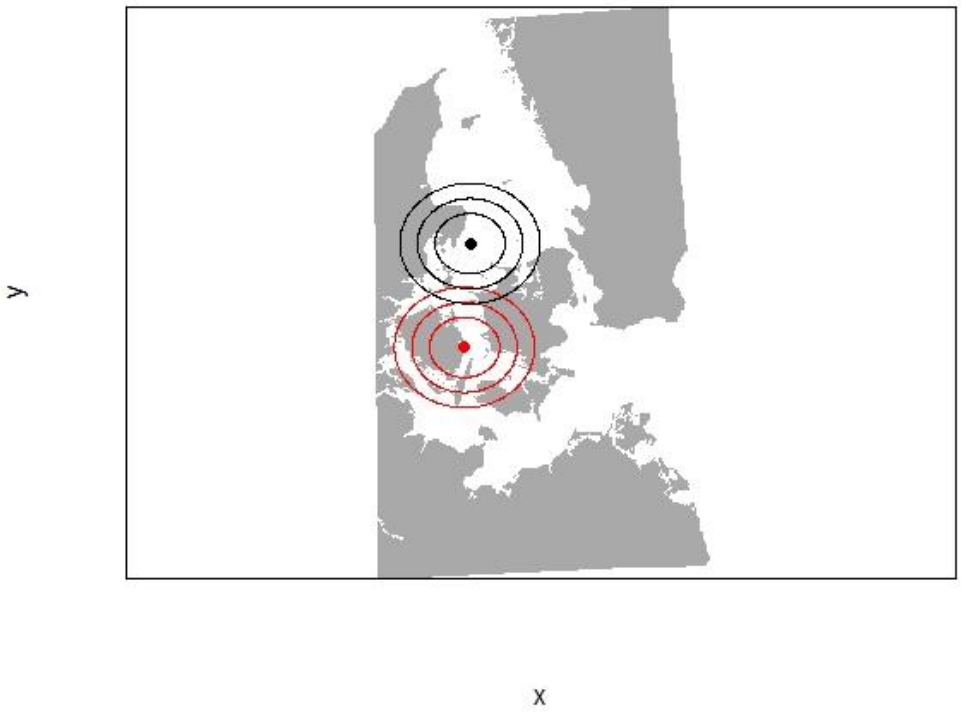

Figure 46. Locations of two disturbances with contrasting potential effect: ‘high’ (red) where observed density of animals is high and ‘low’ (black), where observed density of animals is low. Each location has then 30, 45 and 60 km radius of potential effect of disturbance defined.

We then constructed a matrix to identify the number of hours per day each individual spends within any of these defined areas over the entire 5 years simulations (Figure 47).

This kind of matrix provides the kind of information conceptually required for transposing to iPCoD to inform analysis on harbour porpoises.

	ID	1	2	3	4	5	6	7	8	9	10	11	12	13
1	0_2010_1	24.0	24.0	13.0	18.0	8.0	0.0	0.0	0.0	0.0	0.0	0.0	0.0	0.0
2	0_2011_1	24.0	24.0	24.0	24.0	9.5	0.0	0.0	0.0	0.0	0.0	0.0	0.0	0.0
3	0_2012_1	0.0	0.0	0.0	0.0	0.0	0.0	0.0	0.0	0.0	0.0	0.0	0.0	0.0
4	0_2013_1	24.0	24.0	24.0	24.0	24.0	24.0	24.0	24.0	24.0	24.0	24.0	24.0	24.0
6	3_2010_1	24.0	24.0	24.0	24.0	24.0	9.5	23.5	24.0	24.0	24.0	24.0	24.0	14.5
7	3_2011_1	0.0	0.0	0.0	0.0	0.0	0.0	0.0	0.0	0.0	0.0	0.0	0.0	0.0
8	3_2012_1	0.0	0.0	0.0	0.0	0.0	0.0	0.0	0.0	0.0	0.0	0.0	0.0	0.0
9	3_2013_1	22.5	15.0	0.0	0.0	2.0	0.0	0.0	13.0	0.0	16.5	22.0	19.5	10.5
10	3_2014_1	2.0	24.0	16.5	24.0	17.5	21.0	24.0	3.0	11.0	24.0	24.0	24.0	24.0
11	4_2010_1	0.0	0.0	0.0	0.0	0.0	0.0	0.0	0.0	0.0	0.0	0.0	0.0	0.0
12	4_2011_1	24.0	24.0	11.5	16.0	24.0	24.0	17.0	0.0	0.0	0.0	0.0	1.0	17.0

Figure 47. Example of a matrix showing number of hours per day each tracked individual spent within one of the defined areas of disturbance. Each column is therefore a day of year (365 columns) and each row is an individual tracked a given year.

This kind of approach could be explored further to allows other movement and exposure variables to be estimated:

- Individual and seasonal differences in the exposure history
- Frequency of occurrence within a disturbed area
- Inter-individual variability in duration and frequency of occurrence within the disturbed area.

All of these variables will sum to affect the realism of probability of exposure estimates.

10.2.1 Pitfalls

As mentioned above, DEPONS only allows for tracking of individuals which are created at the beginning of each simulation and the tracking stops when animals die. Individuals born after the start of the simulation are not tracked. DEPONS is also designed to simulate movement of so-called super-individuals: individuals which represent collectively larger number of individuals. Hence, DEPONS for Inner Danish Waters is designed to simulate maximum 200 ‘super-individuals’ and the results can then be extrapolated to the entire population in this area.

These above issues result in small number of individuals which can be tracked during actual simulations, after the end of burn-in period (Figure 48). As a consequence, the simulation of movement can only be performed for limited period of time – a maximum 10 years. After this period, there are very few or no animals which can be tracked by the model. This problem with low number of simulated and tracked individuals would be even more pronounced for simulations over large geographical space such as the North Sea.

Therefore, this is one of the limitations of this approach, that whilst it can provide the kind of information required to improve iPCoD simulations, it is limited by the sample size available (in terms of the number of animals that animals that can be tracked given simulation length and burn in period). This is a consideration that should be taken into account. But this approach demonstrates how movement models can be used to inform more realistic iPCoD simulations.

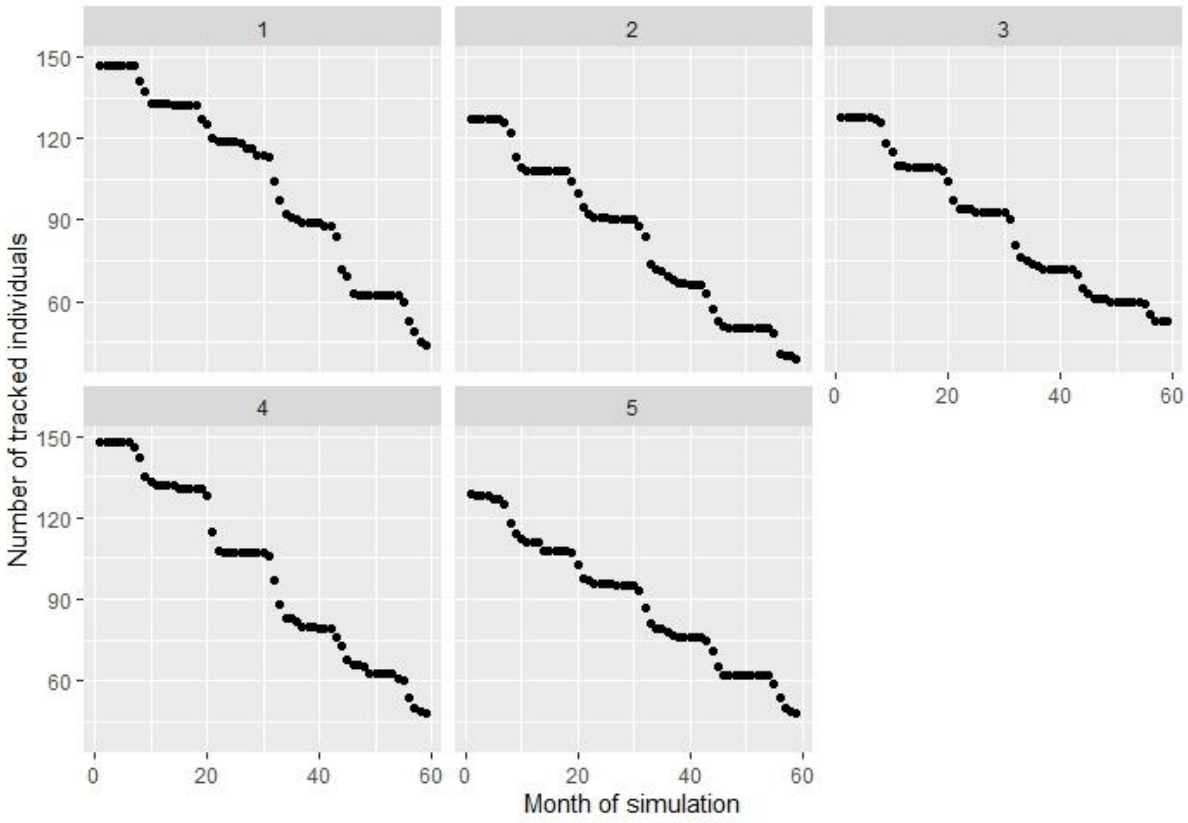

Figure 48. Examples from five simulations showing total number of tracked individuals during 5-year simulations, excluding burn-in period. At the beginning of each simulation, 200 individuals are created and tracked but, as some of these individuals die during the burn-in period, smaller number of individuals is tracked at the beginning of actual simulations and even smaller number by the end of these simulations.

11 Summary and future requirements

In this report we have provided detailed descriptions of DEB models for harbour seals, grey seals, bottlenose dolphins and minke whales in UK waters. These can be added to the suite of DEB models, all based on the template developed by Hin et al. (2019), that already includes models for harbour porpoise, long-finned pilot whale, Cuvier's beaked whale, Blainville's beaked whale, beluga and Pacific walrus. In principle, the same template could be used to develop DEB models for other cetacean species (e.g., Risso's dolphin, white-sided and white-beaked dolphins) likely to be affected by offshore wind farm construction in UK waters. However, this

would be challenging because of the lack of data on key demographic parameters (age-specific growth rates, age-specific survival rates, length-mass relationships, and lactation durations) for these species. In addition, there is little or no information on how these species react to the noise associated with wind farm construction. Although it may be possible to “borrow” values for the relevant parameters from other related species, this would introduce additional uncertainty into model predictions that would be difficult to quantify.

The model descriptions in this report have been structured using the ODD protocol recommended by Grimm et al. (2020) for documenting agent-based models. Descriptions of this kind are widely accepted as Supplementary Information (SI) for journal articles that report results obtained using such models and will simplify the production of such articles because the same SI can be used multiple times. The models have also been calibrated using the POM approach developed by Grimm et al. (2005).

We investigated the effects of disturbance on vital rates for harbour seals, grey seals, bottlenose dolphins and minke whales (Sections 5.3, 6.3, 7.3 and 8.3). Grey seals appear to be more vulnerable to the effects of disturbance than the other three species, but these results should be treated with caution because only a relatively small set of plausible model parameter values was used in the simulations for the other three species.

We have demonstrated in Section 9.3 how the DEB models developed for this study and the harbour porpoise DEB model are capable of generating the relationships required to replace the transfer functions in iPCoD. These transfer functions, which established the relationship between days of disturbance experienced and their effect on vital rates, were derived using formal EE approaches. Although the way in which these transfer functions were derived is more precisely documented than those developed using EE, it should be recognised that the DEB-derived functions rely on two key sets of assumptions. First, they are based on a set of equations and parameter values sourced from across the marine mammal and energetics literature that may not be appropriate for the species to which they are applied. Second, they assume that the only effect of disturbance from human noise on vital rates is the result of a reduction in energy intake and that this reduction is directly related to the duration of any behavioural changes caused by disturbance. The predictions of a DEB model are highly dependent on how many hours of lost foraging are specified to occur as a result of disturbance. The validity of this assumption will need to be evaluated carefully if DEB-derived functions are used to replace the EE-derived transfer functions in iPCoD.

Loss of foraging opportunities is only one of the three potential effects of behavioural change on vital rates documented by Southall et al. 2021. The others are increased predation risk and impaired reproductive behaviour. It is likely that the experts involved in the iPCoD EEs took account of all three potential effects when they predicted the effects of different amounts of disturbance on vital rates. On the other hand, the experts were asked to evaluate the effects of disturbance at any time of year on vital rates. However, the DEB models have clearly indicated that a reduction in energy intake is only likely to affect the vital rates of certain life history stages (particularly pregnant and lactating females, and recently weaned calves or pups) at certain times of year. These findings can be used to identify opportunities for risk mitigation through the timing of operations in a way that is not possible using the EE-derived transfer functions.

We have also described how the uncertainty associated with the many model parameter values can be accounted for and developed a novel and efficient method using ABC to quantify the uncertainty associated with parameters that are not directly observable. By sampling from the resulting posterior probability distributions, it will be possible to generate the equivalent of the thousands of different “virtual” expert relationships between vital rates and the number of days of disturbance that are currently used to evaluate uncertainty in iPCoD. This method can be readily applied to any of the existing DEB models developed using the Hin et al. (2019) template. However, it should be recognised that the uncertainty that is captured by this approach (which relates to uncertainty in model parameter values) is fundamentally different from the uncertainty associated with the EE-derived transfer functions. The latter related to the variation among experts in the predicted form of the transfer functions and the experts’ evaluations of their confidence in the shape of the functions.

Finally, we carried out preliminary trials using output from the DEPONS model (Nabe-Nielsen et al., 2018) to show how telemetry data can be used to estimate the cumulative exposure of different individuals in a harbour porpoise population to disturbance from piling activity.

It is clear from the uncertainty and sensitivity analyses that much of the uncertainty about the effects of disturbance on vital rates is related to uncertainty around the choice of a suitable value for the FMR multiplier (sigma_M). Further research to clarify the causes of variation in FMR between and within species would provide a more robust quantification of this uncertainty than we have been able to provide.

The other set of parameters that make a substantial contribution to uncertainty are those relating to the development of foraging efficiency. Information regarding the way in which the foraging efficiency of pups and calves develops in the post-weaning period, either from direct observation or telemetry, would be particularly valuable.

Finally, understanding the effects of disturbance on foraging remains key to such models.

The final set of parameters that contribute substantially to uncertainty are those relating to the threshold body condition for starvation (ρ_s) and the risk of starvation-related mortality (μ_s). Further research on the relationship between body condition and the risk of mortality is required to resolve this.

Finally, in the time available, we were unable to consider the effects on the predictions of the DEB models of environmental stochasticity and individual variation in the parameters that determine growth, feeding efficiency and the threshold for reproduction. Incorporation of this variation would undoubtedly make the model predictions more realistic. Further research is required to determine the magnitude and importance of their effects.

12 References

Arso Civil, M., Cheney, B., Quick, N. J., Thompson, P. M., & Hammond, P. S. (2017). A new approach to estimate fecundity rate from inter-birth intervals. Ecosphere, 8(4), e01796.

Arso Civil, M., B. Cheney, N. J. Quick, V. Islas-Villanueva, J. A. Graves, V. M. Janik, P. M. Thompson, and P. S. Hammond. 2018. Variations in age-and sex-specific survival rates help explain population trend in a discrete marine mammal population. Ecology and Evolution

Barlow, J. and P. Boveng. 1991. Modeling age-specific mortality for marine mammal populations. Marine Mammal Science 7(1):50-65.

Bejarano, A. C., R. S. Wells, and D. P. Costa. 2017. Development of a bioenergetic model for estimating energy requirements and prey biomass consumption of the bottlenose dolphin Tursiops truncatus. Ecological Modelling 356:162-172.

Bennett, K. A., J. R. Speakman, S. E. Moss, P. Pomeroy, and M. A. Fedak. 2007. Effects of mass and body composition on fasting fuel utilisation in grey seal pups (Halichoerus grypus Fabricius): an experimental study using supplementary feeding. Journal of Experimental Biology 210:3043-3053.

Blix, A., and L. Folkow. 1995. Daily energy expenditure in free living minke whales. Acta Physiologica 153(1):61-66.

Boness, D. J., W. D. Bowen, and O. T. Oftedall. 1994. Evidence of a maternal foraging cycle resembling that of otariid seals in a small phocid, the harbor seal. Pages 95-104 Behavioral Ecology and Sociobiology.

Bonner, W. 1981. Grey Seal *Halichoerus grypus Fabricius*, 1791. Pages Pp 111-144 Ridgway, S.H. & Harrison, R.J. (eds.) Handbook of Marine Mammals Volume 2 Seals. Academic Press, London.

Booth, C. G., F. Heinis, and H. J. 2019. Updating the Interim PCoD Model: Workshop Report - New transfer functions for the effects of disturbance on vital rates in marine mammal species. Report Code SMRUC-BEI-2018-011, submitted to the Department for Business, Energy and Industrial Strategy (BEIS), February 2019 (unpublished).

Booth, C., and F. Heinis. 2018. Updating the Interim PCoD Model: Workshop Report - New transfer functions for the effects of permanent threshold shifts on vital rates in marine mammal species. Report Code SMRUC-UOA-2018-006, submitted to the University of Aberdeen and Department for Business, Energy and Industrial Strategy (BEIS), June 2018 (unpublished).

Boveng, P., Bowen, W., S. J. Iverson, J. McMillan, and D. Boness. 2006. Reproductive performance in grey seals: age-related improvement and senescence in a capital breeder. Journal of Animal Ecology 75:1340-1351.

Bowen, W.D., Iverson, S.J., Boness, D.J., Oftedal, O.T., 2001. Foraging effort, food intake and lactation performance depend on maternal mass in a small phocid seal. Funct. Ecol. 15, 325–334. https://doi.org/10.1046/j.1365-2435.2001.00530.x

Bowen, W.D., Oftedal, O.T., Boness, D.J., 1992. Mass and Energy Transfer during Lactation in a Small Phocid, the Harbor Seal (Phoca vitulina). Physiol. Zool. 65, 844–866. https://doi.org/10.1086/physzool.65.4.30158543

Bowen, W.D., Oftedal, O.T., Boness, D.J., Iverson, S.J., 1994. The effect of maternal age and other factors on birth mass in the harbour seal. Can. J. Zool. 72, 8–14. https://doi.org/10.1139/z94-002

Boyd, I. 1984. The relationship between body condition and the timing of implantation in pregnant grey seals (Halichoerus grypus). Journal of Zoology 203:113-123.

Braithwaite, J. E., J. J. Meeuwig, and M. R. Hipsey. 2015. Optimal migration energetics of humpback whales and the implications of disturbance. Conservation Physiology 3:cov001.

Brody, S. 1968. Bioenergetics and growth, revised 1945 edn. Hafner Publishing, New York, NY.

Cheney, B., T. J. Thompson, and L. Cordes. 2019. Increasing trends in fecundity and calf survival of bottlenose dolphins in a marine protected area. Scientific Reports **9**:1767.

Cheney, B., R. Wells, T. Barton, and P. Thompson. 2018. Laser photogrammetry reveals variation in growth and early survival in free-ranging bottlenose dolphins. Animal Conservation 21:252-261.

Christensen, I. (1981). Age determination of minke whales, Balaenoptera acutorostrata, from laminated structures in the tympanic bullae. Reports of the International Whaling Commission, 31, 245–253.

Christiansen, F., and D. Lusseau. 2015. Linking Behavior to Vital Rates to Measure the Effects of Non-Lethal Disturbance on Wildlife. Conservation Letters 8:424-431.

Christiansen, F., G. A. Víkingsson, M. H. Rasmussen, and D. Lusseau. 2013. Minke whales maximise energy storage on their feeding grounds. Journal of Experimental Biology 216: 427-436.

Christiansen, F., G. A. Víkingsson, M. H. Rasmussen, and D. Lusseau. 2014. Female body condition affects foetal growth in a capital breeding mysticete. Functional Ecology 28(3):579-588.

Cockcroft, V., and G. Ross. 1990. Observations on the early development of a captive bottlenose dolphin calf. The bottlenose dolphin 461:478.

Cordes, L.S., Thompson, P.M., 2013. Variation in breeding phenology provides insights into drivers of long-term population change in harbour seals. Proc. R. Soc. B Biol. Sci. https://doi.org/10.1098/rspb.2013.0847

Costa, D., B. L. Boeuf, A. Huntley, and C. Ortiz. 1986. The energetics of lactation in the northern elephant seal, Mirounga angustirostris. Journal of Zoology 209:21-33.

Czapanskiy, M. F., M. S. Savoca, W. T. Gough, P. S. Segre, D. M. Wisniewska, D. E. Cade, and J. A. Goldbogen. 2021. Modelling short-term energetic costs of sonar disturbance to cetaceans using high-resolution foraging data. Journal of Applied Ecology.

De Roos, A. M., N. Galic, and H. Heesterbeek. 2009. How resource competition shapes individual life history for nonplastic growth: ungulates in seasonal food environments. Ecology 90:945-960.

Dubé, Y., Hammill, M.O., Barrette, C., 2003. Pup development and timing of pupping in harbour seals (Phoca vitulina) in the St. Lawrence River estuary, Canada. Can. J. Zool. 81, 188–194. https://doi.org/10.1139/z02-231

Durbach, I.N., C.M. Harris, C. Martin, T.A. Helble, E.E. Henderson, G. Ierley, L. Thomas, and S.W. Martin. (2021). Changes in the behavior of minke whales (Balaenoptera acutorostrata) in response to Navy training. Frontiers in Marine Science 8: Article 660122.

Finney, D. J. (1979). Bioassay and the Practice of Statistical Inference. International Statistical Review / Revue Internationale de Statistique, 47(1), 1. https://doi.org/10.2307/1403201

Folkow, L. P., T. Haug, T., K.T. Nilssen, and E.S. Nordøy. (2000). Estimated food consumption of minke whales Balaenoptera acutorostrata in Northeast Atlantic waters in 1992-1995. NAMMCO Scientific Publications, 2, 65–80.

Goedegebuure, M., J. Melbourne-Thomas, S. P. Corney, C. R. McMahon, and M. A. Hindell. 2018. Modelling southern elephant seals Mirounga leonina using an individual-based model coupled with a dynamic energy budget. PloS one 13(3):e0194950.

Grellier, K., Hammond, P. S., Wilson, B., Sanders-Reed, C. A., & Thompson, P. M. (2003). Use of photo-identification data to quantify mother calf association patterns in bottlenose dolphins. Canadian Journal of Zoology, 81(8), 1421-1427.

Grimm, V., Railsback, S. F., Vincenot, C. E., Berger, U., Gallagher, C., Deangelis, D. L., Ayllón, D. (2020). The ODD protocol for describing agent-based and other simulation models: A second update to improve clarity, replication, and structural realism. JASSS, 23(2). https://doi.org/10.18564/jasss.4259

Grimm, V., Revilla, E., Berger, U., Jeltsch, F., Mooij, W. M., Railsback, S. F., … DeAngelis, D. L. (2005). Pattern-oriented modeling of agent-based complex systems: Lessons from ecology. Science, 310(5750), 987–991. https://doi.org/10.1126/science.1116681

Groemping, U., 2011. FrF2: Fractional Factorial Designs with 2-Level Factors . http://cran.r-project.org/web/packages/FrF2/ Archived at: http://www.webcitation.org/6H9NO65Hn.

Groemping, U., 2013. DoE.base: Full Factorials, Orthogonal Arrays and Base Utilities for DoE Packages. http://cran.rproject. org/web/packages/DoE.base/ Archived at: http://www.webcitation.org/6H9NV5KCl.

Hall, A. J., and B. J. McConnell. 2007. Measuring changes in juvenile gray seal body composition. Marine Mammal Science 23:650-665.

Hall, A. J., McConnell. B. J. and Barker, R. J., 2001. Factors affecting first-year survival in grey seals and their implications for life history strategy. Journal of Animal Ecology, 70(1), pp.138-149.

Hall, A.J., Kershaw, J., Thompson, P., 2012. Age-length and condition relationships and age distributions among live-captured UK harbour seals, 1999-2012., SCOS Briefing Paper 12/11.

Hall, A.J., Mackey, B., Kershaw, J., Thompson, P., 2019. Age-length relationships in UK harbour seals during a period of decline in abundance. Aquat. Conserv. Mar. Freshw. Ecosyst. 29, 61–70.

Hall, A. J., and D. J. Russell. 2018. Gray Seal: Halichoerus grypus. Pages 420-422 Encyclopedia of marine mammals. Elsevier

Hanson, N., S. Smout, S. Moss, and P. Pomeroy. 2019. Colony-specific differences in decadal longitudinal body composition of a capital-breeding marine top predator. Aquatic Conservation Marine and Freshwater Ecosystems. **29(S1)**:131-143.

Harding, K., M. Fujiwara, Y. Axberg, and T. Härkönen. 2005. Mass-dependent energetics and survival in Harbour Seal pups. Functional Ecology **19**:129-135.

Härkönen, T., Heide-Jørgensen, M.P., 1990. Comparative life histories of east atlantic and other harbour seal populations. Ophelia 32, 211–235. https://doi.org/10.1080/00785236.1990.10422032

Hart, L. B., R. S. Wells, and L. H. Schwacke. 2013. Reference ranges for body condition in wild bottlenose dolphins Tursiops truncatus. Aquatic Biology 18:63-68.

Harwood, J., C. Booth, R. Sinclair, and E. Hague. 2020. Developing marine mammal Dynamic Energy Budget models and their potential for integration into the iPCoD framework. Scottish Marine and Freshwater Science Vol 11 No 11, 74pp. DOI: 10.7489/12328-1.

Harwood, J., S. King, R. Schick, C. Donovan, and C. Booth. 2014. A protocol for Implementing the Interim Population Consequences of Disturbance (PCoD) approach: Quantifying and assessing the effects of UK offshore renewable energy developments on marine mammal populations. Report Number SMRUL-TCE-2013-014. Scottish Marine And Freshwater Science, 5(2).

Hauksson, E. 2007. Growth and reproduction in the Icelandic grey seal. NAMMCO Scientific Publications **6**:153-162.Harwood, J., C. G. Booth, and D. Tollit. 2019. Walrus Interim PCoD Model: Workshop Report - New transfer functions for the effects of acoustic disturbance on vital rates in Pacific Walrus. US Fish and Wildlife Service, Anchorage.

Hauksson, E., G. Vikingsson, S. Halldorsson, D. Olafsdottir, and J. Sigurjonsson. 2011. Preliminary report on biological parameters for North Atlantic minke whales in Icelandic waters, IWC 2011 SC/63/O15.

Hin, V., J. Harwood, and A. M. de Roos. 2019. Bio-energetic modeling of medium-sized cetaceans shows high sensitivity to disturbance in seasons of low resource supply. Ecological Applications:e01903.

Hin, V., J. Harwood, and A. M. De Roos. 2021. How density-dependent processes hide the population consequences of disturbance. Journal of Animal Ecology TBC:TBC.

Jabot, F., T. Faure, and N. Dumoulin. 2013. Easy ABC: performing efficient approximate Bayesian computation sampling schemes using R. Methods in Ecology and Evolution 4 (7): 684-687.

Jonsgård, Å. 1951. Studies on the Little Piked Whale Or Minke Whale (Balaenoptera acutorostrata Lacépède): Report on Norwegian Investigations Carried Out in the Years 1943-1950. OEEC.

Jørgensen, C., Lydersen, C., Brix, O., Kovacs, K.M., 2001. Diving development in nursing harbour seal pups. J. Exp. Biol. 204, 3993–4004.

Kastelein, R. A., L. Helder-Hoek, N. Jennings, R. van Kester, and R. Huisman. 2019. Reduction in body mass and blubber thickness of harbor porpoises (Phocoena phocoena) due to near-fasting for 24 hours in four seasons. Aquatic Mammals **45**:37-47.

Kastelein, R. A., and R. Van Battum. 1990. The relationship between body weight and morphological measurements in harbour porpoises (Phocoena phocoena) from the North Sea. Aquat Mamm **16**:48-52.

Kastelein, R. A., Vaughan, N., Walton, S., & Wiepkema, P. R. (2002). Food intake and body measurements of Atlantic bottlenose dolphins (Tursiops truncates) in captivity. Marine Environmental Research, 53(2), 199–218. https://doi.org/10.1016/S0141-1136(01)00123-4

Keen, K. A., Beltran, R. S., Pirotta, E., & Costa, D. P. (2021). Emerging themes in Population Consequences of Disturbance models. Proceedings of the Royal Society B, 288(1957), 20210325.

King, S. L., R. S. Schick, C. Donovan, C. G. Booth, M. Burgman, L. Thomas, and J. Harwood. 2015. An interim framework for assessing the population consequences of disturbance. Methods in Ecology and Evolution **6**:1150-1158.

Klanjscek, T., R. M. Nisbet, H. Caswell, and M. G. Neubert. 2007. A model for energetics and bioaccumulation in marine mammals with applications to the right whale. Ecological Applications 17:2233-2250.

Kleiber, M. 1975. The fire of life. Robert E. Kreiger, New York

Kooijman, S.A.L.M., 2010. Dynamic Energy Budget theory for metabolic organisation - Th, Cambridge University Press. https://doi.org/10.1098/rstb.2010.0167

Koopman, H. N. 2007. Phylogenetic, ecological, and ontogenetic factors influencing the biochemical structure of the blubber of odontocetes. Marine Biology 151:277-291.

Koopman, H. N., D. A. Pabst, W. A. Mclellan, R. Dillaman, and A. Read. 2002. Changes in blubber distribution and morphology associated with starvation in the harbor porpoise (Phocoena phocoena): evidence for regional differences in blubber structure and function. Physiological and Biochemical Zoology **75**:498-512.

Kvadsheim, P.H., S. DeRuiter, L. D. Sivle, J. Goldbogen, R. Roland-Hansen, P.J.O. Miller, F-P. A. Lam, J. Calambokidis, A. Friedlaender, F. Visser, P. L. Tyack, L. Kleivane, and B. Southall. (2017). Avoidance responses of minke whales to 1–4 kHz naval sonar. Marine Pollution Bulletin 121: 60-68.

Lang, S.L.C., Iverson, S.J., Bowen, W.D., 2011. The influence of reproductive experience on milk energy output and lactation performance in the grey seal (Halichoerus grypus). PLoS One 6, e19487. https://doi.org/10.1371/journal.pone.0019487

Lockyer, C., 1993. Seasonal changes in body fat condition of northeast Atlantic pilot whales, and their biological significance. IWC Special Issue 14: Biology of the Northern Hemisphere Pilot Whales, pp.205-324.

Lockyer, C. 2007. All creatures great and smaller: a study in cetacean life history energetics. Journal of the Marine Biological Association of the United Kingdom 87(4):1035-1045. doi: 10.1017/S0025315407054720

Lockyer, C., G. Desportes, K. Hansen, S. Labberté, and U. Siebert. 2003. Monitoring growth and energy utilisation of the harbour porpoise (*Phocoena phocoena*) in human care. NAMMCO Scientific Publications **5**:107-120.Lorscheid, I., Heine, B.O., Meyer, M., 2012. Opening the “Black Box” of Simulations: Increased Transparency

and Effective Communication Through the Systematic Design of Experiments. Comput. Math. Organ. Theory 18, 22–62. https://doi.org/10.1007/s10588-011-9097-3

Mann, J., and B. Smuts. 1999. Behavioral development in wild bottlenose dolphin newborns (Tursiops sp.). Behaviour 136:529-566.

McHuron, E. A., D. P. Costa, L. Schwarz, and M. Mangel. 2016. State-dependent behavioural theory for assessing the fitness consequences of anthropogenic disturbance on capital and income breeders. Methods in Ecology and Evolution:n/a-n/a.

McHuron, E. A., L. K. Schwarz, D. P. Costa, and M. Mangel. 2018. A state-dependent model for assessing the population consequences of disturbance on income-breeding mammals. Ecological Modelling 385:133-144.

McHuron, E. A., M. Mangel, L. K. Schwarz, and D. P. Costa. 2017. Energy and prey requirements of California sea lions under variable environmental conditions. Marine Ecology Progress Series 567:235-247.

McLaren, I. 1993. Growth in pinnipeds. Biological Reviews **68**:1-79.

Moretti, D. 2019. Determining the effect of Mid-Frequency Active (MFA) sonar on fitness of Blainville's beaked whales (Mesoplodon densirostris) in the Tongue of the Ocean. University of St Andrews.

Muelbert, M.M.C., Bowen, W.D., 1993. Duration of lactation and postweaning changes in mass and body composition of harbour seal, Phoca vitulina , pups . Can. J. Zool. 71, 1405–1414. https://doi.org/10.1139/z93-194

Muelbert, M.M.C., Bowen, W.D., Iverson, S.J., 2003. Weaning mass affects changes in body composition and food intake in harbour seal pups during the first month of independence. Physiol. Biochem. Zool. 76, 418–427. https://doi.org/10.1086/375427

Nabe-Nielsen, J., F. van Beest, V. Grimm, R. Sibly, J. Teilmann, and P. M. Thompson. 2018. Predicting the impacts of anthropogenic disturbances on marine populations. Conservation Letters e12563. https://doi.org/10.1111/conl.12563

Nabe-Nielsen, J., R. M. Sibly, J. Tougaard, J. Teilmann, and S. Sveegaard. 2014. Effects of noise and by-catch on a Danish harbour porpoise population. Ecological Modelling 272:242-251.

Neuenhoff, R. D., D. F. Cowan, H. Whitehead, and C. D. Marshall. 2011. Prenatal data impacts common bottlenose dolphin (Tursiops truncatus) growth parameters estimated by length-at-age curves. Marine Mammal Science 27:195-216.

New, L. F., J. S. Clark, D. P. Costa, E. Fleishman, M. Hindell, T. Klanjšček, D. Lusseau, S. Kraus, C. McMahon, and P. Robinson. 2014. Using short-term measures of behaviour to estimate long-term fitness of southern elephant seals. Marine Ecology Progress Series 496:99-108.

New, L. F., D. J. Moretti, S. K. Hooker, D. P. Costa, and S. E. Simmons. 2013. Using Energetic Models to Investigate the Survival and Reproduction of Beaked Whales (family Ziphiidae). PLoS ONE **8**.

Nisbet, R., E. Muller, K. Lika, and S. Kooijman. 2000. From molecules to ecosystems through dynamic energy budget models. Journal of Animal Ecology 69:913-926.

Nordøy, E., L. Folkow, P. Mårtensson, and A. Blix. 1995. Food requirements of Northeast Atlantic minke whales. Whales, Seals, Fish and Man. AS Blix, L. Walløe, and Ø. Ulltang (eds.). Dev. Mar. Bio 4:307-317.

Noren, D., D. Crocker, T. Williams, and D. Costa. 2003. Energy reserve utilization in northern elephant seal (Mirounga angustirostris) pups during the postweaning fast: size does matter. Journal of Comparative Physiology B 173:443-454.

Noren, S. R., M. S. Udevitz, and C. V. Jay. 2014. Energy demands for maintenance, growth, pregnancy, and lactation of female pacific walruses (odobenus rosmarus divergens). Pages 837-854 Physiological and Biochemical Zoology.

Noren, S. R., and R. S. Wells. 2009. Blubber deposition during ontogeny in free-ranging bottlenose dolphins: balancing disparate roles of insulation and locomotion. Journal of Mammalogy 90:629-637.

Noren, S. R., D. J. Boness, S. J. Iverson, J. McMillan, and W. D. Bowen. 2008. Body condition at weaning affects the duration of the postweaning fast in gray seal pups (Halichoerus grypus). Physiological and Biochemical Zoology 81:269-277.

O'Brien, J. K., and T. R. Robeck. 2012. The relationship of maternal characteristics and circulating progesterone concentrations with reproductive outcome in the bottlenose dolphin (Tursiops truncatus) after artificial insemination, with and without ovulation induction, and natural breeding. Theriogenology 78:469-482.

Olsen, E., and J. Sunde. (2002). Age determination of minke whales (Balaenoptera acutorostrata) using the aspartic acid racemization technique. Sarsia, 87(1), 1–8. https://doi.org/10.1080/003648202753631686

Paterson, W., D. Russell, G. Wu, B. McConnell, J. Currie, D. J. McCafferty, and D. Thompson. 2019. Post-disturbance haulout behaviour of harbour seals. Aquatic Conservation Marine and Freshwater Ecosystems. **29(S1)**:144-156.

Paterson, W., Sparling, C.E., Thompson, D., Pomeroy, P.P., Currie, J.I., McCafferty, D.J., 2012. Seals like it hot: Changes in surface temperature of harbour seals (Phoca vitulina) from late pregnancy to moult. J. Therm. Biol. 37, 454–461. https://doi.org/10.1016/j.jtherbio.2012.03.004

Peddemors, V., M. Fothergill, and V. Cockcroft. 1992. Feeding and growth in a captive-born bottlenose dolphin Tursiops truncatus. African Zoology 27:74-80.

Perrin, W. F., and S. B. Reilly. 1984. Reproductive parameters of dolphins and small whales of the family Delphinidae. Report of the International Whaling Commission (Special Issue 6):97-133.

Perrin, W. F., S. D. Mallette, and R. L. Brownell Jr. 2018. Minke whales: Balaenoptera acutorostrata and B. bonaerensis. Pages 608-613 Encyclopedia of marine mammals. Elsevier.

Pirotta, E., C. G. Booth, D. P. Costa, E. Fleishman, S. D. Kraus, D. Lusseau, D. Moretti, L. F. New, R. S. Schick, and L. K. Schwarz. 2018a. Understanding the population consequences of disturbance. Ecology and Evolution.

Pirotta, E., M. Mangel, D. P. Costa, B. Mate, J. A. Goldbogen, D. M. Palacios, L. A. Hückstädt, E. A. McHuron, L. Schwarz, and L. New. 2018b. A Dynamic State Model of Migratory Behavior and Physiology to Assess the Consequences of Environmental Variation and Anthropogenic Disturbance on Marine Vertebrates. The American Naturalist 191:E000-E000.

Pomeroy, P., M. Fedak, P. Rothery, and S. Anderson. 1999. Consequences of maternal size for reproductive expenditure and pupping success of grey seals at North Rona, Scotland. Journal of Animal Ecology 68:235-253.

Pirotta, E., L. K. Schwarz, D. P. Costa, P. W. Robinson, and L. New. 2018c. Modeling the functional link between movement, feeding activity, and condition in a marine predator. Behavioral Ecology 30:434-445.

Reddy, M., Kamolnick, T., Curry, C., & Skaar, D. (1994). Energy Requirements for the Bottlenose Dolphin (Tursiops truncatus) in Relation to Sex, Age, & Reproductive Status. Marine Mammals: Public Display and Research, 1(1), 26–31.

Reijnders, P.J.H., Brasseur, S.M.J.M., Meesters, E.H.W.G., 2010. Earlier pupping in harbour seals, Phoca vitulina. Biol. Lett. 6, 854–857. https://doi.org/10.1098/rsbl.2010.0468

Reilly, J. J., M. A. Fedak, D. H. Thomas, W. A. A. Coward, and S. S. Anderson. 1996. Water balance and the energetics of lactation in grey seals (Halichoerus grypus) as studied by isotopically labelled water methods. Pages 157-165 Journal of Zoology.

Renouf, D., Gales, R., Noseworthy, E., 1993. Seasonal variation in energy intake and condition of harp seals: Is there a harp seal morph? Problems for bioenergetic modelling. J. Zool. 230, 513–528. https://doi.org/10.1111/j.1469-7998.1993.tb02703.x

Renouf, D., Noseworthy, E., 1991. Changes in food intake, mass, and fat accumulation in association with variations in thyroid hormone levels of harbour seals (Phoca vitulina). Can. J. Zool. 69, 2470–2479.

Russell, D.J.F., Hastie, G.D., Thompson, D., Janik, V.M., Hammond, P.S., Scott-Hayward, L.A.S., Matthiopoulos, J., Jones, E.L., McConnell, B.J., 2016. Avoidance of wind farms by harbour seals is limited to pile driving activities. J. Appl. Ecol. 53, 1642–1652. https://doi.org/10.1111/1365-2664.12678

Sauvé, C.C., Van De Walle, J., Hammill, M.O., Arnould, J.P.Y., Beauplet, G., 2014. Stomach temperature records reveal nursing behaviour and transition to solid food consumption in an unweaned mammal, the harbour seal pup (Phoca vitulina). PLoS One 9. https://doi.org/10.1371/journal.pone.0090329

Schick, R. S., L. F. New, L. Thomas, D. P. Costa, M. A. Hindell, C. R. McMahon, P. W. Robinson, S. E. Simmons, M. Thums, and J. Harwood. 2013. Estimating resource acquisition and at-sea body condition of a marine predator. Journal of Animal Ecology 82:1300-1315.

Sinclair, R. R., C.E. Sparling, and J. Harwood. (2020). Review of demographic parameters and sensitivity analysis to inform inputs and outputs of Population Consequences of Disturbance assessments for marine mammals. Scottish Marine and Freshwater Science, 11(14).

Smout, S., R. King, and P. Pomeroy. 2019. Environment-sensitive mass changes influence breeding frequency in a capital breeding marine top predator. Journal of Animal Ecology

Southall, B. L., Nowacek, D. P., Bowles, A. E., Senigaglia, V., Bejder, L., & Tyack, P. L. (2021). Marine Mammal Noise Exposure Criteria: Assessing the Severity of Marine Mammal Behavioral Responses to Human Noise. *Aquatic Mammals*, *47*(5), 421-464.

Sparling, C. E., and M. A. Fedak. 2004. Metabolic rates of captive grey seals during voluntary diving. Journal of Experimental Biology 207:1615-1624.

Sparling, C. E., J. R. Speakman, and M. A. Fedak. 2006. Seasonal variation in the metabolic rate and body composition of female grey seals: fat conservation prior to high-cost reproduction in a capital breeder? Journal of Comparative Physiology B 176:505-512.

Stolen, M. K., D. K. Odell, and N. B. Barros. 2002. Growth of bottlenose dolphins (Tursiops truncatus) from the Indian River Lagoon system, Florida, USA. Marine Mammal Science 18:348-357.

Sveegard S., Teilmann J., Tougaard J., Dietz R., 2011, High-density areas for harbor porpoises (Phocoena phocoena) identified by satellite tracking, Marine Mammal Science, 27(1), 230-246

Taylor, B., S. Chivers, J. Larese, and W. Perrin. 2007. Generation length and percent mature estimates for IUCN assessments of cetaceans. Administrative Report LJ-07-01National Marine Fisheries Service, Southwest Fisheries Science Center.

Thiele, J.C., Kurth, W., Grimm, V., 2014. Facilitating parameter estimation and sensitivity analysis of agent-based models: A cookbook using NetLogo and R. JASSS 17, 11. https://doi.org/10.18564/jasss.2503

Thomas, L., D.J.F. Russell, C.D. Duck, C.D. Morris, M. Lonergan, F. Empacher, D. Thompson, and J. Harwood. 2019. Modeling the population size and dynamics of the British grey seal. Aquatic Conservation: Marine and Freshwater Ecosystems 29(S1):6-23.

Thompson, P. M., D. Miller, R. Cooper, and P. S. Hammond. 1994. Changes in the Distribution and Activity of Female Harbour Seals During the Breeding Season: Implications for their Lactation Strategy and Mating Patterns. Journal of Animal Ecology **63**:24-30.

Villegas-Amtmann, S., L. Schwarz, G. Gailey, O. Sychenko, and D. Costa. 2017. East or west: the energetic cost of being a gray whale and the consequence of losing energy to disturbance. Endangered Species Research 34:167-183.

Villegas-Amtmann, S., L. Schwarz, J. Sumich, and D. Costa. 2015. A bioenergetics model to evaluate demographic consequences of disturbance in marine mammals applied to gray whales. Ecosphere 6:1-19.

Wells, R. S., & Scott, M. D. (2018). Bottlenose dolphin, Tursiops truncatus, Common Bottlenose Dolphin. In Encyclopedia of Marine Mammals (pp. 118–125).

White, J.W., Rassweiler, A., Samhouri, J.F., Stier, A.C., White, C., 2014. Ecologists should not use statistical significance tests to interpret simulation model results. Oikos 123, 385–388. https://doi.org/10.1111/j.1600-0706.2013.01073.x

Winship, A. 2009. Estimating the impact of bycatch and calculating bycatch limits to achieve conservation objectives as applied to harbour porpoise in the North Sea. University of St Andrews.

Worthy, G. A., and D. Lavigne. 1987. Mass loss, metabolic rate, and energy utilization by harp and grey seal pups during the postweaning fast. Physiological Zoology 60:352-364.

This publication is available at **www.gov.scot**

Any enquiries regarding this publication should be sent to us at

The Scottish Government
St Andrew's House
Edinburgh
EH1 3DG

ISBN: 978-1-83521-067-3 (web only)

Published by The Scottish Government, October 2023

Produced for The Scottish Government by APS Group Scotland, 21 Tennant Street, Edinburgh EH6 5NA
PPDAS1318062 (10/23)

w w w . g o v . s c o t